Convergence of a Reformulated Boundary Integral Method for Two Fluid Interfaces with Surface Tension

Héctor Daniel Ceniceros Angulo

May, 1995

A dissertation in the Department of Mathematics submitted to the faculty of the Graduate School of Arts and Sciences in partial fulfillment of the requirements for the degree of Doctor of Philosophy at New York University.

Approved: _____

Thomas Y. Hou
Advisor

Convergence of a Reformulated Boundary Integral Method for Two Fluid Interfaces with Surface Tension

Author: Héctor Daniel Ceniceros Angulo

Advisor: Thomas Y. Hou

Abstract

Numerical instability is a common difficulty in simulations of interfacial flows. In addition, when surface tension is included into the model, the evolution equations of the interface become stiff, that is, stable explicit time integration methods require a severe constraint in the size of the time step, and the application of implicit methods is difficult because the surface tension enters into the interface dynamics nonlinearly and nonlocally.

Hou, Lowengrub and Shelley [*J. Comp. Phys.* 114:312–338, 1994] design semi-implicit time integration methods for a spectral discretization in space of a new boundary integral formulation for computing the motion of an interface between two irrotational, inviscid, and incompressible fluids in two dimensions. Their methods remove the high order stiffness and perform remarkably well even in the full nonlinear regime of motion, though they apply some numerical filtering at each time step to suppress an observed aliasing instability.

In this thesis we study the nonlinear stability and convergence of a method based on the spectral discretization of Hou *et. al.*, keeping time continuous and including de-aliasing filtering only at suitable places. We are able to prove rigorously the convergence of the method provided the solution is sufficiently smooth. The proof relies on delicate energy estimates for the errors in discrete Sobolev spaces.

We also give an alternative formulation and a scheme for water waves which is more efficient numerically than the method for the general two-density fluid interface applied to this special case. We state a convergence theorem and outline its proof. Bottom topography is also considered.

Applications to Rayleigh-Taylor instability, droplet formation in a single fluid, and breaking waves with bottom topography are given. We find that surface tension leads to an interesting phenomenon in overturning waves: the interface curvature develops a concentrated spike at a certain time and subsequent capillary waves appear on the forward side of the crest.

Acknowledgements

I am most indebted to my advisor Thomas Y. Hou for his invaluable guidance, constant encouragement and extraordinary patience.

To the most wonderful people I have ever met, my parents, Juan and Elizalda for all they have given me.

To my brothers and sister for their support.

To my friends at the Courant Institute and Caltech for making my graduate studies a unique experience.

I would like to acknowledge the support of the Consejo Nacional de Ciencia y Tecnológia CONACyT Mexico for a fellowship during 1990-1994 and the Office of Naval Research ONR Grant: N00014-94-1-0310.

Contents

Abstract iii

Acknowledgements iv

1 Introduction 1

2 A Boundary Integral Reformulation for Two Fluid Interfaces 8

2.1 Tangent Angle-Arclength Stretching Reformulation 9

2.2 Stiffness and Small Scale Decomposition 13

3 The Numerical Method for Two Fluid Interfaces with Surface Tension and its Convergence 16

3.1 The Numerical Method 16

3.2 Consistency 20

3.3 Stability 24

3.3.1 Estimates for the Variations of the Velocities 24

3.3.2 Evolution Equations for the Errors 34

3.3.3 Energy Estimates 44

3.4 Appendix : Proof of Technical Lemmas 52

4 Water Waves with Surface Tension 70

4.1 A Tangent Angle-Arclength Stretching Formulation for Water Waves on a Fluid of Infinite Depth 70

4.2 A Convergent Numerical Method for Water Waves with Surface Tension . . 72

4.3 Sketch of Proof 74

4.4 Water Waves with Bottom Topography 78

5 Numerical Examples **82**

5.1 Time Discretization 82

5.2 Some Details about the Implementation 84

5.2.1 Equal Arclength Initialization 84

5.2.2 Solving the Integral Equation 85

5.2.3 Constructing R for the Nonuniform Mesh 85

5.2.4 Fourier Filtering 87

5.3 Numerical Experiments 87

5.3.1 An Interfacial Standing Wave 88

5.3.2 Raleigh-Taylor Instability 89

5.3.3 Drop Formation in a Single Fluid 91

5.3.4 Breaking Waves 92

Bibliography **115**

1. Introduction

An interface between two immiscible fluids of different properties experiences surface tension due to uneven intermolecular forces of attraction at or near the interface. For example, if one of the fluids is water and the other is air, then the molecules of water that are near the boundary are not surrounded by enough molecules to balance the attractive forces from the interior of the liquid. As a result, the interface tends to contract.

We can also regard the interfacial phenomenon of surface tension as a source of a special form of energy of amount proportional to the area of the surface [10]. This accounts for the spherical shape observed in small liquid drops and gas bubbles. Surface tension is also crucial to understanding the process of droplet formation and many other physical phenomena such as capillarity, cavitation, hydrodynamic stability, the motion of waves on a free surface , the formation of patterns in Hele-Shaw flows [20, 47], crystal growth and solidification [39, 55] , and noise generation at the ocean surface [50].

From the dynamical point of view, the surface tension of a curved interface acts to balance the difference in pressures across it. This boundary condition, in the case of incompressible inviscid fluids, is expressed by Laplace's formula [38]

$$[p] \equiv p_1 - p_2 = \tau\kappa, \tag{1.1}$$

where p_1 and p_2 are the limiting values of the pressure below and above the interface respectively, τ is the surface tension coefficient, and κ is the local curvature of the interface. Here, τ is assumed to be constant, though as a function of state, it may vary with temperature, the presence of pollutant particles on the surface, or other state parameters. However, a variation of τ in space introduces a tangential stress that can only be balanced in viscous fluids. Since in this study we limit ourselves to inviscid flows, we treat τ as a constant. Examples of variable surface tension can be found in [1, 3, 30].

How does surface tension affect the motion and shape of a fluid interface? At the

linear level, surface tension provides a stabilizing mechanism for perturbations about the equilibrium state (a flat surface) [24]. Furthermore, in a recent works [12, 14], Beale, Hou and Lowengrub prove that if surface tension is included then the linearized motion about any smooth solution, even far from equilibrium is well-posed. This linear well-posedness does not preclude the growth of linear disturbances; in fact they can grow exponentially in time, but the rate of growth is bounded, that is, it does not increase indefinitely with the wavenumber.

It is natural to ask if this linear regularization effect prevails in the full nonlinear regime of motion, or if nonlinear interactions could take over and lead to singularity formation. Motivated by this question several researchers have studied numerically the nonlinear behavior of interfacial flows with surface tension [6, 11, 15, 17, 21, 34, 51, 52]. Boundary integral methods are a popular choice among these works because these methods reduce the dimension of the problem by involving quantities along the interface only [49]. Methods of boundary integral type have been used to compute nonlinear surface waves [8, 23, 41, 43, 46, 51, 53], vortex sheet (no density difference) motion [2, 9, 26, 33, 36, 37, 45, 52, 56], Rayleigh-Taylor instability [7, 35, 51, 62] and interfaces in Hele-Shaw cells [20, 34, 63]. However, boundary integral methods designed for computing interface motion are very sensitive to *numerical instabilities* because the underlying problem is fairly singular. If left uncontrolled, these instabilities usually destroy the accuracy of the computations.

Longuet-Higgins and Cokelet [43] were the first to encounter a sawtooth instability in their simulations of nonlinear water waves without surface tension; the computed position of successive particles oscillated and the instability increased in time. By applying 5-point or 7-point averaging to the numerical solution every five time steps or so, Longuet-Higgins and Cokelet were able to delay the onset of this instability for the spatial resolutions they used. It is important to note that this *ad hoc* smoothing technique and others describe below do not completely eliminate the numerical instability.

High mode instability was also observed by Baker, Meiron and Orszag [8] in their computations of free surface flows using a boundary integral method.

In [23], Dold reported a steep-wave instability that he associated with the magnitude of the radius of curvature of the wave crest and that appeared no matter how small the time step was. He conjectured that the use of spectral methods could remove this type of

instability. Dold also studied time discretization-related instabilities. The works of Baker *et al.* [8] and Dold did not consider surface tension and both applied polynomial averaging smoothing to limit the anomalous growth of high modes .

Computations of interfacial flows with surface tension are even more sensitive to numerical instabilities because surface tension introduces nonlinear terms with high order spatial derivatives into the interface evolution equations. Straightforward discretizations of the surface tension term may lead to numerical instabilities. Pullin [51] was of the first to experience this difficulty. Using a boundary integral method for computing two fluid interfacial flows, Pullin noted small-scale corrugations in regions of high curvature in the interface profile that appeared with nonzero surface tension, in addition to a sawtooth instability of the type described by Longuet-Higgins and Cokelet [43]. While he could partially delay the sawtooth instability with similar polynomial averaging smoothing techniques, eventually the appearance of the first type of instability, associated with surface tension, caused the computations to end. Pullin questioned if this instability was physical or numerical.

Using also a boundary integral method, Rangel and Sirignano [52] limited the growth of modes with high wavenumbers by doing redistribution and point insertion of vortices. This procedure gives a smoothing effect very similar to that of the vortex-blob method [19, 36] or the vortex-in-cell method used by Tryggvason [62]. It becomes difficult to distinguish the real effects of surface tension with this regularization.

Linear analysis about equilibrium has helped to identify common sources of instability in boundary integral methods. Without surface tension, Roberts [53] showed how to remove a sawtooth instability.

In recent works [6, 11], numerical stability analyses were presented in two different contexts of interfacial flows with surface tension. Baker and Nachbin [6], performed normal mode analysis for several boundary integral schemes to study the linear evolution of periodic perturbations of a flat vortex sheet. With this linear analysis, Baker and Nachbin were able to identify common causes for numerical instability. However, their study did not consider the behavior of perturbations away from equilibrium and left open the questions of nonlinear stability and convergence. These questions were addressed by Beale, Hou and Lowengrub [11], hereafter referred to as BHL, in a rigorous convergence proof of a

boundary integral method for water waves with or without surface tension. Following a framework developed in [13] for linearized motion perturbed about an arbitrary smooth solution at the continuous level, BHL found that very delicate balances among terms with singular integrals and derivatives must be preserved at the discrete level in order to maintain numerical stability. They also realized that suitable numerical filtering is necessary at certain places to prevent the discretization from introducing new instabilities in the modes with high wavenumber. This filtering depends on the choices for approximating spatial derivatives and quadrature rules for singular integrals. BHL also noted that the periodicity of the numerical solution introduces aliasing errors which ultimately become another source of instability. Thus, spectral approximations also require some Fourier filtering.

Another major difficulty in numerical simulations of interfacial flows with surface tension, is related to time discretizations. Through Laplace's formula, surface tension introduces terms with high order derivatives both nonlinear and nonlocal into the interface dynamics. This leads to severe stability constraints for explicit time integration methods and makes the application of implicit methods difficult [17, 34]. For two fluid interfaces in Euler flow, the stability constraint is of the form $\Delta t \leq C \cdot (\Delta s)^{3/2}$, and for Hele-Shaw flows is $\Delta t \leq C \cdot (\Delta s)^3$, where Δt is the size of the time step and Δs is the minimum grid spacing in arclength. In practice, these time-dependent constraints become more severe by point clustering along the interface. This imposes a serious limitation for well resolved computations. The presence of such restrictions on the time step is known as *stiffness*.

In [34], Hou, Lowengrub and Shelley, hereafter referred to as HLS, introduced methods that remove the high order stiffness in computing the motion of fluid interfaces with surface tension in two-dimensional, irrotational and incompressible fluids. Their schemes are based on a spectral discretization of a boundary integral reformulation using two natural variables: the tangent angle θ to the curve and the arclength stretching σ, which is the derivative of the arclength with respect to a Lagrangian marker α. In these variables, the surface tension term has a very simple form because $\kappa = \theta_\alpha/\sigma$. HLS identify the leading order stiff terms and treat them implicitly in time discretizations. These semi-implicit methods can be solved easily once a suitable parametrization of the interface is chosen. The methods give an enormous saving in computational time. HLS have used their schemes to compute the motion of a vortex sheet, Hele-Shaw and Boussinesq flows. In particular, with their

non-stiff methods, HLS have discovered a new type of singularity in vortex sheets: the formation of trapped bubbles through the self-intersection of the fluid interface [33].

In this thesis, we study the nonlinear stability and convergence of a method based on the spectral spatial discretization used by HLS and keeping time continuous. We apply certain Fourier filtering at places suggested by our stability analysis to preserve the balance among most singular terms. With this filtering as part of the method, we are able to prove rigorously that the method converges to the exact solution with spectral accuracy provided the solution is sufficiently regular. This is our main result (Theorem 3.1).

Our proof follows a framework developed in [12, 14] to study the linearized motion about smooth solution of two fluid interfaces with surface tension in the continuous case, in the same spirit of BHL's convergence proof of a method for water waves [11]. The key is to identify the most singular or leading order terms of the method and to make sure that a delicate balance among these terms is satisfied. The situation is more complicated than that in the water waves scheme studied by BHL. In our case, the formulation is different and more general because it applies to two fluid interfaces of which water waves is a special case, and uses σ and θ as evolution variables to determine the interface position rather than the Cartesian variables x and y.

By adding a tangential velocity, we select a parametrization such that, $\sigma = R(\alpha) < \sigma >$, where the brackets denote average in space and R is a smooth function of mean one. R can be chosen at our advantage to obtain some control on the positioning of the interface Lagrangian particles. Thus, we may cluster particles in neighborhoods of singular points (taking R small there) and separate the particles in over-resolved regions. While this parametrization can give a substantial improvement in the resolution, it introduces new difficulties into the analysis. In particular, we find that a natural variable to use in the computation of the velocity is the true vortex sheet strength $\tilde{\gamma} = \gamma/\sigma$, where γ is the unnormalize vortex sheet strength. By filtering $\tilde{\gamma}$ in the velocity, we are able to show, through energy estimates, that the most singular terms of the method balance one another.

The selection of the places where Fourier filtering is applied when solving a discrete version of an integral equation for $d\gamma/dt$ is also a difficult problem. Terms that arise from the derivative in time of the velocity, have to be filtered at different places to guarantee both the solvability of the discrete integral equation and the stability balance. We do not

claim that the application of Fourier filtering to eliminate aliasing errors is unique but we do show that our choice gives a nonlinearly stable and convergent discretization.

We also present an alternative method for water waves computations which is more efficient numerically than the method for the general two fluid interface applied to the extreme case of a free surface on a single fluid. The scheme is based on a different boundary integral formulation that uses the velocity potential as an evolution variable rather than the vortex sheet strength [8, 11], and on a reformulation using the tangent angle and arclength stretching variables. We state a convergence result for this method (Theorem 4.1) and outline the main ideas of its proof. An extension of the method to simulate water waves with bottom topography is also presented.

We implement our methods with a fourth order implicit-explicit time discretization of the type studied by Ascher *et al.* in [4]. Several numerical examples demonstrate the robustness and efficiency of the methods. We are able to compute with high accuracy the process of drop formation on a falling fluid very close to the pinch-off time, when a topological singularity occurs. This is one of the simplest hydrodynamic examples in which physical quantities become discontinuous in finite time. Our computations show that the interface stretches forming a long neck with a minimum thickness that goes to zero in finite time. This is consistent with what has been observed experimentally [48, 57].

We present also computations for Rayleigh-Taylor instability. We find that for small density differences, the interface rolls up. This behavior agrees qualitatively with other Rayleigh-Taylor computations such as the early marker-in-cell simulations of Daly [21], the vortex-in-cell method of Tryggvason [62] and the projection method of Bell and Marcus [16]. But, unlike these methods, surface tension is the only regularization in our computations. We find evidence that the interface in the roll-up region self-intersects forming trapped bubbles of fluid as was observed by HLS [33] in their vortex sheet computations. This peculiar process of singularity formation is purely due to surface tension effects. The structure of the roll-up appears to be generic.

Another challenging test for our methods is the simulation of breaking waves. Without surface tension, recent boundary integral methods have been able to compute close to the time when the tip of the wave reaches the lower part of the free surface [11, 41]. Moreover, the computations in [11] also show that the interface profile remains smooth though the

magnitude of the curvature is very large at the wave tip.

In our simulations with surface tension, we find an interesting phenomenon in overturning waves. At some point on the forward face of the wave, the curvature develops a concentrated spike and subsequent oscillations appear on one side of it. The spectra of the numerical solution show no sign of instability. By varing the surface tension we observe the appearance of a strong vortical region, or roller [42], in the wave crest and the generation of capillary waves on the forward edge of the roller. This is a phenomenon that has been observed experimentally [25].

This thesis is organized as follows: In Chapter 2, We describe the tangent angle-arclength stretching reformulation of HLS for two fluid interfaces and outline their ideas to remove the stiffness introduced by surface tension. The numerical method, using a spectral discretization in space and keeping time continuous, is presented in Chapter 3 along with the precise statement of the convergence result (Theorem 3.1) and its proof.

The alternative method for water waves is given in Chapter 4, where we also state a convergence result (Theorem 4.1) and outline its proof. In addition, we extend our method to include bottom topography.

Finally, in Chapter 5 we discuss implementation issues of our methods and present the numerical experiments.

2. A Boundary Integral Reformulation for Two Fluid Interfaces

In this chapter, we present the boundary integral reformulation introduced by HLS for two fluid interfaces and describe their ideas to remove the high order stiffness caused by surface tension. Specifically, we concentrate on the motion of an interface Γ separating two infinite layers of inviscid, incompressible and irrotational fluids in two dimensions. Under these assumptions, potential flows exist in the interior of the layers and the flow can be described by variables defined on the interface only. The boundary conditions we impose are

$$(i) \quad [\mathbf{u}]_\Gamma \cdot \hat{\mathbf{n}} = 0 \ ,$$

$$(ii) \quad [p]_\Gamma = \tau\kappa \ ,$$

where $[\mathbf{u}]_\Gamma$ denotes the velocity jump across the interface, and $\hat{\mathbf{n}}$ is a normal unit vector to the interface. The kinematic condition (i) is the usual requirement that particles on the surface, remain there [64]. Condition (ii) is Laplace's formula (1.1). With these hypotheses we can obtain a boundary integral formulation for the interface evolution equations. Here we give only the equations, the details of the derivation can be found in [5, 8]. Denoting the interface position by $\mathbf{X}(\alpha,t) = (x(\alpha,t), y(\alpha,t))$, where α is a Lagrangian parameter, the surface evolves according to

$$\mathbf{X}_t = U^N\hat{\mathbf{n}} + (U^T + U^A)\hat{\mathbf{s}} \tag{2.1}$$

$$\gamma_t = (\frac{U^A\gamma}{\sigma})_\alpha - 2A[\sigma\mathbf{W}_t\cdot\hat{\mathbf{s}} + \frac{1}{8}(\frac{\gamma}{\sigma})_\alpha^2 + gy_\alpha - U^A\mathbf{W}_\alpha\cdot\hat{\mathbf{s}}] + S\kappa_\alpha \tag{2.2}$$

$$\mathbf{W} = \frac{1}{2\pi}\int_{-\infty}^{\infty}\gamma(\alpha')\frac{(-(y(\alpha)-y(\alpha')), x(\alpha)-x(\alpha'))}{(x(\alpha)-x(\alpha'))^2 + (y(\alpha)-y(\alpha'))^2}d\alpha' \tag{2.3}$$

$$U^N = \mathbf{W}\cdot\hat{\mathbf{n}} \quad ; \quad U^T = \mathbf{W}\cdot\hat{\mathbf{s}} \ , \tag{2.4}$$

where $\hat{\mathbf{n}}$ and $\hat{\mathbf{s}}$ are unit normal and tangential vectors to the interface, γ is the unnormalized vortex sheet strength given by $\gamma = \sigma(\mathbf{U}_1 - \mathbf{U}_2)|_\Gamma\cdot\hat{\mathbf{s}}$ and $\sigma = (x_\alpha^2 + y_\alpha^2)^{1/2}$ is the arclength

stretching variable. $A = (\rho_1 - \rho_2)/(\rho_1 + \rho_2)$ is called the Atwood number and measures the stratification of the flows. The local curvature κ is given by

$$\kappa = \frac{y_{\alpha\alpha} x_\alpha - x_{\alpha\alpha} y_\alpha}{(x_\alpha^2 + y_\alpha^2)^{3/2}} \ . \tag{2.5}$$

$S = 2\tau/(\rho_1 + \rho_2)$ is a rescaled surface tension coefficient and g the gravity acceleration. The tangential velocity U^A is arbitrary and its choice determines the frame of reference. In (2.3) the slashed integral denotes Cauchy's principal value. We omit writing the time-dependence to simplify the notation.

From these set of equations we observe that the surface tension enters into the interface dynamics terms with high (third) order derivatives nonlinearly and nonlocally, making implicit time discretizations very difficult.

A "frozen coefficient" linear analysis about an arbitrary smooth solution for the evolution equations (2.1-2.2) gives the following stability constraint for an explicit time-integration method [17, 34]

$$\Delta t < \frac{C}{S} (\bar{\sigma} h)^{3/2} \quad \text{with} \ \ \bar{\sigma} = \min_\alpha \sigma \tag{2.6}$$

Although the exponent 3/2 may not seem very restrictive, this stability constraint is still very severe because of its dependence on $\bar{\sigma}$. As the interface evolves , Lagrangian particles tend to cluster in some regions and cause $\bar{\sigma}$ to be very small. This time-dependent behavior usually leads to prohibitively stiff systems.

HLS exploit the freedom in choosing the tangential velocity U^A to have some control over the point clustering. But their first strategy is to reformulate the interface evolution equations in terms of the tangent angle θ and the arclength stretching σ. In these two new variables, the surface tension term becomes linear : $S\kappa_\alpha = S(\theta_\alpha/\sigma)_\alpha$. This approach has been used previously by Strain [59] in the context of solidification, and by Goldstein and Petrich [27] in the context of integrable closed curve dynamics. We include next a derivation of the evolution equations for σ and θ.

2.1. Tangent Angle-Arclength Stretching Reformulation

Let $z(\alpha) = x(\alpha) + iy(\alpha)$ denote the complex position of the interface. Moreover let us assume that the interface is periodic in the x-direction, that is, $z(\alpha) = \alpha + s(\alpha)$ where $s(\alpha)$

is a 2π-periodic function. By definition, the tangent angle θ and the arclength stretching σ are related to z by the identity

$$z_\alpha = \sigma e^{i\theta} \ . \tag{2.7}$$

Hence, given σ and θ, the position of the interface can be reconstructed by integrating this expression, or equivalently

$$z(\alpha) = \alpha + \int_0^\alpha (\sigma(\alpha')e^{i\theta(\alpha')} - < \sigma e^{i\theta} >)d\alpha' + z_0 \ , \tag{2.8}$$

where the brackets denote the mean or average in space, that is

$$< f > \equiv \frac{1}{2\pi}\int_0^{2\pi} f(\alpha')d\alpha' \ , \tag{2.9}$$

and we have also used that $< z_\alpha >= 1 + < s_\alpha >= 1$ as $s(\alpha)$ is periodic.

The integration constant z_0 can be obtained by evolving one single point of the interface in time. When the two layers of fluid are infinite in the y-direction, z_0 provides just a translation to the curve and does not influence its dynamics. On the other hand in water waves problems with bottom topography (finite depth) the relative position of the interface and the bottom affects the dynamics; thus we need to track z_0 in this case. For simplicity we take $z_0 = 0$ whenever this constant is irrelevant.

We remark also that although (2.8) is equivalent to integrating (2.7) at the continuous level, a discretization of (2.8) is preferable because it enforces the periodicity assumption in z, namely $z(\alpha) - \alpha = s(\alpha)$ should be a 2π-periodic function .

Conversely, given $z(\alpha)$ we can obtain σ and θ by the following transformation

$$\sigma = (x_\alpha^2 + y_\alpha^2)^{1/2} \ , \tag{2.10}$$

$$\theta = \tan^{-1}(y_\alpha/x_\alpha) \ . \tag{2.11}$$

However, as pointed out by HLS [34], to avoid possible branching of the inverse tangent it is better to determine θ numerically using the relation $\theta_\alpha = \sigma\kappa$. Thus an alternative mapping from (x, y) to (σ, θ) takes the form

$$\sigma = (x_\alpha^2 + y_\alpha^2)^{1/2} \ , \tag{2.12}$$

$$\theta = \int_0^\alpha \frac{x_\alpha y_{\alpha\alpha} - y_\alpha x_{\alpha\alpha}}{x_\alpha^2 + y_\alpha^2}\, d\alpha' + \theta_0 \ , \tag{2.13}$$

where the constant of integration θ_0 is obtained from the inverse tangent formula for the point $\alpha = 0$.

We need to find now evolution equations for σ and θ. Differentiating (2.10) with respect to time we get

$$\sigma_t = \frac{1}{\sigma}(x_\alpha x_{\alpha t} + y_\alpha y_{\alpha t}) = (x_t, y_t)_\alpha \cdot \hat{\mathbf{s}} \ . \tag{2.14}$$

To compute $(x_t, y_t)_\alpha$ we differentiate (2.1) with respect to α,

$$(x_t, y_t)_\alpha = U^T_\alpha \hat{\mathbf{s}} + U^N_\alpha \hat{\mathbf{n}} + U^A_\alpha \hat{\mathbf{s}} + U^T \hat{\mathbf{s}}_\alpha + U^N \hat{\mathbf{n}}_\alpha + U^A \hat{\mathbf{s}}_\alpha \ ,$$

and making use of the Frênet formulae $\hat{\mathbf{n}}_\alpha = -\kappa\sigma\hat{\mathbf{s}}$ and $\hat{\mathbf{s}}_\alpha = \kappa\sigma\hat{\mathbf{n}}$, we get

$$(x_t, y_t)_\alpha = [(U^T + U^A)_\alpha - \theta_\alpha U^N]\hat{\mathbf{s}} + [U^N_\alpha + \theta_\alpha(U^T + U^A)]\hat{\mathbf{n}} \ . \tag{2.15}$$

Now substituting (2.15) into (2.14) we obtain

$$\sigma_t = (U^T + U^A)_\alpha - \theta_\alpha U^N \ . \tag{2.16}$$

We can find an evolution equation for θ by differentiating (2.11) with respect to time, we have

$$\theta_t = \frac{1}{1 + (\frac{y_\alpha}{x_\alpha})^2}(\frac{y_\alpha}{x_\alpha})_t = \frac{1}{\sigma}(x_t, y_t)_\alpha \cdot \hat{\mathbf{n}} \ ,$$

and substituting (2.15) into this expression we obtain

$$\theta_t = \frac{1}{\sigma}[U^N_\alpha + \theta_\alpha(U^T + U^A)] \ . \tag{2.17}$$

Note that the evolution equations (2.16-2.17) can be used in many other different contexts depending how the velocity is determined. Examples include motion by mean curvature, dendritic solidification and Hele-Shaw interfaces.

We specify now U^A such that the following condition is satisfied

$$\sigma(\alpha, t) = R(\alpha) < \sigma > \ , \tag{2.18}$$

for some given smooth function $R(\alpha)$ with mean one, that is, we have some control on the positioning of the Lagrangian markers. In particular, if we know in advance where some complexity of the curve is located, we can select R to cluster particles about that region to achieve better resolution.

To find such velocity U^A, we note that condition (2.18) implies that $\sigma_t = R < \sigma_t >$. From (2.16) we get

$$(U^T + U^A)_\alpha - \theta_\alpha U^N = R(\alpha) < (U^T + U^A)_\alpha - \theta_\alpha U^N > = -R(\alpha) < \theta_\alpha U^N > \ .$$

Solving this expression for U^A_α and integrating we find

$$U^A = -U^T + \int_0^\alpha [\theta_\alpha U^N - R(\alpha) < \theta_\alpha U^N >] d\alpha' + U^A(0,t) \ . \tag{2.19}$$

Therefore, if (2.18) is satisfied initially, the choice (2.19) will enforce this constraint in time. This implies that an initial parametrization of the curve is preserved, up to a time-dependent scaling. Following HLS, we refer to this as the *scaled initial parametrization frame*. If $R \equiv 1$ then σ is independent of α and equal everywhere to its mean. This particular parametrization is referred to as the *equal arclength frame* , because the Lagrangian grid points on the interface are equally spaced in arclength.

The spatial constant $U^A(0,t)$ gives just a temporal shift on the frame but does not alter condition (2.18). For simplicity we will take this constant to be zero.

The velocity $\mathbf{W} \equiv (U, V)$ defined in (2.3) has a succinct form if we use the complex position variable z,

$$W = \frac{1}{2\pi i} \int_{-\infty}^{\infty} \frac{\gamma(\alpha')}{z(\alpha) - z(\alpha')} d\alpha' = U - iV \tag{2.20}$$

and using the periodicity of $z(\alpha) - \alpha$, it can be shown [5] that

$$W = \frac{1}{4\pi i} \int_{-\pi}^{\pi} \gamma(\alpha') \cot \frac{1}{2}(z(\alpha) - z(\alpha')) d\alpha' \ . \tag{2.21}$$

We write now the complete set of equations in the σ-θ variables for future reference.

$$\sigma_t = -R(\alpha) < \theta_\alpha U^N > \tag{2.22}$$

$$\theta_t = \frac{1}{\sigma}[U^N_\alpha + \theta_\alpha (U^T + U^A)] \tag{2.23}$$

$$\gamma_t = S(\frac{\theta_\alpha}{\sigma})_\alpha - 2A[Re\{\sigma e^{i\theta} W_t\} + \frac{1}{8}(\frac{\gamma}{\sigma})^2_\alpha + g\sigma \sin\theta - U^A Re\{e^{i\theta} W_\alpha\}] + (\frac{\gamma}{\sigma} U^A)_\alpha \tag{2.24}$$

$$z = \alpha + \int_0^\alpha (\sigma e^{i\theta} - < \sigma e^{i\theta} >) d\alpha' \tag{2.25}$$

$$W = \frac{1}{4\pi i} \int_{-\pi}^{\pi} \gamma(\alpha') \cot \frac{1}{2}(z(\alpha) - z(\alpha')) d\alpha' \tag{2.26}$$

$$U^T = Re\{e^{i\theta} W\} \quad ; \quad U^N = -Im\{e^{i\theta} W\} \tag{2.27}$$

$$U^A = -U^T + \int_0^\alpha (\theta_\alpha U^N - R < \theta_\alpha U^N >) d\alpha' \ . \tag{2.28}$$

2.2. Stiffness and Small Scale Decomposition

The surface tension term $S(\theta_\alpha/\sigma)_\alpha$ affects the evolution of θ through the vortex sheet strength γ in the velocity field. Thus U_α^N is the term that contributes the most to the stiffness in (2.23). This nonlocal effect makes difficult the application of implicit time discretizations. However, we are not taking into account that stiffness arises form high order terms only at small spatial scales; the time step has to be small enough to resolve the propagation of capillary waves [17]. Let us illustrate the problem with a simple example.

Consider the Heat Equation in one dimension with periodic boundary conditions, say in $[-\pi, \pi]$

$$u_t = u_{xx} \quad ; \quad u(0,x) = u_0(x) \quad ; \quad u(-\pi,t) = u(\pi,t) \ .$$

We can use a spectral method to solve this problem by discretizing in Fourier space,

$$\frac{d\hat{u}_k}{dt} = -k^2 \hat{u}_k \quad ; \quad k = -N/2+1, \ldots, N/2 \ ,$$

where $\hat{u}_k$ stands for the discrete Fourier transform. Of course we can solve analytically this system of ODEs, but for the sake of illustration, let us take a simple forward Euler discretization instead. For each k we have

$$\frac{\hat{u}_k^{n+1} - \hat{u}_k^n}{\Delta t} = -k^2 \hat{u}_k^n \ ,$$

where the superindex in $\hat{u}_k^m$ refers to the time $m\Delta t$, and Δt is the size of the time step. Solving for $\hat{u}_k^{n+1}$ we obtain

$$\hat{u}_k^{n+1} = (1 - \Delta t k^2)\hat{u}_k^n \ .$$

Stability requires that $|1 - \Delta t k^2| \leq 1$. This imposes a severe restriction on Δt, namely

$$\Delta t \leq \frac{2}{k^2} \quad \Rightarrow \quad \Delta t \leq Ch^2 \ , \tag{2.29}$$

where $h = 2\pi/N$ is the spatial mesh size. We say that the problem is *stiff* because of this strong constraint to ensure stability.

This simple example tells us that terms with high order derivatives, u_{xx} in this case, introduce stiffness. Moreover, from expression (2.29), it also tells us that *stiffness arises only for the high modes* or equivalently at *small scales*. We note too, that an implicit

discretization removes the high order constraint. As we shall see, the semi-implicit methods of HLS are based on these ideas.

Let us return now to the interface problem. The next step in HLS approach is to extract the leading part of the velocity at high modes (small scales). To this end, we consider the expression (2.20) for W and write the kernel as follows

$$\frac{1}{z(\alpha)-z(\alpha')} = \frac{1}{z_\alpha(\alpha)(\alpha-\alpha')} + \left[\frac{1}{z(\alpha)-z(\alpha')} - \frac{1}{z_\alpha(\alpha)(\alpha-\alpha')}\right] .$$

Using this expression, we can write W as

$$W = \frac{1}{2\pi i}\int_{-\infty}^{\infty} \frac{\gamma(\alpha')}{z(\alpha)-z(\alpha')}d\alpha' = \frac{1}{2iz_\alpha}\mathcal{H}[\gamma] + \int_{-\infty}^{\infty}\gamma(\alpha')g(\alpha,\alpha')d\alpha' , \tag{2.30}$$

where $\mathcal{H}$ is the Hilbert transform defined by

$$\mathcal{H}[f](\alpha) = \frac{1}{\pi}\int_{-\infty}^{\infty}\frac{f(\alpha')}{\alpha-\alpha'}d\alpha' . \tag{2.31}$$

The last term in (2.30) is a smoothing operator because γ is integrated against the smooth function g. Therefore, it follows that [34]

$$U^N(\alpha,t) = \frac{1}{2i\sigma}\mathcal{H}[\gamma](\alpha,t) + R_s[\gamma](\alpha,t) ,$$

where R_s is a smoothing operator in the sense that if $x(\alpha,t)$ and $y(\alpha,t)$ are real analytic functions of α for $t \le T$, the interface does not self-intersects, and $\sigma \neq 0$ then the Fourier transform of R satisfies $\hat{R}_s[\gamma] = O(e^{-\rho|k|}\hat{\gamma})$ for large wavenumber $|k|$. Here, $\rho > 0$ is the width of the strip of analyticity about the real axis. If $x(\alpha,t)$ and $y(\alpha,t)$ are not analytic but C^m then $\hat{R}_s[\gamma] = O(|k|^{-m}\hat{\gamma})$. Thus, at high modes,

$$\frac{1}{\sigma}U^N_\alpha \sim \frac{1}{2\sigma}\left(\frac{1}{\sigma}\mathcal{H}[\gamma]\right)_\alpha ,$$

where by $\sim$ we mean equivalent modulo a smoothing operator. The evolution equations for θ and γ can now be written in a form that reveals the leading order behavior at small scales.

$$\theta_t = \frac{1}{2\sigma}\left(\frac{1}{\sigma}\mathcal{H}[\gamma]\right)_\alpha + P , \tag{2.32}$$

$$\gamma_t = S(\frac{\theta_\alpha}{\sigma})_\alpha + Q , \tag{2.33}$$

where P is defined as the right hand side of (2.23) minus the high mode leading term and Q is the right hand side of (2.24) without the surface tension term.

The leading order terms simplify considerably if σ is independent of α. This can be achieved by taking the parametrization function R identically equal to one. In this particular case, the system (2.32-2.33) in Fourier space becomes

$$\hat{\theta}_t(k) = \frac{1}{2\sigma^2}\,|k|\,\hat{\gamma}(k) + \hat{P}(k) \tag{2.34}$$

$$\hat{\gamma}_t(k) = -\frac{S}{\sigma}k^2\hat{\theta}(k) + \hat{Q}(k)\ , \tag{2.35}$$

where we have used that $\widehat{\mathcal{H}f}(k) = -i\mathrm{sgn}(k)\hat{f}(k)$. An implicit time discretization of the high mode leading order terms is now trivial to solve. If $R \not\equiv 1$, we can recast the system of equations obtained by a semi-implicit discretization in a form suitable for an efficient iterative method. We leave the discussion of specific time discretizations to Chapter 5. In the next chapter we present and analize a spectral spatial discretization for the interface evolution equations.

3. The Numerical Method for Two Fluid Interfaces with Surface Tension and its Convergence

We devote this chapter to prove rigorously the convergence of a numerical method to study the evolution of a two fluid interface with surface tension using the tangent angle-arclength stretching boundary integral reformulation and the scaled initial parametrization frame introduced in Chapter 2, under the assumption of sufficiently regular solutions. In the first section, we present the numerical method and state a convergence theorem. The proof of this result is divided in two main parts: Consistency and Stability. The latter is the most technical part of the proof and it is divided itself into three subsections. Several technical lemmas are also used; their proofs are deferred to the Appendix.

3.1. The Numerical Method

We need to make a few definitions before presenting the method. Let f be a function whose values are known on a uniform grid of mesh size $h = 2\pi/N$. We define a discrete Fourier transform of f by

$$\hat{f}_k = \frac{1}{N} \sum_{j=-N/2+1}^{N/2} f(\alpha_j) e^{-ik\alpha_j} \quad ; \quad \alpha_j = jh \ , \tag{3.1}$$

with inverse or Fourier interpolant given by

$$f(\alpha_j) = \sum_{k=-N/2+1}^{N/2} \hat{f}_k e^{ik\alpha_j} \ . \tag{3.2}$$

Here we assume that N is even.

We denote by S_h the pseudo spectral derivative operator defined in Fourier space as

$$\widehat{(S_h f)}_k = ik\hat{f}_k \ . \tag{3.3}$$

It is well known that pseudo-spectral approximations without smoothing introduce aliasing errors [28, 29, 61]. To eliminate these errors, we introduce the following Fourier filtering:

$$(\widehat{f^p})_k = \rho(kh)\hat{f}_k \ , \tag{3.4}$$

where the function ρ is chosen such that

$$\begin{aligned}
&(i) \quad \rho(-x) = \rho(x) \ ; \ \rho(x) \geq 0 \\
&(ii) \quad \rho(x) \in C^r \ ; \ r > 2 \\
&(iii) \quad \rho(\pm\pi) = \rho'(\pm\pi) = 0 \\
&(iv) \quad \rho(x) = 1 \quad \text{for } |x| \leq \lambda\pi \quad 0 < \lambda < 1 \ .
\end{aligned}$$

In other words $\rho(x)$ plays the role of Fourier cutoff smoothing while preserving the spectral accuracy, which is guaranteed by condition (iv). Using this filtering, we define a smoothed derivative operator:

$$(\widehat{D_h f})_k = ik\rho(kh)\hat{f}_k \ . \tag{3.5}$$

By z^p we mean $z^p = \alpha + s^p$. In addition, $S_h z_i = 1 + S_h s_i$ and similarly for $D_h z$.

We also need to provide a discrete integral operator. We select this to be the pseudo-spectral operator, which we denote by Int_h, given in Fourier space by

$$(\widehat{Int_h f})_k = \begin{cases} \frac{1}{ik}\hat{f}_k & \text{for } k \neq 0 \ , \\ 0 & \text{for } k = 0 \ , \end{cases} \tag{3.6}$$

for any 2π-periodic function f of mean zero .

The discrete mean is computed using the trapezoidal rule,

$$< f >_h \equiv \frac{1}{N} \sum_{i=-N/2+1}^{N/2} f_i \ . \tag{3.7}$$

Hereafter we denote by $\sigma(\alpha_i)$, $\theta(\alpha_i)$, $\gamma(\alpha_i)$, etc., the exact continuous solution evaluated at the grid points, and by σ_i, θ_i, γ_i, etc., the discrete approximation. To simplify the notation we omit writing the time dependence on the functions unless otherwise noted.

Throughout the proof of convergence, constants are written generically as C and smooth functions as f and g whenever their specific forms are not relevant to the analysis.

We are now ready to present the numerical method:

$$\frac{d\sigma_i}{dt} = -R(\alpha_i) < S_h \theta U^N >_h \tag{3.8}$$

$$\frac{d\theta_i}{dt} = \frac{1}{\sigma_i}[S_h U_i^N + D_h \theta_i (U_i^T + U_i^A)] \tag{3.9}$$

$$\begin{aligned} \frac{d\gamma_i}{dt} &= SD_h(\frac{1}{\sigma_i} D_h \theta_i) + S_h(U_i^A \tilde{\gamma}_i^p) \\ &- 2ARe\{\frac{\sigma_i e^{i\theta_i}}{4\pi i} \sum_{\substack{j=-N/2+1 \\ (j-i)\text{odd}}}^{N/2} \frac{d\gamma_j}{dt} \cot\frac{1}{2}(z_i^p - z_j^p) 2h\} \\ &+ ARe\{\frac{\sigma_i e^{i\theta_i}}{4\pi i} \sum_{\substack{j=-N/2+1 \\ (j-i)\text{odd}}}^{N/2} \gamma_j^p \frac{\frac{dz_i}{dt} - \frac{dz_j}{dt}}{\sin^2\frac{1}{2}(z_i^p - z_j^p)} 2h\} \\ &- 2A[\frac{1}{8} D_h \tilde{\gamma}_i^2 + g\sigma_i \sin\theta_i - U^A Re\{e^{i\theta_i} S_h W_i\}] \end{aligned} \tag{3.10}$$

$$z_i = \alpha_i + Int_h(\sigma e^{i\theta} - < \sigma e^{i\theta} >_h)_i \tag{3.11}$$

$$W_i = \frac{1}{4\pi i} \sum_{\substack{j=-N/2+1 \\ (j-i)\text{odd}}}^{N/2} \tilde{\gamma}_j^p \sigma_j \cot\frac{1}{2}(z_i^p - z_j^p) 2h \tag{3.12}$$

$$U_i^T = Re\{e^{i\theta_i^p} W_i\} \quad ; \quad U_i^N = -Im\{e^{i\theta_i^p} W_i\} \tag{3.13}$$

$$U_i^A = -U_i^T + Int_h(D_h \theta U^N - R < D_h \theta U^N >_h)_i \tag{3.14}$$

where $\tilde{\gamma}_j = \gamma_j / \sigma_j$ approximates the true vortex sheet strength.

The derivative of z with respect to time in the fourth term of equation (3.10) is obtained from (3.11), that is

$$\frac{dz_i}{dt} = Int_h(\frac{d\sigma}{dt} e^{i\theta} + i\sigma e^{i\theta} \frac{d\theta}{dt} - < \frac{d\sigma}{dt} e^{i\theta} + i\sigma e^{i\theta} \frac{d\theta}{dt} >_h)_i \ , \tag{3.15}$$

where $d\sigma/dt$ and $d\theta/dt$ are computed from (3.8) and (3.9).

The quadrature we use to approximate the singular integrals is the alternate-point trapezoidal rule. Sidi and Israeli [58] showed that this quadrature applied to periodic Cauchy kernels such as the kernels considered here, gives spectral accuracy. The altenate-point trapezoidal rule has been used extensively in votex sheet computations [5, 6, 26, 32, 36, 56].

We remark that when $A \neq 0$, equation (3.10) is solved for $d\gamma_i/dt$ by fixed point iteration. Note also that no filtering is applied to $d\gamma_i/dt$ in the sum with the cotangent kernel. As we will show, the filtering comes implicitly from the other terms once we solve for $d\gamma_i/dt$.

We state now a convergence theorem for this numerical method.

THEOREM 3.1. *Assume that for $0 \le t \le T$ there exist a regular solution of the evolution equations of the interface (2.22-2.28) with $\sigma(\cdot,t)$, $\theta(\cdot,t)$ and $\gamma(\cdot,t)$ belonging to $C^{m+3}[-\pi,\pi]$ for $m > 4$ and that $|z(\alpha,t) - z(\beta,t)| \ge C|\alpha - \beta|$ holds for some $C > 0$. If σ_h, θ_h and γ_h denote the numerical solution of (3.8 -3.13), then for $h \le h_0(T)$ we have,*

$$\begin{aligned} \|\sigma_h(t) - \sigma(\cdot,t)\|_{l^2} &\le C(T)h^m \\ \|\theta_h(t) - \theta(\cdot,t)\|_{H_h^{1/2}} &\le C(T)h^m \\ \|\gamma_h(t) - \gamma(\cdot,t)\|_{l^2} &\le C(T)h^m \end{aligned}$$

where

$$\|u\|_{l^2}^2 = \sum_{j=-N/2+1}^{N/2} |u_j|^2 h \ , \tag{3.16}$$

$$\|u\|_{H_h^{1/2}}^2 = 2\pi \sum_{k=-N/2+1}^{N/2} (1 + \rho(kh)|k|)|\hat{u}_k|^2 \ . \tag{3.17}$$

To be consistent with the hypothesis on the regularity of $\sigma(\cdot,t)$, we assume that the parametrization function R is a given $C^{m+3}[-\pi,\pi]$ function of mean one.

The main idea of the proof is to show that there is a balance among the most singular terms of the method. To this end, we obtain evolution equations for the errors between the numerical and the exact solutions. These errors separate into consistency and stability parts. While consistency is almost immediate, the stability issue is difficult. We are guided by the techniques used in [11] for the convergence of a boundary integral method for water waves, and by the the estimates of BHL for the linearized motion of two fluid interfaces in the continuous case [12, 14]. However, our method is based on a different and more general formulation, of which, water waves is a special case.

The use of suitable Fourier filtering is crucial to maintain the desired balance among most singular terms at the discrete level. This requires a careful selection of the places where the filtering is applied. Note for example that W_t is not obtained directly by differentiating W_i.

The parametrization also introduces new difficulties into the analysis. Unless the equal arclength frame is used, in which case σ is constant in space, using γ_i instead of $\tilde{\gamma}_i^p \sigma_i$ in the velocity, introduces a term that would upset the stability balance.

In addition, many nonlinear terms have to be estimated for the general case $A \neq 0$. These terms are controlled by the smallness of the truncation error achieved by the method for sufficiently regular solutions.

3.2. Consistency

We examine next how accurately the exact solution satisfies the discrete system of equations. First note the spectral accuracy of the pseudo-spectral operators (see, e.gr., [61]). If $f(\alpha)$ is a periodic $C^{s+1}[-\pi,\pi]$ function then

$$|S_h f(\alpha_i) - f_\alpha(\alpha_i)| \leq Ch^s \|f\|_{H^{s+1}} , \tag{3.18}$$

$$|D_h f(\alpha_i) - f_\alpha(\alpha_i)| \leq Ch^s \|f\|_{H^{s+1}} , \tag{3.19}$$

and for our Fourier smoothing we have

$$|f^p(\alpha_i) - f(\alpha_i)| \leq Ch^{s+1} \|f\|_{H^{s+1}} . \tag{3.20}$$

It is well known that the trapezoidal rule quadrature, when applied to periodic functions gives spectral accuracy [31], that is,

$$|\sum_{j=-N/2+1}^{N/2} f(\alpha_j)h - \int_{-\pi}^{\pi} f| \leq Ch^{s+1} \|f\|_{H^{s+1}} . \tag{3.21}$$

Similarly for the pseudo spectral integral operator we have,

$$|Int_h(g(\cdot))_i - \int_0^{\alpha_i} g(\alpha)d\alpha| \leq Ch^{s+1} \|g\|_{H^s} , \tag{3.22}$$

for zero-mean and periodic $g(\alpha) \in C^s[-\pi,\pi]$.

Thus, from these observations and from the assumption on the regularity of the exact solution it follows that

$$\begin{aligned} z_h(\alpha_i) \equiv \alpha_i + Int_h(\sigma(\cdot)e^{i\theta(\cdot)} - < \sigma e^{i\theta} >_h)_i = \\ \alpha_i + \int_0^{\alpha_i} (\sigma e^{i\theta} - 1)d\alpha + O(h^{m+3}) = z(\alpha_i) + O(h^{m+3}) , \end{aligned} \tag{3.23}$$

where we have also used that $< z_\alpha >= 1$.

We denote by $W_h(\alpha_i)$, $U_h^T(\alpha_i)$, $U_h^N(\alpha_i)$, and $U_h^N(\alpha_i)$ the velocities obtained by substituting the exact solution $\sigma(\cdot,t)$, $\theta(\cdot,t)$ and $\gamma(\cdot,t)$ into the discrete equations (3.12 - 3.14) to distinguish them from the corresponding exact velocities.

We now examine the accuracy of the approximation for the velocity. Note that

$$\tilde{\gamma}^p(\alpha_j) = \tilde{\gamma}(\alpha_j) + O(h^{m+3}) = \frac{\gamma(\alpha_j)}{\sigma(\alpha_j)} + O(h^{m+3}) \ . \tag{3.24}$$

Thus, using the spectral accuracy of the smoothing and (3.23) we get

$$\tilde{\gamma}^p(\alpha_j)\sigma(\alpha_j)\cot\frac{1}{2}(z_h^p(\alpha_i) - z_h^p(\alpha_j)) = \gamma(\alpha_j)\cot\frac{1}{2}(z(\alpha_i) - z(\alpha_j)) + O(h^{m+3}) \ . \tag{3.25}$$

Hence, we only need to check the accuracy of the alternate-point trapezoidal quadrature rule used to approximate the velocity integral W [11]. To this end, we make a change of variables and use the periodicity of the integrand to obtain,

$$\begin{aligned}\int_{-\pi}^{\pi} \gamma(\alpha')\cot\frac{1}{2}(z(\alpha) - z(\alpha'))d\alpha' &= \int_{-\pi}^{\pi} \gamma(\alpha+\beta)\cot\frac{1}{2}(z(\alpha) - z(\alpha+\beta))d\beta \\ &= \int_{-\pi}^{\pi} [\gamma(\alpha+\beta)\cot\frac{1}{2}(z(\alpha) - z(\alpha+\beta)) + \frac{\gamma(\alpha)}{z_\alpha(\alpha)}\cot\frac{1}{2}\beta]d\beta \ ,\end{aligned}$$

where we have used that $\cot\frac{1}{2}\beta$ is an odd function and thus, its principal value integral is zero. Let us define

$$F(\alpha,\beta) \equiv \gamma(\alpha+\beta)\cot\frac{1}{2}(z(\alpha) - z(\alpha+\beta)) + \frac{\gamma(\alpha)}{z_\alpha(\alpha)}\cot\frac{1}{2}\beta \ . \tag{3.26}$$

$F(\alpha,\beta)$ has a removable singularity at $\beta = 0$. More precisely

$$\lim_{\beta\to 0} F(\alpha,\beta) = \frac{\gamma(\alpha)z_{\alpha\alpha}}{z_\alpha^2(\alpha)} - \frac{2\gamma_\alpha(\alpha)}{z_\alpha(\alpha)} \tag{3.27}$$

and since $\gamma(\cdot,t)$, $z_\alpha(\cdot) \in C^{m+3}[-\pi,\pi]$, it follows that $F(\alpha,\cdot) \in C^{m+2}[-\pi,\pi]$, which incidentally shows that the exact velocities $W(\alpha)$, $U^T(\alpha)$ and $U^N(\alpha)$ are in $C^{m+2}[-\pi,\pi]$. Let us denote

$$J_h(\alpha_i) \equiv \sum_{j=-N/2+1}^{N/2} F(\alpha_i,\beta_j)h - \int_{-\pi}^{\pi} F(\alpha_i,\beta)d\beta \quad ; \quad \beta_j = jh \ . \tag{3.28}$$

Then in view of (3.21) and the smoothness of F we have that

$$|J_h(\alpha_i)| \le Ch^{m+2}\|D_\beta^{m+2}F(\alpha_i,\cdot)\|_{L^2} \ . \tag{3.29}$$

Moreover, Richardson extrapolation gives us the alternate-point trapezoidal rule:

$$\begin{aligned}2J_h(\alpha_i) - J_{2h}(\alpha_i) &= \\ &2\sum_{j=-N/2+1}^{N/2} F(\alpha_i,\beta_j)h - \sum_{j=-N/4+1}^{N/4} F(\alpha_i,\beta_{2j})2h - \int_{-\pi}^{\pi} F(\alpha_i,\beta)d\beta \\ = &\sum_{\substack{j=-N/2+1 \\ (j-i)\text{odd}}}^{N/2} F(\alpha_i,\beta_j)2h - \int_{-\pi}^{\pi} F(\alpha_i,\beta)d\beta \ ,\end{aligned} \tag{3.30}$$

which implies that

$$\sum_{\substack{j=-N/2+1\\(j-i)\text{odd}}}^{N/2} F(\alpha_i,\beta_j)2h - \int_{-\pi}^{\pi} F(\alpha_i,\beta)d\beta = O(h^{m+2}) \ . \tag{3.31}$$

Thus, substituting (3.26) into (3.31) we obtain

$$\begin{aligned}\sum_{\substack{j=-N/2+1\\(j-i)\text{odd}}}^{N/2} \gamma(\alpha_i+\beta_j)\cot\frac{1}{2}(z(\alpha_i)-z(\alpha_i+\beta_j))2h \\ - \quad \fint_{-\pi}^{\pi} \gamma(\alpha_i+\beta)\cot\frac{1}{2}(z(\alpha_i)-z(\alpha_i+\beta))d\beta = O(h^{m+2}) \ ,\end{aligned} \tag{3.32}$$

where we have used that $\cot\frac{1}{2}\beta$ is an odd function of β and N is even. Changing variables again and using (3.25) we find

$$\begin{aligned}\sum_{\substack{j=-N/2+1\\(j-i)\text{odd}}}^{N/2} \tilde{\gamma}^p(\alpha_j)\sigma(\alpha_j)\cot\frac{1}{2}(z^p(\alpha_i)-z^p(\alpha_j))2h \\ - \quad \int_{-\pi}^{\pi} \gamma(\alpha')\cot\frac{1}{2}(z(\alpha_i)-z(\alpha'))d\alpha' = O(h^{m+2}) \ ,\end{aligned} \tag{3.33}$$

which shows the spectral accuracy of the approximation for the velocity, that is

$$W_h(\alpha_i) = W(\alpha_i) + O(h^{m+2}) \ . \tag{3.34}$$

Note that since $\theta^p(\alpha_i) = \theta(\alpha_i) + O(h^{m+3})$, it follows that

$$U_h^N(\alpha_i) \quad = \quad U^N(\alpha_i) + O(h^{m+2}) \ , \tag{3.35}$$

$$U_h^T(\alpha_i) \quad = \quad U^T(\alpha_i) + O(h^{m+2}) \ , \tag{3.36}$$

and using (3.19-3.22) we also have

$$U_h^A(\alpha_i) = U^A(\alpha_i) + O(h^{m+2}) \ . \tag{3.37}$$

It is now easy to check the consistency for the σ-equation (3.8) because

$$\begin{aligned}< S_h\theta(\cdot)U_h^N(\cdot) >_h \quad &= \quad < \theta_\alpha(\cdot)U^N(\cdot) >_h + O(h^{m+2}) \\ &= \quad < \theta_\alpha(\cdot)U^N(\cdot) > + O(h^{m+2})\end{aligned} \tag{3.38}$$

and consequently

$$\frac{d\sigma}{dt}(\alpha_i) = -R(\alpha_i) < S_h\theta(\cdot)U_h^N(\cdot) >_h + O(h^{m+2}) \ . \tag{3.39}$$

Analogously, for the θ-equation (3.9) we obtain

$$\frac{d\theta}{dt}(\alpha_i) = \frac{1}{\sigma(\alpha_i)}[S_h U_h^N(\alpha_i) + D_h\theta(\alpha_i)(U^T(\alpha_i) + U^A(\alpha_i))] + O(h^{m+1}) \ . \tag{3.40}$$

Now from (3.15), using (3.21) and (3.22) it follows that

$$\frac{dz_h}{dt}(\alpha_i) = \frac{dz}{dt}(\alpha_i) + O(h^{m+2}) \ . \tag{3.41}$$

Note also that we may write

$$\begin{aligned} &\sum_{\substack{j=-N/2+1 \\ (j-i)\text{odd}}}^{N/2} \gamma(\alpha_j)^p \frac{\frac{dz_h}{dt}(\alpha_i) - \frac{dz_h}{dt}(\alpha_j)}{\sin^2\frac{1}{2}(z_h^p(\alpha_i) - z_h^p(\alpha_j))} 2h \\ &\quad = \sum_{\substack{j=-N/2+1 \\ (j-i)\text{odd}}}^{N/2} G(\alpha_i,\alpha_j)\cot\frac{1}{2}(z(\alpha_i) - z(\alpha_j))2h + O(h^{m+2}) \ , \end{aligned} \tag{3.42}$$

where

$$G(\alpha_i,\alpha_j) \equiv 2\gamma(\alpha_j)\frac{\frac{dz}{dt}(\alpha_i) - \frac{dz}{dt}(\alpha_j)}{\sin(z(\alpha_i) - z(\alpha_j))} \ . \tag{3.43}$$

Hence $G(\cdot,\cdot) \in C^{m+1}[-\pi,\pi]$ (it has a removable singularity) and, as a result, the alternate point trapezoidal rule yields an $O(h^m)$ approximation for this integral. On the other hand, in view of (3.19) we also have

$$D_h\left(\frac{1}{\sigma(\alpha_i)}D_h\theta(\alpha_i)\right) = \left(\frac{1}{\sigma(\alpha_i)}\theta_\alpha(\alpha_i)\right)_\alpha + O(h^m) \tag{3.44}$$

and similarly for the other terms of the γ-equation (3.10). The next lemma summarizes the accuracy of the numerical method.

Consistency Lemma. *The exact solution of the interface equations (2.22-2.28) satisfies the discrete evolution system (3.8-3.10) with truncation error of order $O(h^{m+2})$ for equation (3.8), of order $O(h^{m+1})$ for equation (3.9), and of order $O(h^m)$ for equation (3.10).*

3.3. Stability

Let us define the errors or variations between exact and numerical solutions as,

$$\dot{\sigma_j} \equiv \sigma_j - \sigma(\alpha_j) \ , \tag{3.45}$$

$$\dot{\theta_j} \equiv \theta_j - \theta(\alpha_j) \ , \tag{3.46}$$

$$\dot{\gamma_j} \equiv \gamma_j - \gamma(\alpha_j) \ . \tag{3.47}$$

Our goal is to obtain a system of evolution equations for the errors and perform energy estimates on this system to show that these errors remain bounded in suitable discrete norms for $t \leq T$. Because this task is long and technical we divide it into three parts. First, we obtain estimates for the errors in the approximations to the velocities. Then, we use these estimates to obtain evolution equations for $\dot{\sigma}$, $\dot{\theta}$ and $\dot{\tilde{\gamma}}$, identifying the most singular terms of the method. Finally, we complete the proof by showing, through energy estimates, that these terms balance one another, and that the errors are bounded in the appropriate discrete norms.

Before we proceed, let us introduce some notation that will be used extensively in the analysis that follows. We define a discrete s-th order smoothing operator, written generically A_{-s}, as an operator satisfying

$$\|D_h^l(A_{-s}(\dot{\phi}))\|_{l^2} \leq C\|\dot{\phi}\|_{l^2} \tag{3.48}$$

and

$$\|A_{-s}(S_h^l\dot{\phi})\|_{l^2} \leq C\|\dot{\phi}\|_{l^2} \quad \text{for } 0 \leq l \leq s \ . \tag{3.49}$$

Note in particular that $A_0(\dot{\phi_i})$ is a l^2-bounded operator, that is

$$\|A_0(\dot{\phi})\|_{l^2} \leq C\|\dot{\phi}\|_{l^2} \ . \tag{3.50}$$

Moreover, it is easy to see that $h^s A_0(\dot{\phi_i}) = A_{-s}(\dot{\phi_i})$. To simplify notation we also write

$$A_{-s}(\dot{\phi_i}, \dot{\psi_i}, \ldots, \dot{\eta_i}) \equiv A_{-s}(\dot{\phi_i}) + A_{-s}(\dot{\psi_i}) + \cdots + A_{-s}(\dot{\eta_i}) \ .$$

3.3.1. Estimates for the Variations of the Velocities

To obtain evolution equations for the errors, we need to estimate the variation of the velocities. As noted by BHL [11], it is easier to work with the kernels defined on the entire

line rather than in $[-\pi,\pi]$. The extension can be accomplished by noting that [44]

$$\frac{1}{2}\cot\frac{1}{2}z=\frac{1}{z}+\sum_{k=1}^{\infty}\frac{2z}{z^2-(2k\pi)^2}\ , \tag{3.51}$$

which converges uniformly in any compact set not containing the points $z=2k\pi$, with k integer. Thus for any 2π-periodic function f we have,

$$\begin{aligned}\frac{1}{2}\sum_{\substack{j=-N/2+1\\(j-i)\text{odd}}}^{N/2} f(\alpha_j)\cot\frac{1}{2}(z(\alpha_i)-z(\alpha_j))2h=\\ \sum_{\substack{j=-N/2+1\\(j-i)\text{odd}}}^{N/2}\frac{f(\alpha_j)}{z(\alpha_i)-z(\alpha_j)}2h+\sum_{k=1}^{\infty}\sum_{\substack{j=-N/2+1\\(j-i)\text{odd}}}^{N/2}\frac{2f(\alpha_j)(z(\alpha_i)-z(\alpha_j))}{(z(\alpha_i)-z(\alpha_j))^2-(2k\pi)^2}2h\ ,\end{aligned} \tag{3.52}$$

but $z(\alpha,t)=\alpha+s(\alpha,t)$ and $s(\cdot,t)$ is 2π-periodic. Hence

$$\begin{aligned}&\sum_{k=1}^{M}\sum_{\substack{j=-N/2+1\\(j-i)\text{odd}}}^{N/2}\frac{2f(\alpha_j)(z(\alpha_i)-z(\alpha_j))}{(z(\alpha_i)-z(\alpha_j))^2-(2k\pi)^2}2h=\\ &\sum_{k=1}^{M}\sum_{\substack{j=-N/2+1\\(j-i)\text{odd}}}^{N/2}[\frac{f(\alpha_j)}{z(\alpha_i)-z(\alpha_j)-2k\pi}+\frac{f(\alpha_j)}{z(\alpha_i)-z(\alpha_j)+2k\pi}]2h=\\ &\sum_{k=1}^{M}\sum_{\substack{j=-N/2+1\\(j-i)\text{odd}}}^{N/2}[\frac{f(\alpha_j)}{z(\alpha_i)-(\alpha_j+2k\pi+s(\alpha_j))}+\frac{f(\alpha_j)}{z(\alpha_i)-(\alpha_j-2k\pi+s(\alpha_j))}]2h\ .\end{aligned}$$

If we define $\alpha_{j+kN}\equiv\alpha_j+2k\pi$ and extend the functions periodically, we obtain

$$\begin{aligned}\sum_{k=1}^{M}\sum_{\substack{j=-N/2+1\\(j-i)\text{odd}}}^{N/2}\frac{2f(\alpha_j)(z(\alpha_i)-z(\alpha_j))}{(z(\alpha_i)-z(\alpha_j))^2-(2k\pi)^2}2h=\\ \sum_{\substack{j=-N/2+1\\(j-i)\text{odd}}}^{N(M+1/2)}\frac{f(\alpha_j)}{z(\alpha_i)-z(\alpha_j)}2h+\sum_{\substack{j=-N(M+1/2)\\(j-i)\text{odd}}}^{-N/2}\frac{f(\alpha_j)}{z(\alpha_i)-z(\alpha_j)}2h\ .\end{aligned} \tag{3.53}$$

We combine now (3.52) and (3.53) into a single expression to get

$$\frac{1}{2}\sum_{\substack{j=-N/2+1\\(j-i)\text{odd}}}^{N/2} f(\alpha_j)\cot\frac{1}{2}(z(\alpha_i)-z(\alpha_j))2h=\lim_{M\to\infty}\sum_{\substack{j=-N(M+1/2)+1\\(j-i)\text{odd}}}^{N(M+1/2)}\frac{f(\alpha_j)}{z(\alpha_i)-z(\alpha_j)}2h\ .$$

To simplify the notation, we define

$$\sum_{(j-i)\text{odd}} \frac{f(\alpha_j)}{z(\alpha_i)-z(\alpha_j)}2h \equiv \lim_{M\to\infty} \sum_{\substack{j=-N(M+1/2)+1 \\ (j-i)\text{odd}}}^{N(M+1/2)} \frac{f(\alpha_j)}{z(\alpha_i)-z(\alpha_j)}2h \ . \tag{3.54}$$

Analogously, the numerical solution can be extended periodically. We have

$$\sum_{\substack{j=-N/2+1 \\ (j-i)\text{odd}}}^{N/2} f_j \cot\frac{1}{2}(z_i-z_j)2h = \sum_{(j-i)\text{odd}} \frac{f_j}{z_i-z_j}2h \ . \tag{3.55}$$

Similarly for the term in (3.10) involving the kernel $1/\sin^2 z$, we find

$$\sum_{\substack{j=-N/2+1 \\ (j-i)\text{odd}}}^{N/2} \gamma_j^p \frac{\frac{dz_i}{dt}-\frac{dz_j}{dt}}{\sin^2\frac{1}{2}(z_i^p-z_j^p)}2h = \sum_{(j-i)\text{odd}} \gamma_j^p \frac{\frac{dz_i}{dt}-\frac{dz_j}{dt}}{(z_i^p-z_j^p)^2}2h \ . \tag{3.56}$$

Let us consider now the variation of the velocity $\dot{W}_i \equiv W_i - W_h(\alpha_i)$, where

$$W_h(\alpha_i) \equiv \frac{1}{2\pi i} \sum_{(j-i)\ \text{odd}} \frac{\sigma(\alpha_j)\tilde{\gamma}^p(\alpha_j)}{z_h^p(\alpha_i)-z_h^p(\alpha_j)}2h \tag{3.57}$$

and $z_h(\alpha_i)$ is given by (3.23). We can write $\dot{W}$ as a sum of linear and nonlinear terms in the errors $\dot{\sigma}$, $\dot{\tilde{\gamma}}$, and $\dot{z}$ as follows

$$\begin{aligned} \dot{W}_i &= \frac{1}{2\pi i} \sum_{(j-i)\ \text{odd}} \frac{\sigma(\alpha_j)\dot{\tilde{\gamma}}_j^p}{z_h^p(\alpha_i)-z_h^p(\alpha_j)}2h + \frac{1}{2\pi i} \sum_{(j-i)\ \text{odd}} \frac{\dot{\sigma}_j\tilde{\gamma}^p(\alpha_j)}{z_h^p(\alpha_i)-z_h^p(\alpha_j)}2h \\ &- \frac{1}{2\pi i} \sum_{(j-i)\ \text{odd}} \sigma(\alpha_j)\tilde{\gamma}^p(\alpha_j)\frac{\dot{z}_i^p-\dot{z}_j^p}{(z_h^p(\alpha_i)-z_h^p(\alpha_j))^2}2h + \dot{W}_i^{NL} \ , \end{aligned} \tag{3.58}$$

where $\dot{W}_i^{NL}$ stands for the nonlinear part given by

$$\begin{aligned} \dot{W}_i^{NL} &= \frac{1}{2\pi i} \sum_{(j-i)\ \text{odd}} \frac{\dot{\sigma}_j\dot{\tilde{\gamma}}_j^p}{z_h^p(\alpha_i)-z_h^p(\alpha_j)}2h + \frac{1}{2\pi i} \sum_{(j-i)\ \text{odd}} \frac{(\sigma\dot{\tilde{\gamma}}^p)_j(\dot{z}_i^p-\dot{z}_j^p)}{(z_h^p(\alpha_i)-z_h^p(\alpha_j))^2}2h \\ &- \frac{1}{2\pi i} \sum_{(j-i)\ \text{odd}} \frac{\sigma_j\tilde{\gamma}_j^p(\dot{z}_i^p-\dot{z}_j^p)^2 2h}{(z_h^p(\alpha_i)-z_h^p(\alpha_j))^2(z_h^p(\alpha_i)-z_h^p(\alpha_j)+\dot{z}_i^p-\dot{z}_j^p)} \ . \end{aligned} \tag{3.59}$$

Our immediate task now is to estimate $\dot{z}$ in terms of $\dot{\sigma}$ and $\dot{\theta}$ and to establish a bound for the nonlinear terms. To this end, let us define

$$T^* \equiv \text{Sup}\{t | t \le T,\ \|\dot{\sigma}\|_{l^2},\ \|\dot{\theta}\|_{l^2},\ \|\dot{\gamma}\|_{l^2} \le h^{7/2} \ \text{ and } \ \|\frac{d\dot{\gamma}}{dt}\|_{l^2} \le h^{3/2}\} \ . \tag{3.60}$$

Unless otherwise noted, *all the estimates we obtain hereafter are valid for* $t \le T^*$. At the end, we close this so called T^*-argument, by showing that $T^* = T$.

Note that since

$$h|\dot\theta_i|^2 \le \sum_{i=-N/2+1}^{N/2} |\dot\theta_i|^2 h = \|\dot\theta\|_{l^2} \ , \tag{3.61}$$

we have that $\|\dot\theta\|_\infty \le h^{-1/2}\|\dot\theta\|_{l^2} \le h^3$, and similarly for $\dot\sigma$ and $\dot\gamma$. Thus

$$\|\dot\sigma\|_\infty \le h^3, \quad \|\dot\theta\|_\infty \le h^3 \quad \text{and} \quad \|\dot{\dot\gamma}\|_\infty \le h^3 \ . \tag{3.62}$$

On the other hand, the variation $\dot z_i \equiv z_i - z_h(\alpha_i)$ is given by

$$\dot z_i = Int_h[(\sigma e^{i\theta})\dot{}_i - < (\sigma e^{i\theta})\dot{}_i >_h] \ , \tag{3.63}$$

where

$$(\sigma e^{i\theta})\dot{}_i \equiv \sigma_i e^{i\theta_i} - \sigma(\alpha_i)e^{i\theta(\alpha_i)} = \dot\sigma_i e^{i\theta(\alpha_i)} + \sigma_i(e^{i\theta_i} - e^{i\theta(\alpha_i)}) \ ,$$

but

$$e^{i\theta_i} - e^{i\theta(\alpha_i)} = e^{i(\theta(\alpha_i)+\dot\theta_i)} - e^{i\theta(\alpha_i)} = ie^{i\theta(\alpha_i)}\dot\theta_i + r(\alpha_i)\dot\theta_i^2$$

with $\|r\|_\infty \le 1/2$. Thus, noting that $\|\dot\theta^2\|_{l^2} \le Ch^3\|\dot\theta\|_{l^2}$, we get

$$e^{i\theta_i} - e^{i\theta(\alpha_i)} = ie^{i\theta(\alpha_i)}\dot\theta_i + A_{-3}(\dot\theta_i) \ . \tag{3.64}$$

Therefore using (3.62) and (3.64), we conclude that

$$(\sigma e^{i\theta})\dot{}_i = i\sigma(\alpha_i)e^{i\theta(\alpha_i)}\dot\theta_i + \dot\sigma_i e^{i\theta(\alpha_i)} + A_{-3}(\dot\theta_i) \ . \tag{3.65}$$

Now clearly, $< f(\cdot)\dot\phi >_h = A_{-s}(\dot\phi)$ for $f \in C^s$. Therefore substituting (3.65) into (3.63) we obtain

$$\dot z_i = Int_h(i\sigma(\cdot)e^{i\theta(\cdot)}\dot\theta)_i + Int_h(e^{i\theta(\cdot)}\dot\sigma)_i + A_{-3}(\dot\sigma_i, \dot\theta_i) \tag{3.66}$$

Recall that the frame is selected such that the initial parametrization is preserved up to a time dependent scaling. Thus

$$\dot\sigma_i = R(\alpha_i)[< \sigma >_h - < \sigma(\cdot) >] = R(\alpha_i) < \dot\sigma >_h + O(h^{m+3}) \ , \tag{3.67}$$

where we have also used (3.21). The relation (3.67) tells us that terms involving $\dot\sigma$ are of lower order. In particular

$$\begin{aligned} Int_h(f(\cdot)\dot\sigma)_i &= < \dot\sigma >_h Int_h(R(\cdot)f(\cdot))_i + O(h^{m+3}) \\ &= \tilde f(\alpha_i) < \dot\sigma >_h + O(h^{m+3}) = A_{-s}(\dot\sigma_i) + O(h^{m+3}) \ , \end{aligned} \tag{3.68}$$

because both the parametrization function R and f are smooth. Similarly we have

$$D_h(f(\alpha_i)\dot{\sigma}_i) = g(\alpha_i) < \dot{\sigma} >_h + O(h^{m+2}) = A_{-s}(\dot{\sigma}_i) + O(h^{m+2}) \tag{3.69}$$

and the same is true for S_h instead of D_h. With these two observations and noting that $z_\alpha(\alpha) = \sigma(\alpha)e^{i\theta(\alpha)}$, we can rewrite equation (3.66) as

$$\dot{z}_i = iInt_h(z_\alpha(\cdot)\dot{\theta})_i + A_{-3}(\dot{\sigma}_i, \dot{\theta}_i) + O(h^{m+3}) \ , \tag{3.70}$$

from which we obtain the following estimates

$$\|\dot{z}\|_{l^2} \leq Ch^{7/2} \quad \text{and} \quad \|\dot{z}\|_\infty \leq Ch^3 \ . \tag{3.71}$$

Note that also that sharper estimates hold, because

$$\|D_h\dot{z}\|_{l^2} \leq Ch^{7/2} \quad \text{and} \quad \|D_h\dot{z}\|_\infty \leq Ch^3 \ , \tag{3.72}$$

and similarly for S_h.

We need now to identify the most singular terms in $\dot{W}$. Let us define a discrete Hilbert Transform as follows:

$$H_h f_i \equiv \frac{1}{\pi} \sum_{(j-i) \text{ odd}} \frac{f_j}{\alpha_i - \alpha_j} 2h \ . \tag{3.73}$$

H_h satisfies properties analogous to the usual Hilbert transform at the continuous level. We summarize some of these properties in the following lemma shown by BHL [11].

LEMMA 3.1. *Let f be such that $\hat{f}_0 = \hat{f}_{N/2} = 0$, then*

$$\begin{aligned}
&(i) \quad (\widehat{H_h f})_k = -isgn(k)\hat{f}_k \ . \\
&(ii) \quad H_h(H_h f_i) = -f_i \, . \\
&(iii) \quad H_h(S_h f_i) = \frac{1}{\pi} \sum_{(j-i) \ odd} \frac{f_i - f_j}{(\alpha_i - \alpha_j)^2} 2h \ . \\
&(iv) \quad S_h(H_h f_i) = H_h(S_h f_i) \ .
\end{aligned}$$

The proof of this and all other technical lemmas we use in this chapter are given in the Appendix.

Now let us return to our expression (3.58) for $\dot{W}$. First, we rewrite the kernel:

$$\frac{1}{z(\alpha) - z(\beta)} = \frac{1}{z_\alpha(\alpha)(\alpha - \beta)} + g(\alpha, \beta) \tag{3.74}$$

where $g(\cdot,\cdot)$ is a smooth function in both variables. Also

$$\frac{\gamma(\beta)}{(z(\alpha)-z(\beta))^2} = \frac{\gamma(\alpha)}{z_\alpha^2(\alpha)(\alpha-\beta)^2} + \frac{p(\alpha)}{\alpha-\beta} + q(\alpha,\beta) \tag{3.75}$$

where $q(\cdot,\cdot)$ is again smooth in both variables, and

$$p(\alpha) = \frac{\gamma_\alpha(\alpha) z_\alpha(\alpha) + \gamma(\alpha) z_{\alpha\alpha}(\alpha)}{z_\alpha^3(\alpha)} \ . \tag{3.76}$$

On the other hand, using consistency, we have that

$$\frac{1}{z_h^p(\alpha_i) - z_h^p(\alpha_j)} = (1 + O(h^{m+3}))\frac{1}{z(\alpha_i) - z(\alpha_j)} \ ,$$

and

$$\frac{\sigma(\alpha_j)\tilde{\gamma}^p(\alpha_j)}{(z^p(\alpha_i) - z^p(\alpha_j))^2} = (1 + O(h^{m+2}))\frac{\gamma(\alpha_j)}{(z(\alpha_i) - z(\alpha_j))^2} \ . \tag{3.77}$$

Thus, for the first term in (3.58), we obtain

$$\begin{aligned} \frac{1}{2\pi i} \sum_{(j-i) \text{ odd}} \frac{\sigma(\alpha_j)\dot{\tilde{\gamma}}_j^p}{z_h^p(\alpha_i) - z_h^p(\alpha_j)} 2h = \\ \Big(1 + O(h^{m+3})\Big) \left(\frac{1}{2iz_\alpha} H_h(\sigma\dot{\tilde{\gamma}}_i^p) + \sum_{(j-i) \text{ odd}} \tilde{g}(\alpha_i,\alpha_j)\dot{\tilde{\gamma}}_j^p 2h \right) \ . \end{aligned} \tag{3.78}$$

The term involving $\tilde{g}$ is a discrete operator which deserves special care. Let us denote a general operator of this type by

$$R_h(\phi_i) = \sum_{(j-i) \text{ odd}} g(\alpha_i,\alpha_j)\phi_j 2h \tag{3.79}$$

for $g(\cdot,\cdot) \in C^s$. Clearly the continuous analogue of R_h, is a smoothing operator. However, this is not true at the discrete level, where $R_h(\phi_i)$ can be as singular as ϕ_i, [15, 34]. We overcome this difficulty with the application of Fourier filtering. Using the properties of the cutoff function ρ which defines the filtering we obtain the following result [11]

LEMMA 3.2. *Let $g(\cdot,\cdot)$ in (3.79) be C^s with $s > 3$ then*

$$R_h(\phi_i^p) = A_{-2}(\phi_i) \ . \tag{3.80}$$

This lemma explains the use of filtering on $\tilde{\gamma}$ when computing W. The analysis below will also make evident the reason for performing the smoothing on $\tilde{\gamma} = \gamma/\sigma$ instead of γ.

Note also that the commutator of the discrete Hilbert transform and a smooth function is an R_h operator, that is

$$H_h(f(\alpha_i)\phi_i) - f(\alpha_i)H_h(\phi_i) = R_h(\phi_i) \ . \tag{3.81}$$

Therefore, we can pull the smooth function $\sigma(\alpha)$ outside H_h in (3.78), at the expense of adding a term $R_h(\dot{\gamma}_i^p) = A_{-2}(\dot{\tilde{\gamma}}_i)$. Consequently

$$\frac{1}{2\pi i} \sum_{(j-i) \text{ odd}} \frac{\sigma(\alpha_j)\dot{\tilde{\gamma}}_j^p}{z_h^p(\alpha_i) - z_h^p(\alpha_j)} 2h = \frac{\sigma(\alpha_i)}{2iz_\alpha(\alpha)} H_h \dot{\gamma}_i^p + A_{-2}(\dot{\tilde{\gamma}}_i) \ . \tag{3.82}$$

This expression exhibits clearly the leading order contribution of $\dot{\tilde{\gamma}}$ in the variation of the velocity $\dot{W}$.

The second term in (3.58), involves $\dot{\sigma}$. Then, in view of (3.67)

$$\frac{1}{2\pi i} \sum_{(j-i) \text{ odd}} \frac{\dot{\sigma}_j \tilde{\gamma}^p(\alpha_j)}{z_h^p(\alpha_i) - z_h^p(\alpha_j)} 2h = A_{-s}(\dot{\sigma}_i) + O(h^{m+3}) \ . \tag{3.83}$$

To estimate the third term in (3.58), we take into account (3.75) and (3.77) to get

$$\begin{aligned} \frac{1}{2\pi i} \sum_{(j-i) \text{ odd}} \sigma(\alpha_j)\tilde{\gamma}^p(\alpha_j) \frac{\dot{z}_i^p - \dot{z}_j^p}{(z_h^p(\alpha_i) - z_h^p(\alpha_j))^2} 2h = \\ -\frac{\gamma(\alpha_i)}{2iz_\alpha^2(\alpha_i)} H_h D_h \dot{z}_i + f(\alpha_i) H_h \dot{z}_i^p + g(\alpha_i)\dot{z}_i^p + A_{-2}(\dot{z}_i) \ , \end{aligned} \tag{3.84}$$

where we have also used Lemmas 3.1 and 3.2. We substitute our estimate (3.70) for $\dot{z}$ into the last expression to obtain

$$-\frac{\gamma(\alpha_i)}{2iz_\alpha^2(\alpha_i)} H_h D_h \dot{z}_i = -\frac{\gamma(\alpha_i)}{2z_\alpha^2(\alpha_i)} H_h (z_\alpha \dot{\theta})_i^p + A_{-2}(\dot{\sigma}_i, \dot{\theta}_i) + O(h^{m+2}) \ . \tag{3.85}$$

Let us define the commutator of the filtering by

$$G_h^p(\phi_i) \equiv (f(\alpha_i)\phi_i)^p - f(\alpha_i)\phi_i^p \tag{3.86}$$

for smooth functions $f(\cdot)$. In order to extract the most singular part of (3.85), we write $(z_\alpha \dot{\theta})_i^p = z_\alpha(\alpha_i)\dot{\theta}_i^p + G_h^p \dot{\theta}_i$ and apply Lemma 3.2. Equation (3.85) becomes

$$\begin{aligned} -\frac{\gamma(\alpha_i)}{2iz_\alpha^2(\alpha_i)} H_h D_h \dot{z}_i &= -\frac{\gamma(\alpha_i)}{2z_\alpha(\alpha_i)} H_h \dot{\theta}_i^p - \frac{\gamma(\alpha_i)}{2z_\alpha^2(\alpha_i)} H_h G_h^p \dot{\theta}_i \\ &+ A_{-2}(\dot{\sigma}_i, \dot{\theta}_i) + O(h^{m+2}) \ . \end{aligned} \tag{3.87}$$

The term $G_h^p\dot{\theta}_i$ is not smooth enough to be included in $A_{-2}(\dot{\sigma}_i, \dot{\theta}_i)$. More precisely, we have

LEMMA 3.3.

$$G_h^p(\phi_i) = hA_0(\phi_i) \ . \tag{3.88}$$

The specific form of the operator G_h^p will become important in the energy estimates involving the evolution equation for $\dot{\theta}$.

To complete the estimates for $\dot{W}$, we need to take care of its nonlinear part. This is the content of the following lemma.

LEMMA 3.4. *For $t \leq T^*$ the nonlinear part of $\dot{W}$ is of the form*

$$\dot{W}_i^{NL} = A_{-2}(\dot{\sigma}_i, \dot{\theta}_i, \dot{\tilde{\gamma}}_i) \ . \tag{3.89}$$

We collect now all the estimates for $\dot{W}_i$. Combining (3.82), (3.83), (3.84) , (3.87), and (3.89) we obtain

$$\begin{aligned} \dot{W}_i &= \frac{\sigma(\alpha_i)}{2iz_\alpha(\alpha)} H_h(\dot{\tilde{\gamma}}_i^p) - \frac{\gamma(\alpha_i)}{2z_\alpha(\alpha_i)} H_h\dot{\theta}_i^p + f(\alpha_i)H_hG_h^p\dot{\theta}_i + E(\dot{\theta}_i) \\ &+ A_{-2}(\dot{\sigma}_i, \dot{\theta}_i, \dot{\tilde{\gamma}}_i) + O(h^{m+2}) \ , \end{aligned} \tag{3.90}$$

where we have defined

$$E(\dot{\theta}_i) \equiv f(\alpha_i)Int_h(z_\alpha\dot{\theta})_i^p + g(\alpha_i)H_hInt_h(z_\alpha\dot{\theta})_i^p \ . \tag{3.91}$$

Hereafter, by $E(\dot{\theta})$ we mean an operator of the form given by (3.91) or the real (imaginary) part of it. Again, the structure of the operator E will be important in the energy estimates.

We can proceed now to estimate the variations of tangential and normal velocities U^T and U^N. We have that

$$\begin{aligned} \dot{U}_i^T &\equiv Re\{e^{i\theta_i^p}W_i - e^{i\theta^p(\alpha_i)}W_h(\alpha_i)\} \\ &= Re\{e^{i\theta^p(\alpha_i)}\dot{W}_i + W_h(\alpha_i)(e^{i\theta^p})_i^{\cdot} + \dot{W}_i(e^{i\theta^p})_i^{\cdot}\} \ , \end{aligned} \tag{3.92}$$

where $(e^{i\theta^p})_i^{\cdot} \equiv e^{i\theta_i^p} - e^{i\theta^p(\alpha_i)}$ and W_h as defined in (3.57). It is clear that (3.64) remains valid also for θ^p. Therefore

$$(e^{i\theta^p})_i^{\cdot} = ie^{i\theta(\alpha_i)}\dot{\theta}_i^p + A_{-3}(\dot{\theta}_i) \ . \tag{3.93}$$

Moreover, using our estimate (3.90), we can obtain the following bound for $\dot{W}$,

$$\|\dot{W}\|_{l^2} \leq C(\|\dot{\sigma}\|_{l^2} + \|\dot{\theta}\|_{l^2} + \|\dot{\gamma}\|_{l^2}) \ .$$

Thus, $\|\dot{W}\|_\infty \leq Ch^3$, and as a result

$$\|\dot{W}(e^{i\theta^p})^{\cdot}\|_{l_2} \leq C\|\dot{W}\|_\infty \|(e^{i\theta^p})^{\cdot}\|_{l_2} \leq Ch^3\|(e^{i\theta^p})^{\cdot}\|_{l_2} \ .$$

From (3.64), we conclude that

$$\dot{W}_i(e^{i\theta^p})_i^{\cdot} = A_{-3}(\dot{\theta}_i) \ . \tag{3.94}$$

In addition, using (3.93), (3.94), and $W_h = W + O(h^{m+2})$, we obtain

$$\begin{aligned} \dot{U}_i^T &= Re\{e^{i\theta^p(\alpha_i)}\dot{W}_i\} - Im\{e^{i\theta(\alpha_i)}W(\alpha_i)\}\dot{\theta}_i^p + A_{-3}(\dot{\theta}_i) \\ &= (1+O(h^{m+3}))Re\{\frac{z_\alpha(\alpha_i)}{\sigma(\alpha_i)}\dot{W}_i\} + U^N(\alpha_i)\dot{\theta}_i^p + A_{-3}(\dot{\theta}_i) \ . \end{aligned}$$

We substitute now our estimate (3.90) for $\dot{W}$ into this last equation. We get

$$\begin{aligned} \dot{U}_i^T &= -\frac{1}{2}\tilde{\gamma}(\alpha_i)H_h\dot{\theta}_i^p + U^N(\alpha_i)\dot{\theta}_i^p + f(\alpha_i)H_hG_h^p\dot{\theta}_i + E(\dot{\theta}_i) \\ &+ A_{-2}(\dot{\sigma}_i, \dot{\theta}_i, \dot{\tilde{\gamma}}_i) + O(h^{m+2}) \ . \end{aligned} \tag{3.95}$$

The variation of the normal component of the velocity is estimated similarly;

$$\begin{aligned} \dot{U}_i^N &\equiv -Im\{e^{i\theta_i^p}W_i - e^{i\theta^p(\alpha_i)}W_h(\alpha_i)\} \\ &= -Im\{e^{i\theta^p(\alpha_i)}\dot{W}_i\} - Re\{e^{i\theta(\alpha_i)}W(\alpha_i)\}\dot{\theta}_i^p + A_{-3}(\dot{\theta}_i) \ . \end{aligned}$$

Hence, using again (3.90) we find

$$\begin{aligned} \dot{U}_i^N &= \frac{1}{2}H_h\dot{\tilde{\gamma}}_i^p - U^T(\alpha_i)\dot{\theta}_i^p + f(\alpha_i)H_hG_h^p\dot{\theta}_i + E(\dot{\theta}_i) \\ &+ A_{-2}(\dot{\sigma}_i, \dot{\theta}_i, \dot{\tilde{\gamma}}_i) + O(h^{m+2}) \ . \end{aligned} \tag{3.96}$$

We remind that $f(\cdot)$ denotes different smooth functions whose forms we need not specify.

Let us now turn our attention to the added tangential velocity U^A. We have

$$\begin{aligned} \dot{U}_i^A &= -\dot{U}_i^T + Int_h(U^N(\cdot)D_h\dot{\theta})_i + Int_h(D_h\theta(\cdot)\dot{U}^N)_i \\ &- Int_h(R(\cdot))_i < U^N(\cdot)D_h\dot{\theta} >_h - Int_h(R(\cdot))_i < D_h\theta(\cdot)\dot{U}^N >_h \\ &+ \dot{U}_i^{A,NL} \ , \end{aligned}$$

where the nonlinear part of the variation is given by

$$\dot{U}_i^{A,NL} = Int_h(\dot{U}^N\dot{\theta})_i - Int_h(R(\cdot))_i < \dot{U}^N\dot{\theta} >_h \ .$$

Note that (3.96) and our definition of T^* imply that

$$\|\dot{U}_i^N\|_{l^2} \leq Ch^{7/2} \text{ and } \|\dot{U}_i^N\|_\infty \leq Ch^3 \ .$$

Therefore,

$$\|\dot{U}_i^N D_h\dot{\theta}\|_{l^2} \leq \|\dot{U}_i^N\|_\infty h^{-1}\|\dot{\theta}\|_{l^2} \leq Ch^2\|\dot{\theta}\|_{l^2} \ , \tag{3.97}$$

from which it follows that

$$\dot{U}_i^{A,NL} = A_{-2}(\dot{\theta}_i) \ .$$

Now, from Parseval's identity we have

$$< \phi D_h\psi >_h = - < D_h\phi\psi >_h \ . \tag{3.98}$$

Hence,

$$< U^N(\cdot)D_h\dot{\theta} >_h = - < D_hU^N(\cdot)\dot{\theta} >_h = A_{-m}(\dot{\theta}_i)$$

and similarly we conclude that

$$< D_h\theta(\cdot)\dot{U}^N >_h = A_{-m}(\dot{\sigma}_i, \dot{\theta}_i, \dot{\bar{\gamma}}_i) \ .$$

Thus, we may write an estimate for $\dot{U}_i^A$ in the following form

$$\dot{U}_i^A = -\dot{U}_i^T + B(\dot{\sigma}_i, \dot{\theta}_i, \dot{\bar{\gamma}}_i) + A_{-m}(\dot{\sigma}_i, \dot{\theta}_i, \dot{\bar{\gamma}}_i) \ , \tag{3.99}$$

where B is given by

$$B(\dot{\sigma}_i, \dot{\theta}_i, \dot{\bar{\gamma}}_i) \equiv Int_h(U^N(\cdot)D_h\dot{\theta})_i + Int_h(\theta_\alpha(\cdot)\dot{U}^N)_i \ . \tag{3.100}$$

We would like to "integrate by parts" to obtain the leading order terms of B. At the continuous level, integration by parts follows from the product rule $(fg)_\alpha = fg_\alpha + f_\alpha g$. However, due to aliasing, $S_h(fg)_i \neq f_iS_hg_i + g_iS_hf_i$. Of course, we do not need this to be satisfied exactly but only that the error be a lower order term. This is the content of the following lemma [11].

LEMMA 3.5. *Let $f(\cdot) \in C^3$ and $\phi \in l^2$ then*

$$D_h(f(\cdot)\phi)_i = f(\alpha_i)D_h\phi_i + f_\alpha(\alpha_i)\phi_i^q + hA_0(\phi_i) \ , \tag{3.101}$$

where

$$\hat{\phi}_k^q = q(kh)\hat{\phi}_k \ ; \ q(x) = \frac{d}{dx}(x\rho(x)) \ . \tag{3.102}$$

Hence,

$$\begin{aligned} Int_h(U^N(\cdot)D_h\dot{\theta})_i &= Int_h(D_h(U^N(\cdot)\dot{\theta}))_i + Int_h(U^N_\alpha(\cdot)\dot{\theta}^q + hA_0(\dot{\theta}))_i \\ &= (U^N(\alpha_i)\dot{\theta}_i)^p + A_{-1}(\dot{\theta}_i) = U^N(\alpha_i)\dot{\theta}_i^p + A_{-1}(\dot{\theta}_i) \ , \end{aligned}$$

where we have used that

$$\begin{aligned} Int_h(D_h(U^N(\cdot)\dot{\theta}))_i &= Int_h(S_h(U^N(\cdot)\dot{\theta})^p)_i = (U^N(\alpha_i)\dot{\theta}_i)^p - < U^N(\cdot)\dot{\theta} >_h \\ &= (U^N(\alpha_i)\dot{\theta}_i)^p + A_{-m}(\dot{\theta}_i) = U^N(\alpha_i)\dot{\theta}_i^p + A_{-1}(\dot{\theta}_i) \ , \end{aligned}$$

and the last equallity was obtained from Lemma 3.3. Now, using our estimate (3.96) for $\dot{U}^N$ in the other term of B, we find that

$$B(\dot{\sigma}_i, \dot{\theta}_i, \dot{\bar{\gamma}}_i) = U^N(\alpha_i)\dot{\theta}_i^p + A_{-1}(\dot{\sigma}_i, \dot{\theta}_i, \dot{\bar{\gamma}}_i) \ . \tag{3.103}$$

We proceed now to obtain evolution equations for $\dot{\sigma}_i$, $\dot{\theta}_i$ and $\dot{\bar{\gamma}}_i$.

3.3.2. Evolution Equations for the Errors

It is easy to obtain an evolution equation for $\dot{\sigma}$. Using the Consistency Lemma we have

$$\begin{aligned} \frac{d\dot{\sigma}_i}{dt} &= -R(\alpha_i) < S_h\theta U^N - S_h\theta(\cdot)U^N(\cdot) >_h + O(h^{m+2}) \\ &= R(\alpha_i) < S_h U^N(\cdot)\dot{\theta} + S_h\theta(\cdot)\dot{U}^N + \dot{\theta}\dot{U}^N >_h + O(h^{m+2}) \ . \end{aligned}$$

The nonlinear term can be bound just as in (3.97). It follows that

$$\frac{d\dot{\sigma}_i}{dt} = A_{-m}(\dot{\sigma}_i, \dot{\theta}_i, \dot{\bar{\gamma}}_i) + O(h^{m+2}) \ . \tag{3.104}$$

We use consistency again to obtain an evolution equation for $\dot{\theta}_i$. In this case

$$\begin{aligned} \frac{d\dot{\theta}_i}{dt} &= \frac{1}{\sigma_i}[S_h U_i^N + D_h\theta_i(U_i^T + U_i^A)] \\ &- \frac{1}{\sigma(\alpha_i)}[S_h U_h^N(\alpha_i) + D_h\theta(\alpha_i)(U_h^T(\alpha_i) + U_h^A(\alpha_i))] + O(h^{m+1}) \ , \end{aligned}$$

which can be written as

$$\begin{aligned} \frac{d\dot{\theta}_i}{dt} &= \frac{1}{\sigma(\alpha_i)}S_h\dot{U}_i^N + \frac{U_h^T(\alpha_i) + U_h^A(\alpha_i)}{\sigma(\alpha_i)}D_h\dot{\theta}_i + \frac{D_h\theta(\alpha_i)}{\sigma(\alpha_i)}(\dot{U}_i^T + \dot{U}_i^A) \\ &+ \frac{1}{\sigma(\alpha_i)}(\dot{U}_i^T + \dot{U}_i^A)D_h\dot{\theta}_i \end{aligned} \tag{3.105}$$

$$
\begin{aligned}
&+ \quad [S_h U_h^N(\alpha_i) + D_h\theta(\alpha_i)(U_h^T(\alpha_i) + U_h^A(\alpha_i))](\frac{1}{\sigma})_i^{\cdot} \\
&+ \quad (\frac{1}{\sigma})_i^{\cdot} S_h \dot{U}_i^N + (U_h^T(\alpha_i) + U_h^A(\alpha_i))(\frac{1}{\sigma})_i^{\cdot} D_h\dot{\theta}_i \\
&+ \quad D_h\theta(\alpha_i)(\dot{U}_i^T + \dot{U}_i^A)(\frac{1}{\sigma})_i^{\cdot} + (\frac{1}{\sigma})_i^{\cdot}(\dot{U}_i^T + \dot{U}_i^A) D_h\dot{\theta}_i + O(h^{m+1}) \ ,
\end{aligned}
$$

where

$$
(\frac{1}{\sigma})_i^{\cdot} \equiv \frac{1}{\sigma_i} - \frac{1}{\sigma(\alpha_i)} = -\frac{\dot{\sigma}_i}{\sigma^2(\alpha_i)} + \frac{\dot{\sigma}_i^2}{\sigma^2(\alpha_i)(\sigma(\alpha_i) + \dot{\sigma}_i)} \ .
$$

Recall that by assumption $\sigma(\alpha) \geq C > 0$ thus, for h small, we get

$$
\left\| \frac{\dot{\sigma}^2}{\sigma^2(\sigma + \dot{\sigma})} \right\|_{l^2} \leq C\|\dot{\sigma}\|_\infty \|\dot{\sigma}\|_{l^2} \leq Ch^3 \|\dot{\sigma}\|_{l^2} \ ,
$$

which implies that

$$
(\frac{1}{\sigma})_i^{\cdot} = A_{-2}(\dot{\sigma}_i) \ . \tag{3.106}
$$

Also note that using (3.99) and (3.103) we have that

$$
\|\dot{U}^T + \dot{U}^A\|_{l^2} \leq C(\|\dot{\sigma}\|_{l^2} + \|\dot{\theta}\|_{l^2} + \|\dot{\gamma}\|_{l^2}) \ .
$$

Hence $\|\dot{U}^T + \dot{U}^A\|_\infty \leq Ch^3$. We can bound the nonlinear terms in (3.105) easily. For example,

$$
\|\frac{1}{\sigma}(\dot{U}^T + \dot{U}^A) D_h\dot{\theta}\|_{l^2} \leq C\|\dot{U}^T + \dot{U}^A\|_\infty h^{-1}\|\dot{\theta}\|_{l^2} \leq Ch^2\|\dot{\theta}\|_{l^2} \ , \tag{3.107}
$$

and for the next term involving $\dot{\sigma}$ we have

$$
[S_h U_h^N(\alpha_i) + D_h\theta(\alpha_i)(U_h^T(\alpha_i) + U_h^A(\alpha_i))](\frac{1}{\sigma})_i^{\cdot} = A_{-2}(\dot{\sigma}_i) \ .
$$

The rest of the nonlinear terms are estimated similarly. Thus

$$
\begin{aligned}
\frac{d\dot{\theta}_i}{dt} &= \frac{1}{\sigma(\alpha_i)} S_h \dot{U}_i^N + \frac{U^T(\alpha_i) + U^A(\alpha_i)}{\sigma(\alpha_i)} D_h\dot{\theta}_i + \frac{\theta_\alpha(\alpha_i)}{\sigma(\alpha_i)} B(\dot{\sigma}_i, \dot{\theta}_i, \dot{\gamma}_i) \\
&+ \quad A_{-2}(\dot{\theta}_i, \dot{\sigma}_i) + O(h^{m+1}) \ ,
\end{aligned} \tag{3.108}
$$

but using our estimate for $\dot{U}^N$, equation (3.96), we obtain

$$
\begin{aligned}
S_h \dot{U}_i^N &= \frac{1}{2}\Lambda_h \dot{\tilde{\gamma}}_i - U^T(\alpha_i) D_h\dot{\theta}_i - U_\alpha^T(\alpha_i)\dot{\theta}_i^q + S_h E(\dot{\theta}_i) \\
&+ \quad S_h G_h^p \dot{\theta}_i + S_h f(\alpha_i) H_h G_h^p \dot{\theta}_i + A_{-1}(\dot{\theta}_i, \dot{\sigma}_i, \dot{\tilde{\gamma}}_i) + O(h^{m+1})
\end{aligned} \tag{3.109}
$$

where we have also used (3.86), and Lemma 3.5 for the term $-U^T\dot{\theta}^p$. Substituting (3.109) and (3.103) into (3.108) we get

$$
\begin{aligned}
(3.110) \qquad \frac{d\dot{\theta}_i}{dt} &= \frac{1}{2\sigma(\alpha_i)}\Lambda_h\dot{\tilde{\gamma}}_i + \frac{U^A(\alpha_i)}{\sigma(\alpha_i)}D_h\dot{\theta}_i + f(\alpha_i)\dot{\theta}_i^p + g(\alpha_i)\dot{\theta}_i^q \\
&+ \frac{1}{\sigma(\alpha_i)}S_hE(\dot{\theta}_i) + \frac{1}{\sigma(\alpha_i)}S_hG_h^p\dot{\theta}_i + \frac{1}{\sigma(\alpha_i)}S_hf(\alpha_i)H_hG_h^p\dot{\theta}_i \\
&+ A_{-1}(\dot{\theta}_i, \dot{\sigma}_i, \dot{\tilde{\gamma}}_i) + O(h^{m+1}) \ .
\end{aligned}
$$

Obtaining an evolution equation for $\dot{\tilde{\gamma}}$ requires to estimate many terms. However, only a few terms contribute to the leading order behavior. More precisely, we will show that

$$
\begin{aligned}
\frac{d\dot{\tilde{\gamma}}_i}{dt} &= \frac{S}{\sigma(\alpha_i)}D_h\frac{1}{\sigma(\alpha_i)}D_h\dot{\theta}_i + \frac{\tilde{\gamma}^2(\alpha_i)}{2\sigma(\alpha_i)}\Lambda_h\dot{\theta}_i + f(\alpha_i)D_h\dot{\tilde{\gamma}}_i \\
&+ A_0(\dot{\sigma}_i, \dot{\theta}_i, \dot{\tilde{\gamma}}_i) + O(h^m) \ .
\end{aligned}
$$

To this end, let us write the right hand side of (3.10) as follows

$$
(3.111) \qquad \frac{d\gamma_i}{dt} = F_i^{(1)} + F_i^{(2)} + F_i^{(3)} \ ,
$$

where

$$
(3.112) \qquad F_i^{(1)} \equiv SD_h(\frac{1}{\sigma_i}D_h\theta_i) + S_h(U_i^A\tilde{\gamma}_i^p) \ .
$$

$$
\begin{aligned}
(3.113) \qquad F_i^{(2)} &\equiv -2ARe\{\frac{\sigma_i e^{i\theta_i}}{2\pi i}\sum_{(j-i)\ \text{odd}}\frac{\frac{d\gamma_j}{dt}}{z_i^p - z_j^p}2h\} \\
&+ 2ARe\{\frac{\sigma_i e^{i\theta_i}}{2\pi i}\sum_{(j-i)\ \text{odd}}\gamma_j^p\frac{\frac{dz_i}{dt} - \frac{dz_j}{dt}}{(z_i^p - z_j^p)^2}2h\} \ .
\end{aligned}
$$

$$
(3.114) \qquad F_i^{(3)} \equiv -2A[\frac{1}{8}D_h\tilde{\gamma}_i^2 + g\sigma_i\sin\theta_i - U^ARe\{e^{i\theta_i}S_hW_i\}] \ ,
$$

and similarly for the corresponding continuous terms $F^{(j)}(\alpha_i)$. It follows by the Consistency Lemma that

$$
(3.115) \qquad \frac{d\dot{\gamma}_i}{dt} = \dot{F}_i^{(1)} + \dot{F}_i^{(2)} + \dot{F}_i^{(3)} + O(h^m) \ ,
$$

where

$$
(3.116) \qquad \dot{F}_i^{(j)} \equiv F_i^{(j)} - F^{(j)}(\alpha_i) \quad \text{for} \quad j = 1, 2, 3 \ .
$$

Let us compute the variation of the first term. We have

$$
\begin{aligned}
\dot{F}_i^{(1)} &= SD_h(\frac{1}{\sigma_i}D_h\theta_i) - SD_h(\frac{1}{\sigma(\alpha_i)}D_h\theta(\alpha_i)) \\
&+ S_h(U_i^A\tilde{\gamma}_i^p) - S_h(U_h^A(\alpha_i)\tilde{\gamma}^p(\alpha_i)) \ ,
\end{aligned}
$$

which we can write as

$$\begin{aligned}(3.117)\qquad \dot{F}_i^{(1)} &= SD_h(\frac{1}{\sigma(\alpha_i)}D_h\dot{\theta}_i) - SD_h(D_h\theta(\alpha_i)(\frac{1}{\sigma})_i^{\cdot}) + S_h(U_h^A(\alpha_i)\dot{\tilde{\gamma}}_i^p)\\ &+ S_h(\dot{U}_i^A\tilde{\gamma}^p(\alpha_i)) + SD_h((\frac{1}{\sigma})_i^{\cdot}D_h\dot{\theta}_i) + S_h(\dot{U}_i^A\dot{\tilde{\gamma}}_i^p)\ .\end{aligned}$$

The nonlinear terms can be estimated as in (3.107);

$$SD_h((\frac{1}{\sigma})_i^{\cdot}D_h\dot{\theta}_i) + S_h(\dot{U}_i^A\dot{\tilde{\gamma}}_i^p) = A_{-1}(\dot{\sigma}_i, \dot{\theta}_i, \dot{\tilde{\gamma}}_i)\ .$$

Consequently

$$(3.118)\quad \dot{F}_i^{(1)} = SD_h(\frac{1}{\sigma_i}D_h\dot{\theta}_i) + S_h(U^A(\alpha_i)\dot{\tilde{\gamma}}_i^p) + S_h(\dot{U}_i^A\tilde{\gamma}^p(\alpha_i)) + A_{-1}(\dot{\sigma}_i, \dot{\theta}_i, \dot{\tilde{\gamma}}_i)\ .$$

Moreover

$$\begin{aligned}(3.119)\qquad S_h(U^A(\alpha_i)\dot{\tilde{\gamma}}_i^p) &= D_h(U^A(\alpha_i)\dot{\tilde{\gamma}}_i) + S_hG_h^p\dot{\tilde{\gamma}}_i\\ &= U^A(\alpha_i)D_h\dot{\tilde{\gamma}}_i + A_0(\dot{\tilde{\gamma}}_i)\ .\end{aligned}$$

Now from (3.95) and (3.99),

$$\begin{aligned}S_h\left(\dot{U}_i^A\tilde{\gamma}^p(\alpha_i)\right) &= \frac{1}{2}S_h\left(\tilde{\gamma}^2(\alpha_i)H_h\dot{\theta}_i^p\right) - S_h\left(\tilde{\gamma}(\alpha_i)U^N(\alpha_i)\dot{\theta}_i^p\right)\\ &+ S_h\left(\tilde{\gamma}(\alpha_i)(U^N(\alpha_i)\dot{\theta}_i)^p\right) - S_hInt_h[U_\alpha^N(\cdot)\dot{\theta}^q]_i\\ &+ S_hInt_h[\theta_\alpha(\cdot)\dot{U}^N]_i + S_hE(\dot{\theta}_i) + S_hf(\alpha_i)H_hG_h^p\dot{\theta}_i\\ &+ A_0(\dot{\sigma}_i, \dot{\theta}_i, \dot{\tilde{\gamma}}_i) + O(h^{m+1})\ .\end{aligned}$$

Note that

$$\|S_hInt_h[\theta_\alpha(\cdot)\dot{U}^N]\|_{l^2} \le C\|\dot{U}^N\|_{l^2} \le C(\|\dot{\sigma}\|_{l^2} + \|\dot{\theta}\|_{l^2} + \|\dot{\theta}\|_{l^2})$$

and similarly

$$\|S_hInt_h[U_\alpha^N(\cdot)\dot{\theta}^q]\|_{l^2} \le C\|\dot{\theta}\|_{l^2}\ .$$

On the other hand, Lemma 3.3 implies that $S_hf(\alpha_i)H_hG_h^p\dot{\theta}_i = A_0(\dot{\theta}_i)$. Also from (3.91) we have that $S_hE(\dot{\theta}_i) = A_0(\dot{\theta}_i)$. In addition,

$$S_h\left(\tilde{\gamma}(\alpha_i)(U^N(\alpha_i)\dot{\theta}_i)^p\right) - S_h\left(\tilde{\gamma}(\alpha_i)U^N(\alpha_i)\dot{\theta}_i^p\right) = A_0(\dot{\theta}_i)\ ,$$

and as a result

$$(3.120)\qquad S_h\left(\dot{U}_i^A\tilde{\gamma}^p(\alpha_i)\right) = \frac{1}{2}\tilde{\gamma}^2(\alpha_i)\Lambda_h\dot{\theta}_i + A_0(\dot{\sigma}_i, \dot{\theta}_i, \dot{\tilde{\gamma}}_i)\ .$$

Substituting (3.119) and (3.120) into (3.118) we get

$$\dot{F}_i^{(1)} = SD_h(\frac{1}{\sigma_i}D_h\dot{\theta}_i) + U^A(\alpha_i)D_h\dot{\tilde{\gamma}}_i + \frac{1}{2}\tilde{\gamma}^2(\alpha_i)\Lambda_h\dot{\theta}_i + A_0(\dot{\sigma}_i, \dot{\theta}_i, \dot{\tilde{\gamma}}_i) \ . \tag{3.121}$$

To estimate $\dot{F}_i^{(2)}$, we split it into two parts:

$$\dot{F}_i^{(2)} = \dot{F}_i^{(2)L} + \dot{F}_i^{(2)NL} \ , \tag{3.122}$$

where

$$\begin{aligned}
\dot{F}_i^{(2)L} &= -2ARe\left\{\frac{z_\alpha(\alpha_i)}{2\pi i}\sum_{(j-i)\ \text{odd}}\frac{\frac{d\dot{\gamma}_j}{dt}}{z_h^p(\alpha_i)-z_h^p(\alpha_j)}2h\right\} \\
&+ 2ARe\left\{\frac{z_\alpha(\alpha_i)}{2\pi i}\sum_{(j-i)\ \text{odd}}\frac{d\gamma}{dt}(\alpha_j)\frac{\dot{z}_i^p-\dot{z}_j^p}{(z_h^p(\alpha_i)-z_h^p(\alpha_j))^2}2h\right\} \\
&+ 2ARe\left\{\frac{z_\alpha(\alpha_i)}{2\pi i}\sum_{(j-i)\ \text{odd}}\gamma^p(\alpha_j)\frac{\frac{d\dot{z}_i}{dt}-\frac{d\dot{z}_j}{dt}}{(z_h^p(\alpha_i)-z_h^p(\alpha_j))^2}2h\right\} \\
&+ 2ARe\left\{\frac{z_\alpha(\alpha_i)}{2\pi i}\sum_{(j-i)\ \text{odd}}\dot{\gamma}_j^p\frac{\frac{dz_h}{dt}(\alpha_i)-\frac{dz_h}{dt}(\alpha_j)}{(z_h^p(\alpha_i)-z_h^p(\alpha_j))^2}2h\right\} \\
&- 4ARe\left\{\frac{z_\alpha(\alpha_i)}{2\pi i}\sum_{(j-i)\ \text{odd}}\frac{d\gamma}{dt}(\alpha_j)\frac{(\frac{dz_h}{dt}(\alpha_i)-\frac{dz_h}{dt}(\alpha_j))(\dot{z}_i^p-\dot{z}_j^p)}{(z_h^p(\alpha_i)-z_h^p(\alpha_j))^3}2h\right\} \\
&= (I)+(II)+(III)+(IV)+(V)
\end{aligned} \tag{3.123}$$

The explicit form of $\dot{F}_i^{(2)NL}$, which contains mostly nonlinear terms, is given in the Appendix where we also prove the following result.

LEMMA 3.6. *For $t \le T^*$ and h small,*

$$\dot{F}_i^{(2)NL} = A_0(\dot{\sigma}_i, \dot{\theta}_i, \dot{\gamma}_i) \ . \tag{3.124}$$

Now, the second and third term in (3.123) can be estimated just as we did for similar terms of $\dot{W}$ in (3.82) and (3.84). Hence

$$\begin{aligned}
(II) &\equiv 2ARe\left\{\frac{z_\alpha(\alpha_i)}{2\pi i}\sum_{(j-i)\ \text{odd}}\frac{d\gamma}{dt}(\alpha_j)\frac{\dot{z}_i^p-\dot{z}_j^p}{(z_h^p(\alpha_i)-z_h^p(\alpha_j))^2}2h\right\} \\
&= 2ARe\left\{\frac{\frac{d\gamma}{dt}(\alpha_i)}{2\pi i z_\alpha(\alpha_i)}\Lambda_h\dot{z}_i + A_0(\dot{z}_i)\right\} = A_0(\dot{\sigma}_i, \dot{\theta}_i) \ ,
\end{aligned} \tag{3.125}$$

where we have also used (3.70) in the last identity. For the third term we have

$$(III) \equiv 2ARe\left\{\frac{z_\alpha(\alpha_i)}{2\pi i}\sum_{(j-i)\ \text{odd}}\gamma^p(\alpha_j)\frac{\frac{d\dot z_i}{dt}-\frac{d\dot z_j}{dt}}{(z_h^p(\alpha_i)-z_h^p(\alpha_j))^2}2h\right\} \tag{3.126}$$

$$= 2ARe\left\{\frac{\frac{d\gamma}{dt}(\alpha_i)}{2\pi i z_\alpha(\alpha_i)}\sum_{(j-i)\ \text{odd}}\frac{\frac{d\dot z_i}{dt}-\frac{d\dot z_j}{dt}}{(\alpha_i-\alpha_j)^2}2h\right\}+A_0(\frac{d\dot z_i}{dt})\ .$$

We need now an estimate for $\frac{d\dot z_i}{dt}$. Using (3.15) , (3.104), and (3.110) we obtain

$$\frac{d\dot z_i}{dt} = Int_h[iz_\alpha(\cdot)\frac{d\dot\theta}{dt}+e^{i\theta(\cdot)}\frac{d\dot\sigma}{dt}+A_0(\dot\sigma,\dot\theta)]_i+O(h^{m+1}) \tag{3.127}$$

$$= Int_h[i\frac{z_\alpha(\cdot)}{2\sigma(\cdot)}\Lambda_h\dot{\tilde\gamma}+i\frac{U^A(\cdot)z_\alpha(\cdot)}{\sigma(\cdot)}D_h\dot\theta+A_0(\dot\sigma,\dot\theta)]_i+O(h^{m+1})$$

and "integrating by parts" on $\dot{\tilde\gamma}$ and $\dot\theta$ we get

$$\frac{d\dot z_i}{dt} = i(\frac{z_\alpha(\alpha_i)}{2\sigma(\alpha_i)}H_h\dot{\tilde\gamma}_i)^p+i(\frac{U^A(\alpha_i)z_\alpha(\alpha_i)}{\sigma(\alpha_i)}\dot\theta_i)^p \tag{3.128}$$

$$+ Int_h[A_0(\dot\sigma,\dot\theta,\dot{\tilde\gamma})]_i+O(h^{m+1})\ ,$$

which shows that

$$\|\frac{d\dot z}{dt}\|_{l^2}\le C(\|\dot\sigma\|_{l^2}+\|\dot\theta\|_{l^2}+\|\dot\gamma\|_{l^2})+O(h^{m+1}) \tag{3.129}$$

and thus

$$\|\frac{d\dot z}{dt}\|_\infty\le Ch^3\ . \tag{3.130}$$

Substituting (3.128) into (3.126) and using Lemma 3.1 we obtain

$$(III)=-\frac{1}{2}A\tilde\gamma(\alpha_i)D_h\dot{\tilde\gamma}_i+A\tilde\gamma(\alpha_i)U^A(\alpha_i)\Lambda_h\dot\theta_i+A_0(\dot\sigma_i,\dot\theta_i,\dot{\tilde\gamma}_i)+O(h^m)\ . \tag{3.131}$$

For the fourth term in (3.123), we note that $\frac{dz}{dt}(\cdot)\in C^{m+2}$ and $z_h(\alpha_i)=z(\alpha_i)+O(h^{m+3})$. Thus

$$(IV) \equiv 2ARe\left\{\frac{z_\alpha(\alpha_i)}{2\pi i}\sum_{(j-i)\ \text{odd}}\dot\gamma_j^p\frac{\frac{dz_h}{dt}(\alpha_i)-\frac{dz_h}{dt}(\alpha_j)}{(z_h^p(\alpha_i)-z_h^p(\alpha_j))^2}2h\right\}$$

$$= \left(1+O(h^{m+2})\right)2ARe\left\{\frac{z_\alpha(\alpha_i)}{2\pi i}\sum_{(j-i)\ \text{odd}}\dot\gamma_j^p\frac{\frac{dz}{dt}(\alpha_i)-\frac{dz}{dt}(\alpha_j)}{(z(\alpha_i)-z(\alpha_j))^2}2h\right\}\ ,$$

but

$$2ARe\left\{\frac{z_\alpha(\alpha_i)}{2\pi i}\sum_{(j-i)\text{ odd}}\dot\gamma_j^p\frac{\frac{dz}{dt}(\alpha_i)-\frac{dz}{dt}(\alpha_j)}{(z(\alpha_i)-z(\alpha_j))^2}2h\right\}=$$
$$f(\alpha_i)\sum_{(j-i)\text{ odd}}\frac{\dot\gamma_j^p}{\alpha_i-\alpha_j}2h+\sum_{(j-i)\text{ odd}}\dot\gamma_j^p g(\alpha_i,\alpha_j)2h\ ,$$

where keeping with our notation, f and g denote smooth functions. Hence using Lemma 3.2 it follows that $(IV)=A_0(\dot{\tilde\gamma}_i)$. Proceeding as in the estimate for (III) we can also show that $(V)=A_0(\dot\sigma_i,\dot\theta_i)$.

We collect now our estimates for (I)-(V) and apply Lemma 3.5 to conclude that

$$\begin{aligned}\dot F_i^{(2)} &= -K_h\frac{d\dot\gamma_i}{dt}-\frac{1}{2}A\tilde\gamma(\alpha_i)D_h\dot{\tilde\gamma}_i+A\tilde\gamma(\alpha_i)U^A(\alpha_i)\Lambda_h\dot\theta_i\\ &+ A_0(\dot\sigma_i,\dot\theta_i,\dot{\tilde\gamma}_i)+O(h^m)\ ,\end{aligned}\tag{3.132}$$

where

$$K_h\frac{d\dot\gamma_i}{dt}\equiv 2ARe\left\{\frac{z_\alpha(\alpha_i)}{2\pi i}\sum_{(j-i)\text{ odd}}\frac{\frac{d\dot\gamma_j}{dt}}{z_h^p(\alpha_i)-z_h^p(\alpha_j)}2h\right\}\ .\tag{3.133}$$

We also need to estimate $\dot F_i^{(3)}$ to obtain the leading order terms in the evolution equation for $\dot{\tilde\gamma}$ (3.115). From the definition of $\dot F_i^{(3)}$, we have that

$$\begin{aligned}\dot F_i^{(3)} &= -2A\left[\frac{1}{4}D_h(\tilde\gamma(\alpha_i)\dot{\tilde\gamma}_i)+\frac{1}{8}D_h\dot{\tilde\gamma}_i^{\,2}+g(\sigma\sin\theta)_i^{\cdot}\right]\\ &+ 2A\left[U^A(\alpha_i)Re\{(e^{i\theta}S_hW)_i^{\cdot}\}+\dot U_i^A Re\{e^{i\theta_i}S_hW_i\}\right]\ .\end{aligned}\tag{3.134}$$

We can simplify this expression noting that

$$\|D_h\dot{\tilde\gamma}^2\|_{l^2}\le h^{-1}\|\dot{\tilde\gamma}^2\|_{l^2}\le h^{-1}\|\dot{\tilde\gamma}\|_\infty\|\dot{\tilde\gamma}\|_{l^2}\le h^2\|\dot{\tilde\gamma}\|_{l^2}\tag{3.135}$$

and that, by (3.65), $(\sigma\sin\theta)_i^{\cdot}=A_0(\dot\sigma_i,\dot\theta_i)$. Also

$$Re\{e^{i\theta_i}S_hW_i\}=Re\left\{e^{i\theta(\alpha_i)}S_h\dot W_i+S_hW_h(\alpha_i)(e^{i\theta})_i^{\cdot}+S_h\dot W_i(e^{i\theta})_i^{\cdot}\right\}\ .\tag{3.136}$$

This term can be bounded easily,

$$\|S_h\dot W_i(e^{i\theta})^{\cdot}\|_{l^2}\le h^{-1}\|\dot W\|_\infty\|(e^{i\theta})^{\cdot}\|_{l^2}\le Ch^2\|\dot\theta\|_{l^2}\ ,\tag{3.137}$$

because $\|\dot{W}\|_\infty \le h^3$. Therefore

$$Re\{e^{i\theta_i} S_h W_i\} = Re\left\{e^{i\theta(\alpha_i)} S_h \dot{W}_i\right\} + A_0(\dot{\theta}_i) \ . \tag{3.138}$$

We estimate $S_h\dot{W}$ from (3.90).

$$S_h\dot{W} = S_h\left(\frac{\sigma(\alpha_i)}{2iz_\alpha(\alpha)} H_h(\dot{\tilde{\gamma}}_i^p)\right) - S_h\left(\frac{\gamma(\alpha_i)}{2z_\alpha(\alpha_i)} H_h\dot{\theta}_i^p\right) + A_0(\dot{\sigma}_i, \dot{\theta}_i, \dot{\gamma}_i) \ ,$$

but

$$S_h(f(\alpha_i)H_h\dot{\phi}_i^p) = D_h(f(\alpha_i)H_h\dot{\phi}_i) + A_0(\dot{\phi}_i) = f(\alpha_i)\Lambda_h\dot{\phi}_i + A_0(\dot{\phi}_i) \ .$$

Consequently,

$$S_h\dot{W} = \frac{\sigma(\alpha_i)}{2iz_\alpha(\alpha)}\Lambda_h\dot{\tilde{\gamma}}_i - \frac{\gamma(\alpha_i)}{2z_\alpha(\alpha_i)}\Lambda_h\dot{\theta}_i + A_0(\dot{\sigma}_i, \dot{\theta}_i, \dot{\gamma}_i) \ . \tag{3.139}$$

Now for the last term of $\dot{F}_i^{(3)}$ in (3.134) we get

$$\|\dot{U}^A Re\{e^{i\theta} S_h W\}\|_{l^2} \le \|e^{i\theta} S_h W\|_\infty \|\dot{U}^A\|_{l^2} \le C(\|\dot{\sigma}\|_{l^2} + \|\dot{\theta}\|_{l^2} + \|\dot{\gamma}\|_{l^2}) \tag{3.140}$$

and combining (3.134)- (3.140) we find

$$\dot{F}_i^{(3)} = -\frac{1}{2}A\tilde{\gamma}(\alpha_i)D_h\dot{\tilde{\gamma}}_i - A\tilde{\gamma}(\alpha_i)U^A(\alpha_i)\Lambda_h\dot{\theta}_i + A_0(\dot{\sigma}_i, \dot{\theta}_i, \dot{\tilde{\gamma}}_i) \ . \tag{3.141}$$

Finally substituting our estimates for $\dot{F}_i^{(1)}$, $\dot{F}_i^{(2)}$, and $\dot{F}_i^{(3)}$, that is, expressions (3.121), (3.133) and (3.141) into (3.115) we obtain

$$(I + K_h)\frac{d\dot{\gamma}_i}{dt} = P(\dot{\theta}_i, \dot{\tilde{\gamma}}_i) + A_0(\dot{\sigma}_i, \dot{\theta}_i, \dot{\gamma}_i) + O(h^m) \ , \tag{3.142}$$

where

$$P(\dot{\theta}_i, \dot{\tilde{\gamma}}_i) = SD_h(\frac{1}{\sigma(\alpha_i)}D_h\dot{\theta}_i) + \frac{1}{2}\tilde{\gamma}^2(\alpha_i)\Lambda_h\dot{\theta}_i + f(\alpha_i)D_h\dot{\tilde{\gamma}}_i \ . \tag{3.143}$$

Note that (3.142) is a discrete version of a Fredholm integral equation of second kind. The following result shows that the discrete operator $I+K_h$ has a bounded inverse in l^2 [11].

LEMMA 3.7. *Assume that $z(\cdot;t) \in C^3$ and $z_\alpha \neq 0$. Then there exist constants $h_0 > 0$ and $C > 0$ such that for all h satisfying $0 < h \le h_0$,*

$$\|(I + K_h)^{-1}\|_{l^2} \le C \ . \tag{3.144}$$

We can use now this result to show that $K_h \frac{d\dot{\gamma}_i}{dt}$ is actually a lower order term. Indeed,

$$
\begin{aligned}
K_h \frac{d\dot{\gamma}_i}{dt} &= K_h (I + K_h)^{-1} \left[P(\dot{\theta}_i, \dot{\tilde{\gamma}}_i) + A_0(\dot{\sigma}_i, \dot{\theta}_i, \dot{\gamma}_i) + O(h^m) \right] \\
&= (I + K_h)^{-1} K_h P(\dot{\theta}_i, \dot{\tilde{\gamma}}_i) + A_0(\dot{\sigma}_i, \dot{\theta}_i, \dot{\gamma}_i) + O(h^m) \ ,
\end{aligned} \tag{3.145}
$$

where we have used commutability of the operators, that is

$$
K_h (I + K_h)^{-1} = (I + K_h)^{-1} K_h \ . \tag{3.146}
$$

and the fact that K_h and $(I + K_h)^{-1}$ are bounded in l^2. Moreover, note that

$$
\begin{aligned}
K_h \dot{\phi}_i &= Re \left[\frac{1}{2\pi i} \sum_{(j-i) \text{ odd}} \frac{\dot{\phi}_j}{\alpha_i - \alpha_j} 2h \right] + R_h(\dot{\phi}_i) + A_{-m}(\dot{\phi}_i) \\
&= R_h(\dot{\phi}_i) + A_{-m}(\dot{\phi}_i) \ ,
\end{aligned} \tag{3.147}
$$

where R_h is a discrete 'smoothing' operator of the type defined in (3.79). Here is a place where the right combination of filtering is crucial. By Lemma 3.2 we know that if Fourier smoothing is applied to eliminate aliasing errors, then $R_h = A_{-2}$. Therefore,

$$
\begin{aligned}
R_h(D_h \frac{1}{\sigma(\alpha_i)} D_h \dot{\theta}_i) &= A_{-2}(S_h \frac{1}{\sigma(\alpha_i)} D_h \dot{\theta}_i) = A_0(\dot{\theta}_i) \ , \\
R_h(\Lambda_h \dot{\theta}_i) &= A_{-2}(S_h H_h \dot{\theta}_i) = A_0(\dot{\theta}_i) \ , \\
R_h(D_h \dot{\tilde{\gamma}}_i) &= A_{-1}(\dot{\tilde{\gamma}}_i) \ ,
\end{aligned}
$$

which shows that

$$
K_h \frac{d\dot{\gamma}_i}{dt} = A_0(\dot{\sigma}_i, \dot{\theta}_i, \dot{\tilde{\gamma}}_i) \ . \tag{3.148}
$$

Therefore our previous estimate (3.142) becomes

$$
\begin{aligned}
\frac{d\dot{\gamma}_i}{dt} &= S D_h \frac{1}{\sigma(\alpha_i)} D_h \dot{\theta}_i + \frac{1}{2} \tilde{\gamma}^2(\alpha_i) \Lambda_h \dot{\theta}_i + f(\alpha_i) D_h \dot{\tilde{\gamma}}_i \\
&+ A_0(\dot{\sigma}_i, \dot{\theta}_i, \dot{\tilde{\gamma}}_i) + O(h^m) \ .
\end{aligned} \tag{3.149}
$$

However, we need an evolution equation for $\dot{\tilde{\gamma}}_i$. Recall that $\tilde{\gamma} = \gamma / \sigma$, thus

$$
\begin{aligned}
\frac{d\dot{\tilde{\gamma}}_i}{dt} &= \frac{1}{\sigma(\alpha_i)} \frac{d\dot{\gamma}_i}{dt} + \left(\frac{1}{\sigma} \right)_i^{\cdot} \frac{d\gamma_i}{dt} - \left(\frac{\gamma}{\sigma^2} \frac{d\sigma}{dt} \right)_i^{\cdot} \\
&= \frac{1}{\sigma(\alpha_i)} \frac{d\dot{\gamma}_i}{dt} + A_0(\dot{\sigma}_i, \dot{\theta}_i, \dot{\tilde{\gamma}}_i) + O(h^m)
\end{aligned}
$$

where we have used (3.106), (3.104), and (3.149). Thus dividing equation (3.149) by $\sigma(\alpha_i)$ we obtain

$$\begin{aligned}\frac{d\dot{\tilde{\gamma}}_i}{dt} &= \frac{S}{\sigma(\alpha_i)} D_h \frac{1}{\sigma(\alpha_i)} D_h \dot{\theta}_i + \frac{\tilde{\gamma}^2(\alpha_i)}{2\sigma(\alpha_i)} \Lambda_h \dot{\theta}_i + f(\alpha_i) D_h \dot{\tilde{\gamma}}_i \\ &+ A_0(\dot{\sigma}_i, \dot{\theta}_i, \dot{\tilde{\gamma}}_i) + O(h^m) \ ,\end{aligned}$$

and this completes our system of evolution equations, which we list now as a summary of the estimates obtained in this section.

We have shown that, for $t \leq T^*$,

$$\frac{d\dot{\sigma}_i}{dt} = A_{-2}(\dot{\sigma}_i, \dot{\theta}_i, \dot{\gamma}_i) + O(h^{m+2}) \tag{3.150}$$

$$\frac{d\dot{\theta}_i}{dt} = \frac{1}{2\sigma(\alpha_i)} \Lambda_h \dot{\tilde{\gamma}}_i + f(\alpha_i) D_h \dot{\theta}_i + \Theta(\dot{\theta}_i) + A_{-1}(\dot{\theta}_i, \dot{\sigma}_i, \dot{\tilde{\gamma}}_i) + O(h^{m+1}) \tag{3.151}$$

$$\begin{aligned}\frac{d\dot{\tilde{\gamma}}_i}{dt} &= -\frac{S}{\sigma(\alpha_i)} \Lambda_h \frac{1}{\sigma(\alpha_i)} \left(\Lambda_h - \frac{\tilde{\gamma}^2(\alpha_i)}{2S\sigma(\alpha_i)} \right) \dot{\theta}_i + f(\alpha_i) D_h \dot{\tilde{\gamma}}_i \\ &+ A_0(\dot{\sigma}_i, \dot{\theta}_i, \dot{\tilde{\gamma}}_i) + O(h^m) \ ,\end{aligned} \tag{3.152}$$

where $\Theta(\dot{\theta}_i)$ is of the form

$$\begin{aligned}\Theta(\dot{\theta}_i) &= c_1(\alpha_i) \dot{\theta}_i^p + c_2(\alpha_i) \dot{\theta}_i^q + c_3(\alpha_i) S_h G_h^p(\dot{\theta}_i) \\ &+ c_4(\alpha_i) S_h f(\alpha_i) H_h G_h^p(\dot{\theta}_i) + c_5(\alpha_i) S_h E(\dot{\theta}_i)\end{aligned} \tag{3.153}$$

and all the c_i's are smooth functions.

Note also that, in (3.152), we have combined the two leading order terms in $\dot{\theta}_i$ into a single term. Indeed,

$$\begin{aligned}-\frac{S}{\sigma(\alpha_i)} \Lambda_h \frac{1}{\sigma(\alpha_i)} \left(\Lambda_h - \frac{\tilde{\gamma}^2(\alpha_i)}{2\sigma(\alpha_i) S} \right) \dot{\theta}_i &= -\frac{S}{\sigma(\alpha_i)} \Lambda_h \frac{1}{\sigma(\alpha_i)} \Lambda_h \dot{\theta}_i + \frac{\tilde{\gamma}^2(\alpha_i)}{2\sigma(\alpha_i)} \dot{\theta}_i \\ &= -\frac{S}{\sigma(\alpha_i)} D_h H_h \frac{1}{\sigma(\alpha_i)} H_h D_h \dot{\theta}_i + \frac{\tilde{\gamma}^2(\alpha_i)}{2\sigma(\alpha_i)} \dot{\theta}_i + A_0(\dot{\theta}_i) \\ &= \frac{S}{\sigma(\alpha_i)} D_h \frac{1}{\sigma(\alpha_i)} D_h \dot{\theta}_i - \frac{S}{\sigma(\alpha_i)} R_h \left((S_h H_h \dot{\theta})^p \right) + \frac{\tilde{\gamma}^2(\alpha_i)}{2\sigma(\alpha_i)} \dot{\theta}_i + A_0(\dot{\theta}_i) \\ &= \frac{S}{\sigma(\alpha_i)} D_h \frac{1}{\sigma(\alpha_i)} D_h \dot{\theta}_i + \frac{\tilde{\gamma}^2(\alpha_i)}{2\sigma(\alpha_i)} \dot{\theta}_i + A_0(\dot{\theta}_i) \ ,\end{aligned}$$

where we have also used $H_h^2 = -I$, as $D_h \dot{\theta}_i$ has both modes $k = 0$ and $k = N/2$ equal to zero.

3.3.3. Energy Estimates

From the first term of the evolution equation for $\dot{\tilde{\gamma}}$ we observe that surface tension effects become dominant for modes higher than $\|\gamma^2/(2S\sigma)\|_\infty$. To distinguish these high modes from lower modes, we introduce the following projection operator.

$$(\widehat{P_M u})_k = \begin{cases} \hat{u}_k & \text{if } |k| > M \ , \\ 0 & \text{if } k \leq M \ , \end{cases} \tag{3.154}$$

where M is a constant given by

$$M = 2\left(\|\frac{\gamma^2}{2\sigma S}\|_\infty + 1 \right) \ . \tag{3.155}$$

Note that the definition of the projection operator implies that

$$\|P_M u\|_{l^2} \leq \|u\|_{l^2} \ . \tag{3.156}$$

Let us also denote the usual discrete inner product of two functions whose values are known on a uniform grid of size h, by

$$(\phi \ , \ \psi)_h \equiv \sum_{j=-N+1}^{N/2} \phi_j \psi_j h \ . \tag{3.157}$$

We start the estimates by taking the inner product of (3.152) and $\frac{\sigma}{2S}\dot{\tilde{\gamma}}$. We obtain

$$\begin{aligned} \frac{1}{2S}\left(\sigma\dot{\tilde{\gamma}} \ , \ \frac{d\dot{\tilde{\gamma}}}{dt} \right)_h &= -\frac{1}{2}\left(\dot{\tilde{\gamma}} \ , \ \Lambda_h \frac{1}{\sigma}(\Lambda_h - g)\dot{\theta} \right)_h + \left(f\dot{\tilde{\gamma}} \ , \ D_h\dot{\tilde{\gamma}} \right)_h \\ &+ \frac{1}{2S}\left(\sigma\dot{\tilde{\gamma}} \ , \ A_0(\dot{\sigma}, \dot{\theta}, \dot{\tilde{\gamma}}) + O(h^m) \right)_h \equiv G_1 + G_2 + G_3 \ . \end{aligned} \tag{3.158}$$

We examine next each term G_i separately.

$$\begin{aligned} G_1 &\equiv -\frac{1}{2}\left(\dot{\tilde{\gamma}} \ , \ \Lambda_h \frac{1}{\sigma}(\Lambda_h - g)\dot{\theta} \right)_h \\ &= -\frac{1}{2}\left(\frac{1}{\sigma}\Lambda_h P_M \dot{\tilde{\gamma}} \ , \ (\Lambda_h - g)P_M\dot{\theta} \right)_h \\ &- \frac{1}{2}\left(\frac{1}{\sigma}\Lambda_h (I - P_M)\dot{\tilde{\gamma}} \ , \ (\Lambda_h - g)P_M\dot{\theta} \right)_h \\ &- \frac{1}{2}\left(\frac{1}{\sigma}\Lambda_h \dot{\tilde{\gamma}} \ , \ (\Lambda_h - g)(I - P_M)\dot{\theta} \right)_h \equiv G_{11} + G_{12} + G_{13} \ . \end{aligned} \tag{3.159}$$

The following result gives us a bound for the terms G_{12} and G_{13}.

LEMMA 3.8. *Let $f(\cdot)$ and $g(\cdot) \in C^2[-\pi,\pi]$ and ϕ, $\psi \in l^2$, then*

$$
\begin{aligned}
&(i) \quad |(f\Lambda_h(I-P_M)\phi\ ,\ (\Lambda_h-g)P_M\psi)_h| \le C\|\phi\|_{l^2}\|\psi\|_{l^2}\ .\\
&(ii) \quad |(f\Lambda_h\phi\ ,\ (\Lambda_h-g)(I-P_M)\psi)_h| \le C\|\phi\|_{l^2}\|\psi\|_{l^2}\ .\\
&(iii) \quad |(fD_h(I-P_M)\phi\ ,\ (\Lambda_h-g)\psi)_h| \le C\|\phi\|_{l^2}\|\psi\|_{l^2}\ .\\
&(iv) \quad |(fD_h\phi\ ,\ (\Lambda_h-g)(I-P_M)\psi)_h| \le C\|\phi\|_{l^2}\|\psi\|_{l^2}\ .
\end{aligned}
$$

Parts (i) and (ii) of this lemma imply that

$$
|G_{12}+G_{13}| \le C\|\dot{\tilde{\gamma}}\|_{l^2}\|\dot{\theta}\|_{l^2}\ , \tag{3.160}
$$

and as a result

$$
G_1 \le -\frac{1}{2}\left(\frac{1}{\sigma}\Lambda_h P_M\dot{\tilde{\gamma}}\ ,\ (\Lambda_h-g)P_M\dot{\theta}\right)_h + C\|\dot{\tilde{\gamma}}\|_{l^2}\|\dot{\theta}\|_{l^2}\ . \tag{3.161}
$$

The term G_2 is of lower order, because

$$
\begin{aligned}
\left(f\dot{\tilde{\gamma}}\ ,\ D_h\dot{\tilde{\gamma}}\right)_h &= -\left(D_h(f\dot{\tilde{\gamma}})\ ,\ \dot{\tilde{\gamma}}\right)_h\\
&= -\left(fD_h\dot{\tilde{\gamma}}\ ,\ \dot{\tilde{\gamma}}\right)_h - \left(f_\alpha\dot{\tilde{\gamma}}^q + hA_0(\dot{\tilde{\gamma}})\ ,\ \dot{\tilde{\gamma}}\right)_h\ ,
\end{aligned} \tag{3.162}
$$

and thus

$$
\left(f\dot{\tilde{\gamma}}\ ,\ D_h\dot{\tilde{\gamma}}\right)_h = -\frac{1}{2}\left(f_\alpha\dot{\tilde{\gamma}}^q + hA_0(\dot{\tilde{\gamma}})\ ,\ \dot{\tilde{\gamma}}\right)_h\ . \tag{3.163}
$$

Therefore

$$
|G_2| \le C\|\dot{\tilde{\gamma}}\|_{l^2}^2\ . \tag{3.164}
$$

We estimate G_3 directly using Schwarz inequality. We get

$$
\begin{aligned}
|G_3| &= |\frac{1}{2S}\left(\sigma\dot{\tilde{\gamma}}\ ,\ A_0(\dot{\sigma},\dot{\theta},\dot{\tilde{\gamma}}) + O(h^m)\right)_h|\\
&\le C\|\dot{\tilde{\gamma}}\|_{l^2}\left(\|\dot{\tilde{\gamma}}\|_{l^2} + \|\dot{\sigma}\|_{l^2} + \|\dot{\theta}\|_{l^2} + O(h^m)\right)\ .
\end{aligned} \tag{3.165}
$$

Now, for the left-hand side of (3.158) we note that

$$
\frac{1}{2S}\left(\sigma\dot{\tilde{\gamma}}\ ,\ \frac{d\dot{\tilde{\gamma}}}{dt}\right)_h = \frac{1}{4S}\left(\sigma\ ,\ \frac{d\dot{\tilde{\gamma}}^2}{dt}\right)_h = \frac{1}{4S}\frac{d}{dt}\left(\sigma\ ,\ \dot{\tilde{\gamma}}^2\right)_h - \frac{1}{4S}\left(\sigma_t\ ,\ \dot{\tilde{\gamma}}^2\right)_h\ . \tag{3.166}
$$

Consequently,

$$
\frac{1}{4S}\frac{d}{dt}\left(\sigma\ ,\ \dot{\tilde{\gamma}}^2\right)_h \le C\|\dot{\tilde{\gamma}}\|_{l^2}^2 + G_1 + G_2 + G_3\ ,
$$

and using our estimates (3.161), (3.164), and (3.165) for G_1, G_2, and G_3 respectively, we obtain

$$\begin{aligned} \frac{1}{4S}\frac{d}{dt}\left(\sigma\ ,\ \dot{\tilde{\gamma}}^2\right)_h &\leq -\frac{1}{2}\left(\frac{1}{\sigma}\Lambda_h P_M\dot{\tilde{\gamma}}\ ,\ (\Lambda_h - g)P_M\dot{\theta}\right)_h \\ &+ C\left(\|\dot{\tilde{\gamma}}\|_{l^2}^2 + \|\dot{\sigma}\|_{l^2}^2 + \|\dot{\theta}\|_{l^2}^2 + O(h^m)\|\dot{\tilde{\gamma}}\|_{l^2}\right)\ . \end{aligned} \tag{3.167}$$

In order to balance the first term on the right-hand side of the inequality (3.167), we need to take the inner product of the evolution equation (3.151) and $(\Lambda_h - g)P_M\dot{\theta}$. Thus,

$$\left((\Lambda_h - g)P_M\dot{\theta}\ ,\ \frac{d\dot{\theta}}{dt}\right)_h = T_1 + T_2 + T_3 + T_4 + T_5 + T_6 + T_7\ , \tag{3.168}$$

where

$$T_1 = \frac{1}{2}\left(\frac{1}{\sigma}\Lambda_h\dot{\tilde{\gamma}}\ ,\ (\Lambda_h - g)P_M\dot{\theta}\right)_h\ , \tag{3.169}$$

$$T_2 = \left(fD_h\dot{\theta}\ ,\ (\Lambda_h - g)P_M\dot{\theta}\right)_h\ , \tag{3.170}$$

$$T_3 = \left(\Theta(\dot{\theta})\ ,\ (\Lambda_h - g)P_M\dot{\theta}\right)_h\ , \tag{3.171}$$

$$T_4 = \left(A_{-1}(\dot{\sigma},\dot{\theta},\dot{\tilde{\gamma}}) + O(h^{m+1})\ ,\ (\Lambda_h - g)P_M\dot{\theta}\right)_h\ , \tag{3.172}$$

and $\Theta(\dot{\theta})$ is of the form defined in (3.153).

Let us start with the left hand side of (3.168). Thus,

$$\begin{aligned} \left((\Lambda_h - g)P_M\dot{\theta}\ ,\ \frac{d\dot{\theta}}{dt}\right)_h &= \left((\Lambda_h - g)P_M\dot{\theta}\ ,\ \frac{d}{dt}P_M\dot{\theta}\right)_h \\ &+ \left((\Lambda_h - g)P_M\dot{\theta}\ ,\ (I - P_M)\frac{d\dot{\theta}}{dt}\right)_h\ . \end{aligned} \tag{3.173}$$

However, we also have the following orthogonality property

$$\left(\Lambda_h P_M\dot{\theta}\ ,\ (I - P_M)\frac{d\dot{\theta}}{dt}\right)_h \equiv 0\ . \tag{3.174}$$

Thus we get,

$$\begin{aligned} &\left((\Lambda_h - g)P_M\dot{\theta}\ ,\ (I - P_M)\frac{d\dot{\theta}}{dt}\right)_h = -\left(gP_M\dot{\theta}\ ,\ (I - P_M)\frac{d\dot{\theta}}{dt}\right)_h \\ &= -\left(gP_M\dot{\theta}\ ,\ (I - P_M)\left[\frac{1}{2\sigma}\Lambda_h\dot{\tilde{\gamma}} + fD_h\dot{\theta} + A_0(\dot{\sigma},\dot{\theta}) + A_{-1}(\dot{\tilde{\gamma}}) + O(h^{m+1})\right]\right)_h\ , \end{aligned} \tag{3.175}$$

and using Lemma 3.8, it follows that

$$\left((\Lambda_h - g)P_M\dot{\theta}\ ,\ \frac{d\dot{\theta}}{dt}\right)_h = \left((\Lambda_h - g)P_M\dot{\theta}\ ,\ \frac{d}{dt}P_M\dot{\theta}\right)_h + R\ , \tag{3.176}$$

where

$$|R| \leq C\|\dot{\theta}\|_{l^2}\left(\|\dot{\sigma}\|_{l^2} + \|\dot{\theta}\|_{l^2} + \|\dot{\tilde{\gamma}}\|_{l^2} + h^m\right) \ . \tag{3.177}$$

Furthermore, we can rewrite (3.176) as

$$\left((\Lambda_h - g)P_M\dot{\theta}\ ,\ \frac{d}{dt}P_M\theta\right)_h = \frac{1}{2}\frac{d}{dt}\left((\Lambda_h - g)P_M\dot{\theta}\ ,\ P_M\dot{\theta}\right)_h + R \ . \tag{3.178}$$

We turn our attention now to the right hand side of (3.168). For the first term, we have

$$\begin{aligned} T_1 &\equiv \frac{1}{2}\left(\frac{1}{\sigma}\Lambda_h\dot{\tilde{\gamma}}\ ,\ (\Lambda_h - g)P_M\dot{\theta}\right)_h \\ &= \frac{1}{2}\left(\frac{1}{\sigma}\Lambda_h P_M\dot{\tilde{\gamma}}\ ,\ (\Lambda_h - g)P_M\dot{\theta}\right)_h + \frac{1}{2}\left(\frac{1}{\sigma}\Lambda_h(I - P_M)\dot{\tilde{\gamma}}\ ,\ (\Lambda_h - g)P_M\dot{\theta}\right)_h \end{aligned}$$

and in view of Lemma 3.8,

$$T_1 \leq \frac{1}{2}\left(\frac{1}{\sigma}\Lambda_h P_M\dot{\tilde{\gamma}}\ ,\ (\Lambda_h - g)P_M\dot{\theta}\right)_h + C\|\dot{\theta}\|_{l^2}\|\dot{\tilde{\gamma}}\|_{l^2} \ . \tag{3.179}$$

Similarly, we find the following bound for T_2.

$$T_2 \leq \left(fD_hP_M\dot{\theta}\ ,\ (\Lambda_h - g)P_M\dot{\theta}\right)_h + C\|\dot{\theta}\|_{l^2}^2 \ . \tag{3.180}$$

Despite its appearance, this is a lower order term because

$$\begin{aligned} &\left(fD_hP_M\dot{\theta}\ ,\ (\Lambda_h - g)P_M\dot{\theta}\right)_h = \\ &\qquad \left(fD_hP_M\dot{\theta}\ ,\ \Lambda_hP_M\dot{\theta}\right)_h + \left(\tilde{f}P_M\dot{\theta}\ ,\ D_hP_M\dot{\theta}\right)_h \ , \end{aligned} \tag{3.181}$$

but we have shown already in (3.162-3.164) that, $|(fP_M\dot{\theta}\ ,\ D_hP_M\dot{\theta})_h| \leq C\|\dot{\theta}\|_{l^2}^2$. Moreover,

$$\begin{aligned} \left(fD_h\dot{\phi}\ ,\ \Lambda_h\dot{\phi}\right)_h &= \left(H_hD_h\dot{\phi}\ ,\ fD_h\dot{\phi}\right)_h = -\left(D_h\dot{\phi}\ ,\ H_h(f(S_h\dot{\phi})^p)\right)_h \\ &= -\left(D_h\dot{\phi}\ ,\ f\Lambda_h\dot{\phi}\right)_h - \left(D_h\dot{\phi}\ ,\ A_{-2}(S_h\dot{\phi})\right)_h \ . \end{aligned} \tag{3.182}$$

Hence

$$\left(fD_h\dot{\phi}\ ,\ \Lambda_h\dot{\phi}\right)_h = \frac{1}{2}\left(D_h\dot{\phi}\ ,\ A_{-1}(\dot{\phi})\right)_h = \left(\dot{\phi}\ ,\ A_0(\dot{\phi})\right)_h \ , \tag{3.183}$$

and consequently, we can conclude that

$$T_2 \leq C\|\dot{\theta}\|_{l^2}^2 \ . \tag{3.184}$$

To estimate T_3, we need to use the precise form of the operator Θ. Substituting (3.153) into (3.171), we get

$$
\begin{aligned}
(3.185) \qquad T_3 &= \left(c_1\dot{\theta}^p + c_2\dot{\theta}^q\ ,\ (\Lambda_h - g)P_M\dot{\theta}\right)_h \\
&+ \left(c_3 S_h G_h^p(\dot{\theta}) + c_4 S_h f H_h G_h^p(\dot{\theta})\ ,\ (\Lambda_h - g)P_M\dot{\theta}\right)_h \\
&+ \left(c_5 S_h E(\dot{\theta})\ ,\ (\Lambda_h - g)P_M\dot{\theta}\right)_h\ .
\end{aligned}
$$

One more lemma helps us get the right bound for this expression.

LEMMA 3.9. *Let $f(\cdot) \in C^2$ then*

$$
\begin{aligned}
&(i) \quad |(f\phi\ ,\ \Lambda_h\psi)_h| \le C\|\phi\|_{H_h^{1/2}}\|\psi\|_{H_h^{1/2}}\ . \\
&(ii) \quad |(fH_h\phi\ ,\ \Lambda_h\psi)_h| \le C\|\phi\|_{H_h^{1/2}}\|\psi\|_{H_h^{1/2}}\ . \\
&(iii) \quad \left|(fS_hG_h^p\phi\ ,\ \Lambda_h\psi)_h\right| \le C\|\phi\|_{H_h^{1/2}}\|\psi\|_{H_h^{1/2}}\ . \\
&(iv) \quad \left|(fS_hgG_h^pH_h\phi\ ,\ \Lambda_h\psi)_h\right| \le C\|\phi\|_{H_h^{1/2}}\|\psi\|_{H_h^{1/2}}\ .
\end{aligned}
$$

Therefore,

$$
(3.186) \qquad |T_3| \le C\|\dot{\theta}\|^2_{H_h^{1/2}} + \left|\left(c_5 S_h E(\dot{\theta})\ ,\ (\Lambda_h - g)P_M\dot{\theta}\right)_h\right|\ .
$$

Recall that the operator $E(\dot{\theta})$ has the following general form,

$$
E(\dot{\theta}_i) = f(\alpha_i)Int_h(z_\alpha\dot{\theta})_i^p + g(\alpha_i)H_hInt_h(z_\alpha\dot{\theta})_i^p\ .
$$

Also note that

$$
\begin{aligned}
(3.187) \qquad S_h\left(f(\alpha_i)Int_h(z_\alpha\dot{\theta})_i^p\right) &= D_h\left(f(\alpha_i)Int_h(z_\alpha\dot{\theta})_i\right) + S_hG_h^pInt_h(z_\alpha\dot{\theta})_i \\
&= f(\alpha_i)\dot{\theta}^p + f_\alpha(\alpha_i)\tilde{\dot{\theta}}_i^q + S_hG_h^p\tilde{\dot{\theta}}_i + A_{-1}(\dot{\theta}_i)\ ,
\end{aligned}
$$

where $\tilde{\dot{\theta}}_i \equiv Int_h(z_\alpha\dot{\theta})_i$. Similarly we can show that,

$$
(3.188) S_h\left(g(\alpha_i)H_hInt_h(z_\alpha\dot{\theta})_i^p\right) = g(\alpha_i)H_h\dot{\theta}^p + g_\alpha(\alpha_i)H_h\tilde{\dot{\theta}}_i^q + S_hG_h^pH_h\tilde{\dot{\theta}}_i + A_{-1}(\dot{\theta}_i)\ .
$$

Moreover,

$$
(3.189) \qquad \|\tilde{\dot{\theta}}\|^2_{H_h^{1/2}} \equiv \left((\Lambda_h + I)Int_h(z_\alpha\dot{\theta})\ ,\ Int_h(z_\alpha\dot{\theta})\right)_h \le C\|\dot{\theta}\|^2_{H_h^{1/2}}\ .
$$

Therefore, Lemma 3.9 implies that

$$
\left|\left(c_5 S_h E(\dot{\theta})\ ,\ (\Lambda_h - g)P_M\dot{\theta}\right)_h\right| \le C\|\dot{\theta}\|^2_{H_h^{1/2}}\ ,
$$

and using this estimate in (3.186), we get

$$|T_3| \leq C\|\dot\theta\|^2_{H_h^{1/2}} \ . \tag{3.190}$$

Finally,

$$\begin{aligned} |T_4| &= \left|\left(A_{-1}(\dot\sigma,\dot\theta,\dot{\tilde\gamma}) + O(h^{m+1})\ ,\ (\Lambda_h - g)P_M\dot\theta\right)_h\right| \\ &\leq C\|\dot\theta\|_{l^2}\left(\|\dot\theta\|_{l^2} + \|\dot\sigma\|_{l^2} + \|\dot{\tilde\gamma}\|_{l^2} + h^m\right) \end{aligned} \tag{3.191}$$

Combining the bounds we obtained for the terms T_i, $i = 1,\ldots,4$, we get the following energy estimate for the $\dot\theta$-equation.

$$\begin{aligned} \frac{1}{2}\frac{d}{dt}\left((\Lambda_h - g)P_M\dot\theta\ ,\ P_M\dot\theta\right)_h &\leq \frac{1}{2}\left(\frac{1}{\sigma}\Lambda_h P_M\dot{\tilde\gamma}\ ,\ (\Lambda_h - g)P_M\dot\theta\right)_h \\ &+ C\|\dot\theta\|_{H_h^{1/2}}\left(\|\dot\theta\|_{H_h^{1/2}} + \|\dot\sigma\|_{l^2} + \|\dot{\tilde\gamma}\|_{l^2} + h^m\right) \ . \end{aligned} \tag{3.192}$$

Now taking the inner product of (3.150) and $\dot\sigma$, it follows immediately that

$$\frac{1}{2}\frac{d}{dt}\|\dot\sigma\|^2_{l^2} \leq C\|\dot\theta\|_{l^2}\left(\|\dot\theta\|_{l^2} + \|\dot\sigma\|_{l^2} + \|\dot{\tilde\gamma}\|_{l^2} + h^{m+2}\right) \ . \tag{3.193}$$

To complete the estimates, we need to consider the contribution of the low modes. Take the inner product of equation (3.151) and $(I - P_M)\dot\theta$. We have,

$$\begin{aligned} \left((I-P_M)\dot\theta\ ,\ \frac{d\dot\theta}{dt}\right)_h &= \left((I-P_M)\dot\theta\ ,\ \frac{1}{2\sigma}\Lambda_h\dot{\tilde\gamma}\right)_h \\ &+ \left((I-P_M)\dot\theta\ ,\ \frac{U^A}{\sigma}D_h\dot\theta\right)_h \\ &+ \left((I-P_M)\dot\theta\ ,\ \frac{f\dot\theta^p - U_\alpha^T\dot\theta^q}{\sigma}\right)_h \\ &+ \left((I-P_M)\dot\theta\ ,\ \frac{1}{\sigma}S_h G_h^p\dot\theta + \frac{1}{\sigma}S_h f H_h G_h^p\dot\theta\right)_h \\ &+ \left((I-P_M)\dot\theta\ ,\ \frac{1}{\sigma}S_h E(\dot\theta)\right)_h \\ &+ \left((I-P_M)\dot\theta\ ,\ A_{-1}(\dot\sigma,\dot\theta,\dot{\tilde\gamma}) + O(h^{m+1})\right)_h \ . \end{aligned} \tag{3.194}$$

For the left hand side of this expression, we note that

$$\begin{aligned} \left((I-P_M)\dot\theta\ ,\ \frac{d\dot\theta}{dt}\right)_h &= \left((I-P_M)\dot\theta\ ,\ \frac{d}{dt}(I-P_M)\dot\theta\right)_h \\ &= \frac{1}{2}\frac{d}{dt}\|(I-P_M)\dot\theta\|^2_{l^2} \ , \end{aligned} \tag{3.195}$$

where we have used the orthogonality relation,

$$\left((I-P_M)\dot\theta\ ,\ P_M\frac{d\dot\theta}{dt}\right)_h \equiv 0\ . \tag{3.196}$$

In view of Lemma 3.8, (3.187), (3.188), and that $S_h G_h^p \dot\theta = A_0(\dot\theta)$, we conclude that

$$\frac{1}{2}\frac{d}{dt}\|(I-P_M)\dot\theta\|_{l^2}^2 \le C\|\dot\theta\|_{l^2}\left(\|\dot\theta\|_{l^2}+\|\dot\sigma\|_{l^2}+\|\dot{\tilde\gamma}\|_{l^2}+h^{m+1}\right)\ . \tag{3.197}$$

We now put together the two bands of modes by noting that

$$\begin{aligned}
&\left((\Lambda_h-g)P_M\dot\theta\ ,\ P_M\dot\theta\right)_h+\frac{M}{2}\left\|(I-P_M)\dot\theta\right\|_{l^2}^2 \\
&\quad=\ \left(\Lambda_h P_M\dot\theta\ ,\ P_M\dot\theta\right)_h-\left(gP_M\dot\theta\ ,\ P_M\dot\theta\right)_h+\frac{M}{2}\left\|(I-P_M)\dot\theta\right\|_{l^2}^2 \\
&\quad\ge\ \left(\Lambda_h P_M\dot\theta\ ,\ P_M\dot\theta\right)_h-\|g\|_\infty\|P_M\dot\theta\|_{l^2}^2+\frac{M}{2}\left\|(I-P_M)\dot\theta\right\|_{l^2}^2 \\
&\quad=\ 2\pi\sum_{\substack{|k|>M\\ k\in I}}\left[\rho(kh)|k|-\|g\|_\infty\right]|\hat{\dot\theta}_k|^2+2\pi\frac{M}{2}\sum_{\substack{|k|\le M\\ k\in I}}|\hat{\dot\theta}_k|^2\ ,
\end{aligned} \tag{3.198}$$

where $I=\{-N/2+1,\dots,N/2\}$. Recall that $M=2(\|g\|_\infty+1)$. Therefore,

$$\frac{\rho(kh)|k|}{2}>\|g\|_\infty \qquad \text{for}\ \ |k|\ge M\ , \tag{3.199}$$

and as a result,

$$\begin{aligned}
&\left((\Lambda_h-g)P_M\dot\theta\ ,\ P_M\dot\theta\right)_h+\frac{M}{2}\left\|(I-P_M)\dot\theta\right\|_{l^2}^2 \\
&\quad\ge\ 2\pi[\frac{1}{2}\sum_{\substack{|k|>M\\ k\in I}}\rho(kh)|k||\hat{\dot\theta}_k|^2+\frac{M}{2}\sum_{\substack{|k|\le M\\ k\in I}}|\hat{\dot\theta}_k|^2] \\
&\quad=\ \frac{\pi}{2}[\sum_{\substack{|k|>M\\ k\in I}}\rho(kh)|k||\hat{\dot\theta}_k|^2+M\sum_{\substack{|k|\le M\\ k\in I}}|\hat{\dot\theta}_k|^2] \\
&\quad+\ \frac{\pi}{2}[\sum_{\substack{|k|>M\\ k\in I}}\rho(kh)|k||\hat{\dot\theta}_k|^2+M\sum_{\substack{|k|\le M\\ k\in I}}|\hat{\dot\theta}_k|^2]\ge\frac{1}{4}\|\dot\theta\|_{H_h^{1/2}}^2\ .
\end{aligned} \tag{3.200}$$

We now add the estimates (3.167), (3.192), (3.193), and $M/2$ times the low-mode estimate (3.197). Note that the leading order terms of (3.167) and (3.192) cancel each other, and we are left with the following inequality,

$$\begin{aligned}
&\frac{1}{4S}\frac{d}{dt}\left(\sigma\ ,\ \dot{\tilde\gamma}^2\right)_h+\frac{1}{2}\frac{d}{dt}\|\dot\sigma\|_{l^2}^2+\frac{1}{2}\frac{d}{dt}\left((\Lambda_h-g)P_M\dot\theta\ ,\ P_M\dot\theta\right)_h+\frac{M}{2}\frac{d}{dt}\|(I-P_M)\dot\theta\|_{l^2}^2 \\
&\quad\le\ C\left(\|\dot\theta\|_{H_h^{1/2}}^2+\|\dot{\tilde\gamma}\|_{l^2}^2+\|\dot\sigma\|_{l^2}^2\right)+C\left(\|\dot\theta\|_{H_h^{1/2}}+\|\dot{\tilde\gamma}\|_{l^2}+\|\dot\sigma\|_{l^2}\right)h^m\ ,
\end{aligned} \tag{3.201}$$

and integrating in time we find,

$$y_0^2(t) = y_0^2(0) + \int_0^t K\left(y_0^2(s) + y_0(s)h^m\right) ds \ , \tag{3.202}$$

where

$$y_0^2(t) = \|\dot{\theta}\|^2_{H_h^{1/2}} + \|\dot{\tilde{\gamma}}\|^2_{l^2} + \|\dot{\sigma}\|^2_{l^2} \ . \tag{3.203}$$

Using the Gronwall inequality, we conclude that

$$y_0(t) \leq C(T)h^m \qquad\qquad t \leq T^* \ . \tag{3.204}$$

Therefore,

$$\|\dot{\sigma}\|_{l^2} \ , \ \|\dot{\tilde{\gamma}}\|_{l^2} \leq C(T)h^m \ , \tag{3.205}$$

and

$$\|\dot{\theta}\|_{H_h^{1/2}} \leq C(T)h^m \ \text{ or } \ \|\dot{\theta}\|_{l^2} \leq C(T)h^{m-1} \ . \tag{3.206}$$

On the other hand from the evolution equation (3.152) for $\dot{\tilde{\gamma}}$, we have that, for $t \leq T^*$

$$\left\| \frac{d\dot{\tilde{\gamma}}}{dt} \right\|_{l^2} \leq \frac{C}{h^2}\left(\|\dot{\sigma}\|_{l^2} + \|\dot{\theta}\|_{l^2} + \|\dot{\tilde{\gamma}}\|_{l^2}\right) \leq \tilde{C}(T)h^{m-3} \ . \tag{3.207}$$

Since $m > 4$, we get for small h

$$\|\dot{\sigma}\|_{l^2} \ , \ \|\dot{\tilde{\gamma}}\|_{l^2} \leq C(T)h^5 < \frac{1}{2}h^{7/2} \ , \tag{3.208}$$

and

$$\|\dot{\theta}\|_{l^2} \leq B(T)h^4 < \frac{1}{2}h^{7/2} \quad \text{ and } \quad \left\| \frac{d\dot{\tilde{\gamma}}}{dt} \right\|_{l^2} < \frac{1}{2}h^{3/2} \ . \tag{3.209}$$

From the definition (3.60) of T^*, it follows that

$$T = T^* \ , \tag{3.210}$$

which shows that the estimates (3.205-3.206) are valid for the entire interval $0 \leq t \leq T$. This completes the proof of Theorem 3.1 for the convergence of our method. ∎

3.4. Appendix : Proof of Technical Lemmas

We indicate with an asterisk those proofs given in [11], which are included here with little modification.

Unless otherwise noted $I = \{-N/2+1, \ldots, N/2\}$.

PROOF OF LEMMA 3.1 *

The first step in proving part (i) is to express the operator H_h as a convolution.

$$H_h f_i = \frac{1}{\pi} \sum_{(j-i) \text{ odd}} \frac{f_j}{\alpha_i - \alpha_j} 2h = (K * f)(\alpha_i) \ ,$$

where

$$K(\alpha_i) = \begin{cases} \frac{2}{\pi \alpha_i} & \text{if } i \text{ is odd} \\ \\ 0 & \text{if } i \text{ is even} \end{cases}$$

and $*$ is the discrete convolution, that is

$$(K * f)(\alpha_i) = \sum_j K(\alpha_i - \alpha_j) f_j h \ .$$

Therefore, it follows that

$$(\widehat{H_h f})_k = \tilde{K}_k \hat{f}_k \ ,$$

with

$$\tilde{K}_k = \frac{2h}{\pi} \sum_{l=-\infty}^{\infty} \frac{e^{-i(2l+1)kh}}{(2l+1)h} = \frac{2}{\pi} \sum_{l=-\infty}^{\infty} \frac{e^{-i(2l+1)kh}}{2l+1} \ . \tag{3.211}$$

Thus, to prove part (i), we need to show that

$$\frac{2}{\pi i} \sum_{l=-\infty}^{\infty} \frac{e^{i(2l+1)\xi}}{2l+1} = \text{sgn}(\xi) \quad \text{for } |\xi| < \pi \ . \tag{3.212}$$

We extend $\text{sgn}(\xi)$ periodically outside the interval $|\xi| < \pi$. To prove (3.212) is the same as to prove that $\text{sgn}(\xi)$ has the Fourier expansion given by the left hand side of (3.212). Let $F(\xi) = \text{sgn}(\xi)$, then the Fourier coefficients of F are given by

$$\hat{F}_k = \frac{1}{2\pi} \int_{-\pi}^{\pi} F(\xi) e^{-ik\xi} d\xi = \frac{1}{\pi k i} (1 - (-1)^k) \ , \quad \text{for } k \neq 0 \ ,$$

and for $k = 0$, $\hat{F}_0 = 0$. This shows that,

$$\hat{F}_k = \begin{cases} \frac{2}{\pi i (2l+1)} & \text{if } k = 2l+1 \\ \\ 0 & \text{if } k = 2l \ . \end{cases}$$

Hence, by a classical result on the convergence of Fourier series for piecewise smooth functions, we obtain

$$F(\xi) = \mathrm{sgn}(\xi) = \sum_k \hat{F}_k e^{ik\xi} = \frac{2}{\pi i} \sum_{l=-\infty}^{\infty} \frac{e^{i(2l+1)\xi}}{2l+1} \ , \tag{3.213}$$

for $0 < |\xi| < \pi$, on which $F(\xi)$ is smooth. This proves (3.212), and consequently,

$$\tilde{K}_k = \frac{2}{\pi} \sum_{l=-\infty}^{\infty} \frac{e^{-i(2l+1)kh}}{(2l+1)} = i\mathrm{sgn}(-kh) = -i\mathrm{sgn}(k) \ . \tag{3.214}$$

Therefore

$$(\widehat{H_h f})_k = -i\mathrm{sgn}(k)\hat{f}_k \quad \text{for } k < N/2 \ , \tag{3.215}$$

where we have defined $\mathrm{sgn}(0) = 0$. Now from (3.215), it follows at once that

$$H_h(H_h) = (-i)^2 I = -I \ , \tag{3.216}$$

on functions with $\hat{f}_0 = \hat{f}_{N/2} = 0$. We turn now to the evaluation of the symbol for the operator given by

$$\begin{aligned} |D|f_i &\equiv \frac{1}{\pi} \sum_{(j-i)\ \mathrm{odd}} \frac{f_i - f_j}{(\alpha_i - \alpha_j)^2} 2h \\ &= \frac{1}{\pi} f_i \sum_{(j-i)\ \mathrm{odd}} \frac{2h}{(\alpha_i - \alpha_j)^2} - \frac{2h}{\pi} \sum_{(j-i)\ \mathrm{odd}} \frac{f_j}{(\alpha_i - \alpha_j)^2} \end{aligned}$$

Let us define,

$$G(\alpha_i) = \begin{cases} \frac{2}{\pi \alpha_i^2} & \text{if } i \text{ is odd} \\ \\ 0 & \text{if } i \text{ is even} \ . \end{cases}$$

Then $|D|$ may be written as

$$|D|f_i = \frac{1}{\pi h} f_i \sum_{l=-\infty}^{\infty} \frac{1}{(2l+1)^2} - (G * f)(\alpha_i) \ .$$

Hence, in Fourier space we obtain

$$(\widehat{|D|f})_k = \left[\frac{1}{\pi h} \sum_{l=-\infty}^{\infty} \frac{1}{(2l+1)^2} - \tilde{G}_k \right] \hat{f}_k \ ,$$

where

$$\tilde{G}_k = \frac{2h}{\pi} \sum_{l=-\infty}^{\infty} \frac{e^{-i(2l+1)kh}}{(2l+1)^2 h^2} = \frac{2}{\pi h} \sum_{l=-\infty}^{\infty} \frac{e^{-i(2l+1)kh}}{(2l+1)^2}$$

and using the identity

$$\sum_{l=-\infty}^{\infty} \frac{1}{(2l+1)^2} = \frac{\pi^2}{4} \ ,$$

we obtain

$$(\widehat{|D|f})_k = \left(\frac{\pi}{2h} - \frac{2}{\pi h} \sum_{l=-\infty}^{\infty} \frac{e^{-i(2l+1)kh}}{(2l+1)^2} \right) \hat{f}_k \ .$$

We claim that

$$\frac{2}{\pi} \sum_{l=-\infty}^{\infty} \frac{e^{i(2l+1)\xi}}{(2l+1)^2} = \frac{\pi}{2} - |\xi| \quad \text{for } |\xi| < \pi \quad . \tag{3.217}$$

As before, to verify (3.217) we extend $P(\xi) \equiv \frac{\pi}{2} - |\xi|$ periodically outside the interval $|\xi| < \pi$ with period 2π and then compute its Fourier coefficients. We have,

$$\hat{P}_k = \frac{1}{2\pi} \int_{-\pi}^{\pi} P(\xi) e^{-ik\xi} d\xi = \frac{1}{\pi k^2} (1 - (-1)^k) \ , \quad \text{for } k \neq 0 \ ,$$

and $\hat{P}_0 = 0$. This proves (3.217) since $P(\xi)$ is piecewise smooth and continuous at $\xi = 0$. It follows from (3.217) that

$$\frac{\pi}{2h} - \frac{2}{\pi h} \sum_{-\infty}^{\infty} \frac{e^{-i(2l+1)kh}}{(2l+1)^2} = \frac{|-kh|}{h} = |k| \ .$$

Hence

$$(\widehat{|D|f})_k = |k| \hat{f}_k \ . \tag{3.218}$$

On the other hand,

$$(H_h \widehat{(S_h f)})_k = -i \mathrm{sgn}(k) \cdot (ik) \hat{f}_k = |k| \hat{f}_k \quad \text{for } |kh| < \pi \ . \tag{3.219}$$

Therefore we conclude that

$$H_h(S_h f_i) = \frac{1}{\pi} \sum_{(j-i) \text{ odd}} \frac{f_i - f_j}{(\alpha_i - \alpha_j)^2} 2h \ , \tag{3.220}$$

for functions f with $\hat{f}_{N/2} = 0$. In Fourier space it is easy to verify that

$$H_h S_h = S_h H_h \ . \blacksquare \tag{3.221}$$

PROOF OF LEMMA 3.2 *

We have that

$$R_h(\phi_i^p) \equiv \sum_{(j-i) \text{ odd}} g(\alpha_i, \alpha_j)\phi_j^p 2h = \sum_{l=1}^{N/2} g(\alpha_i, \alpha_{i+2l-1})\phi_{i+2l-1}^p \, 2h \ .$$

where, using periodicity, we have switched to the interval $[0, 2\pi]$. Denote by $\hat{g}_k(\alpha)$ the Fourier coefficient of $g(\alpha, \beta)$ as a function of β. Then R_h can be written as

$$\begin{aligned} R_h(\phi_i^p) &= 2h \sum_{l=1}^{N/2} \sum_{k_1,k_2 \in I} \hat{g}_k(\alpha_i)\rho(k_2 h)\hat{\phi}_{k_2} e^{i(k_1+k_2)\alpha_{i+2l-1}} \\ &= 2h \sum_{k_1,k_2 \in I} \hat{g}_k(\alpha_i)\rho(k_2 h)\hat{\phi}_{k_2} e^{i(k_1+k_2)\alpha_{i-1}} \sum_{l=1}^{N/2} e^{i(k_1+k_2)\alpha_{2l}} \ . \end{aligned}$$

Note that if $k_1 + k_2 \neq 0 \bmod N/2$ then

$$\sum_{l=1}^{N/2} e^{i(k_1+k_2)\alpha_{2l}} = 0 \ .$$

Therefore,

$$\begin{aligned} R_h(\phi_i^p) &= \pi \sum_{\substack{k_1,k_2 \in I \\ k_1+k2=0 \bmod(N/2)}} \hat{g}_k(\alpha_i)\rho(k_2 h)\hat{\phi}_{k_2} e^{i(k_1+k_2)\alpha_{i-1}} \\ &= \pi \sum_{k_1 \in I} \hat{g}_{k_1}(\alpha_i)\rho(-k_1 h)\hat{\phi}_{-k_1} \\ &+ \pi \sum_{k_1=1}^{N/2} \hat{g}_{k_1}(\alpha_i)\rho((N/2-k_1)h)\hat{\phi}_{N/2-k_1} e^{i(N/2)\alpha_{i-1}} \\ &+ \pi \sum_{k_1=-N/2+1}^{-1} \hat{g}_{k_1}(\alpha_i)\rho((-N/2-k_1)h)\hat{\phi}_{-N/2-k_1} e^{-i(N/2)\alpha_{i-1}} \equiv I + II + III \ . \end{aligned}$$

Recall that $g(\alpha, \beta)$ is a smooth function in both variables, hence $\hat{g}_{k_1}(\alpha_i)$ is a smooth function in α_i. Moreover, $\hat{g}_{k_1}(\alpha_i)$ and its derivative in α_i decay like $O(k_1^{-m})$, where m is the degree of regularity of g, as a function of the second variable. Therefore, we have

$$|D_h^l I(\phi_i^p)| \leq C\|\phi\|_{l^2} \quad \text{for } 0 \leq l \leq m \ ,$$

and

$$|I(S_h^l \phi_i^p)| \leq C \sum_{k_1 \in I} |\hat{g}_{k_1}| \ |k_1|^l \, |\hat{\phi}_{k_1}| \, C\|\phi\|_{l^2} \quad \text{for } 0 \leq l \leq m-1 \ .$$

As a result $I = A_{-(m-1)}$. Note that in term II, $\hat{g}_{k_1}(\alpha_i)e^{i(N/2)\alpha_{i-1}}$ is not a smooth function in α_i. However since $\rho(\pi) = \rho'(\pi) = 0$, we get

$$|\rho(\pi - k_1 h)| = |\rho(\pi) + \frac{1}{2}\rho''(\pi)k_1^2 h^2 + \ldots| \leq Ck_1^2 h^2 \ .$$

Hence, it follows that

$$\begin{aligned} |II(\phi_i^p)| &\leq \pi \sum_{k_1=1}^{N/2} |\hat{g}_{k_1}(\alpha_i)| \ |\rho((N/2 - k_1)h)\hat{\phi}_{N/2-k_1}| \\ &\leq Ch^2 \sum_{k_1=1}^{N/2} k_1^{-m+2} \, |\hat{\phi}_{N/2-k_1}| \leq Ch^2 \|\phi\|_{l^2} \end{aligned}$$

since $m > 3$. This proves $II(\phi_i^p) = h^2 A_0(\phi_i)$. Similarly we can show $III = A_{-2}$. ∎

Proof of lemma 3.3.

From its definition (3.86), G_h^p may be written as

$$G_h^p \dot{\phi}_i = \sum_{\substack{k_1,k_2 \in I \\ k_1 + k2 = k \bmod N}} (\rho(k_2 h) - \rho(kh))\hat{f}_{k_1}\hat{\dot{\phi}}_{k_2} e^{ik\alpha_i} \ .$$

Now, note that

$$\rho(k_2 h) - \rho(kh) = \rho((k - k_1 \pm N)h) - \rho(kh) = \rho'(\bar{\xi})hk_1 \ .$$

Therefore

$$G_h^p \dot{\phi}_i = h \sum_{\substack{k_1,k_2 \in I \\ k_1 + k2 = k \bmod N}} \rho'(\bar{\xi})k_1 \hat{f}_{k_1}\hat{\dot{\phi}}_{k_2} e^{ik\alpha_i} \ .$$

Thus, $G_h^p \dot{\phi}_i = hA_0(\dot{\phi}_i)$, provided that

$$\sum_{k_1 \in I} |k_1||\hat{f}_{k_1}| \leq C \ ,$$

which holds true for $f \in C^2$. ∎

Proof of lemma 3.4

By the spectral approximation properties of the numerical method we know that

$$z_h^p(\alpha_i) = z(\alpha_i) + O(h^{m+3}) \ . \tag{3.222}$$

Let us consider the first term of $\dot{W}^{NL}$. Using (3.67) and (3.222), we obtain

$$\frac{1}{2\pi i}\sum_{(j-i)\text{ odd}}\frac{\dot{\sigma}_j\dot{\tilde{\gamma}}_j^p}{z_h^p(\alpha_i)-z_h^p(\alpha_j)}2h=(1+O(h^{m+3}))\frac{<\dot{\sigma}>_h}{2\pi i}\sum_{(j-i)\text{ odd}}\frac{R(\alpha_j)\dot{\tilde{\gamma}}_j^p}{z(\alpha_i)-z(\alpha_j)}2h\ ,$$

but

$$\frac{<\dot{\sigma}>_h}{2\pi i}\sum_{(j-i)\text{ odd}}\frac{R(\alpha_j)\dot{\tilde{\gamma}}_j^p}{z(\alpha_i)-z(\alpha_j)}2h=\frac{R(\alpha_i)<\dot{\sigma}>_h}{2\pi i z_\alpha(\alpha_i)}H_h\dot{\tilde{\gamma}}_i^p+\dot{\sigma}_iR_h(\dot{\tilde{\gamma}}_i^p)\ .$$

Therefore

$$\left\|\frac{1}{2\pi i}\sum_{(j-i)\text{ odd}}\frac{\dot{\sigma}_j\dot{\tilde{\gamma}}_j^p}{z_h^p(\alpha_i)-z_h^p(\alpha_j)}2h\right\|_{l^2}\le C\|\dot{\sigma}\|_\infty(\|\dot{\tilde{\gamma}}\|_{l^2}+\|A_{-2}(\dot{\tilde{\gamma}})\|_{l^2})\le Ch^3\|\dot{\tilde{\gamma}}\|_{l^2}\ .$$

The two other terms in $\dot{W}^{NL}$ require a different estimate. We illustrate the idea with one of the terms. First note that by assumption,

$$|z(\alpha_i)-z(\alpha_j)|\ge C|\alpha_i-\alpha_j|\ge Ch\quad\text{for } j-i \text{ odd.}$$

and in view of (3.222), for small h, we have

$$|z_h^p(\alpha_i)-z_h^p(\alpha_j)|\ge C|\alpha_i-\alpha_j|\ge Ch\quad\text{for } j-i \text{ odd.}$$

Also for small h and $t\le T^*$,

$$|z(\alpha_i)-z(\alpha_j)+\dot{z}_i^p-\dot{z}_j^p|\ge C|\alpha_i-\alpha_j|-ch^3\ge\frac{1}{2}C|\alpha_i-\alpha_j|\ . \tag{3.223}$$

Then for the second nonlinear term in $\dot{W}^{NL}$ we obtain

$$\begin{aligned}&\left\|\frac{1}{2\pi i}\sum_{(j-i)\text{ odd}}\frac{(\sigma\dot{\tilde{\gamma}}^p)_j(\dot{z}_i^p-\dot{z}_j^p)}{(z_h^p(\alpha_i)-z_h^p(\alpha_j))^2}2h\right\|_{l^2}\\ &\le\ C\|(\sigma\tilde{\gamma})^{\cdot}\|_\infty\|\dot{z}\|_{l^2}\max_i\sum_{(j-i)\text{ odd}}\frac{h}{|\alpha_i-\alpha_j|^2}\le\frac{C}{h}\|(\sigma\tilde{\gamma})^{\cdot}\|_\infty\|\dot{z}\|_{l^2}\\ &\le\ \frac{C}{h}h^3\|\dot{z}\|_{l^2}\le Ch^2(\|\dot{\sigma}\|_{l^2}+\|\dot{\theta}\|_{l^2})\ ,\end{aligned}$$

where we have used Young's inequality in the estimate that involves $\dot{z}_j^p$ in the numerator. The last term is estimated similarly, except that (3.223) is used instead of (3.222). Therefore we conclude that

$$\dot{W}_i^{NL}=A_{-2}(\dot{\sigma}_i,\dot{\theta}_i,\dot{\tilde{\gamma}}_i).\quad\blacksquare$$

PROOF OF LEMMA 3.5 *.

From the assumption, we know that $\rho \in C^2[-\pi,\pi]$, that ρ is even and $\rho(\pm\pi) = \rho'(\pm\pi) = 0$. Let us define $Q(\xi) \equiv \xi\rho(\xi)$. Then $Q \in C^2[-\pi,\pi]$, $Q(\pm\pi) = Q'(\pm\pi) = 0$, and Q is odd. Note that if Q is extended periodically with period 2π, then Q is C^1 everywhere, and C^2 except for possible jumps in Q'' at $\xi = \pm m\pi$.

Now assume that f is smooth and $\phi \in l^2$. Then we have

$$(f \cdot \phi)(\alpha) = \sum_{k_1,k_2 \in I} \hat{f}_{k_1} \hat{\phi}_{k_2} e^{i(k_1+k_2)\alpha} \ .$$

Let $k = k_1 + k_2$ and consider one term in two cases:

(1) Suppose $k = k_1 + k_2 \in I$. Then we get

$$D_h e^{ik\alpha} = ik\rho(kh)e^{ik\alpha} = \frac{i}{h} Q(kh) e^{ik\alpha} \ .$$

Now use Taylor's theorem with remainder to expand Q around $k_2 h$.

$$Q(kh) = Q(k_2 h) + Q'(k_2 h)k_1 h + k_1^2 h^2 \int_0^1 (1-t)Q''(k_2 h + tk_1 h)dt \ .$$

Thus we obtain

$$D_h e^{ik\alpha} = e^{ik_1\alpha}(D_h e^{ik_2\alpha}) + (ik_1 e^{ik_1\alpha})Q''(k_2 h)e^{ik_2\alpha} + hC_{k_1 k_2} k_1^2 e^{ik\alpha} \ , \tag{3.224}$$

and $C_{k_1 k_2}$ is bounded independent of k_1, k_2.

(2) Suppose $k = k_1 + k_2 > N/2$. Let $\tilde{k} = k - N$. Then

$$D_h e^{i(k_1+k_2)\alpha} = i\tilde{k}\rho(\tilde{k}h)e^{i\tilde{k}\alpha} = \frac{i}{h} Q(\tilde{k}h) e^{i\tilde{k}\alpha} \ .$$

Now extend Q periodically past $\pi = \frac{N}{2}h$. As noted earlier, Q is in C^1 and C^2 except for jumps of Q'' at π. The Taylor's formula is still valid and the same argument works;

$$Q(\tilde{k}h) = Q(kh) = Q(k_2 h) + \ldots$$

Of course, if $k_1 + k_2 < -N/2$, we can argue similarly.

The first two terms in (3.224) give the two main terms of (3.101). We still need to estimate the error term and show that it is bounded in l^2 by $Ch\|\phi\|_{l^2}$. Omitting h the coefficient of $e^{ik\alpha}$, $k \in I$ is

$$\sum_{k_1+k_2=k \bmod N} C_{k_1 k_2} k_1^2 \hat{f}_{k_1} \hat{\phi}_{k_2}$$

We can think of this as a discrete integral operator taking a function of k_2 to a function of k. Using the discrete version of Young's inequality, we conclude that the operator is bounded in l^2 provided that

$$\sum_{k_1 \in I} k_1^2 \, |\hat{f}_{k_1}| \leq C$$

which holds since $f \in C^3$. ∎

PROOF OF LEMMA 3.6

In order to simplify the notation let us write

$$K(\alpha_i, \alpha_j) \equiv \frac{1}{(z_h^p(\alpha_i) - z_h^p(\alpha_j))^2} \quad ; \quad K_{ij} = \frac{1}{(z_i^p - z_j^p)^2}$$

and define the variation

$$\dot{K}_{ij} \equiv K_{ij} - K(\alpha_i, \alpha_j) \; .$$

By direct computation it follows that

$$\begin{aligned}
\dot{F}_i^{(2)NL} &= 2ARe \left\{ \frac{z_\alpha(\alpha_i)}{2\pi i} \sum_{(j-i) \text{ odd}} \frac{d\dot{\gamma}_j}{dt} \frac{\dot{z}_i^p - \dot{z}_j^p}{(z_h^p(\alpha_i) - z_h^p(\alpha_j))^2} 2h \right\} \\
&- 2ARe \left\{ \frac{z_\alpha(\alpha_i)}{2\pi i} \sum_{(j-i) \text{ odd}} \frac{\frac{d\gamma_j}{dt}(\dot{z}_i^p - \dot{z}_j^p)^2 2h}{(z_h^p(\alpha_i) - z_h^p(\alpha_j))^2 (z_h^p(\alpha_i) - z_h^p(\alpha_j) + \dot{z}_i^p - \dot{z}_j^p)} \right\} \\
&+ 2ARe \left\{ \frac{(\sigma e^{i\theta})_i^{\cdot}}{2\pi i} \sum_{(j-i) \text{ odd}} \frac{\frac{d\gamma_j}{dt}}{z_i^p - z_i^p} 2h \right\} \\
&+ 2ARe \left\{ \frac{z_\alpha(\alpha_i)}{2\pi i} \sum_{(j-i) \text{ odd}} \gamma^p(\alpha_j) (\frac{dz_h}{dt}(\alpha_i) - \frac{dz_h}{dt}(\alpha_j)) \dot{K}_{ij}^{NL} 2h \right\} \\
&+ 2ARe \left\{ \frac{z_\alpha(\alpha_i)}{2\pi i} \sum_{(j-i) \text{ odd}} \gamma^p(\alpha_j) (\frac{d\dot{z}_i}{dt} - \frac{d\dot{z}_j}{dt}) \dot{K}_{ij} 2h \right\} \\
&+ 2ARe \left\{ \frac{z_\alpha(\alpha_i)}{2\pi i} \sum_{(j-i) \text{ odd}} \dot{\gamma}_j^p (\frac{d\dot{z}_i}{dt} - \frac{d\dot{z}_j}{dt}) K(\alpha_i, \alpha_j) 2h \right\} \\
&+ 2ARe \left\{ \frac{z_\alpha(\alpha_i)}{2\pi i} \sum_{(j-i) \text{ odd}} \dot{\gamma}_j^p (\frac{d\dot{z}_i}{dt} - \frac{d\dot{z}_j}{dt}) K_{ij} 2h \right\} \\
&\equiv I + II + III + IV + V + VI + VII \; ,
\end{aligned}$$

where

$$\dot{K}_{ij} = -\frac{2(\dot{z}_i^p - \dot{z}_j^p)}{(z_h^p(\alpha_i) - z_h^p(\alpha_j))^3} + \dot{K}_{ij}^{NL}$$

and

$$\dot{K}_{ij}^{NL} = \frac{3(z_h^p(\alpha_i) - z_h^p(\alpha_j))(\dot{z}_i^p - \dot{z}_j^p)^2 + (\dot{z}_i^p - \dot{z}_j^p)^3}{(z_h^p(\alpha_i) - z_h^p(\alpha_j))^3(z_h^p(\alpha_i) - z_h^p(\alpha_j) + \dot{z}_i^p - \dot{z}_j^p)^2} \ .$$

Clearly, terms I and II can be estimated just as we did for similar terms in $\dot{W}^{NL}$. With exactly the same argument, it follows that

$$\begin{aligned} \|I\|_{l^2} &\leq \frac{C}{h}\|\frac{d\dot{\gamma}}{dt}\|_\infty \|\dot{z}\|_{l^2} \leq C(\|\dot{\sigma}\|_{l^2} + \|\dot{\theta}\|_{l^2}) \ , \\ \|II\|_{l^2} &\leq C(\|\dot{\sigma}\|_{l^2} + \|\dot{\theta}\|_{l^2}) \ . \end{aligned}$$

Also, in view of (3.65) we have

$$\begin{aligned} \|(\sigma e^{i\theta})^{\cdot}\|_{l^2} &\leq C(\|\dot{\sigma}\|_{l^2} + \|\dot{\theta}\|_{l^2}) \ , \\ \|(\sigma e^{i\theta})^{\cdot}\|_\infty &\leq Ch^3 \ , \end{aligned}$$

for $t \leq T^*$. Thus, $III = A_0(\dot{\sigma}_i, \dot{\theta}_i)$. In order to estimate term IV, we first note that

$$F(\alpha, \beta) \equiv \gamma(\beta)\frac{\frac{dz}{dt}(\alpha) - \frac{dz}{dt}(\beta)}{z(\alpha) - z(\beta)}$$

is a smooth bounded function since $z_\alpha \neq 0$. Using (3.4) we obtain

$$\begin{aligned} \|IV\|_{l^2} &= \left\| 2ARe\left\{ \frac{z_\alpha(\alpha_i)}{2\pi i} \sum_{(j-i) \text{ odd}} \gamma^p(\alpha_j)(\frac{dz_h}{dt}(\alpha_i) - \frac{dz_h}{dt}(\alpha_j))\dot{K}_{ij}^{NL} 2h \right\} \right\|_{l^2} \\ &\leq C\|\dot{z}\|_\infty \|\dot{z}\|_{l^2} \max_i \sum_{(j-i) \text{ odd}} \frac{h}{|i-j|^3 h^3} \\ &+ C\|\dot{z}\|_\infty^2 \|\dot{z}\|_{l^2} \max_i \sum_{(j-i) \text{ odd}} \frac{h}{|i-j|^4 h^4} \\ &\leq Ch\|\dot{z}\|_{l^2} \leq Ch(\|\dot{\sigma}\|_{l^2} + \|\dot{\theta}\|_{l^2}) \ . \end{aligned}$$

Without much modification, similar arguments can be used to estimate the remaining terms . Therefore

$$\dot{F}_i^{(2)NL} = A_0(\dot{\sigma}_i, \dot{\theta}_i, \dot{\tilde{\gamma}}_i) \tag{3.225}$$

for $t \leq T^*$. ∎

PROOF OF LEMMA 3.7

First we state a result for the corresponding continuous problem. Let

$$K\psi(\alpha) = \int 2ARe\left\{\frac{1}{2\pi i}\left[\frac{z_\alpha(\alpha)}{z(\alpha)-z(\alpha')}\right]\right\}\psi(\alpha')\,d\alpha' \ ,$$

with $z(\alpha,t)$ smooth and $z_\alpha \neq 0$. It has been shown in [8] that $(I+K)$ has a bounded inverse, that is

$$\|(I+K)^{-1}\|_{L^2} \leq C \ .$$

We now proceed to prove that $I+K_h$ is invertible. Let us consider first the operator given by

$$\bar{K}_h\psi_i = \sum_{(j-i)\ \text{odd}} 2ARe\left\{\frac{1}{2\pi i}\left[\frac{z_\alpha(\alpha_i)}{z(\alpha_i)-z(\alpha_j)}\right]\right\}\psi_j\,2h \ .$$

For any discrete l^2 function ψ , we define ϕ by

$$\phi_i = \psi_i + \bar{K}_h\psi_i \ .$$

We shall show that $\phi = 0$ implies that $\psi = 0$, from which it follows the invertibility of $I+\bar{K}_h$. Let $I_i = [\alpha_i - h \ , \ \alpha_i + h]$. We say that $\alpha \in I_i$ if α_i is the closest mesh point to α. If $\alpha \in I_i$ with i odd, we partition the real line as the union of I_i with i even. Define

$$K^o(\alpha,\alpha') = \begin{cases} 2ARe\left\{\frac{1}{2\pi i}\left[\frac{z_\alpha(\alpha_i)}{z(\alpha_i)-z(\alpha_j)}\right]\right\} & \text{if } \alpha \in I_i, \quad \alpha' \in I_j \quad \text{for } i \text{ odd and } j \text{ even} \\ \\ 0 & \text{otherwise.} \end{cases}$$

If $\alpha \in I_i$ with i even, we partition the real line as the union of I_i with i odd. Define $K^e(\alpha,\alpha')$ as the corresponding piecewise constant kernel. Moreover define $f^o(\alpha) = \psi_i$, and $\phi^o(\alpha) = \phi_i$ if $\alpha \in I_i$ and i is odd. Similarly, define $f^e(\alpha) = \psi_i$, and $\phi^e(\alpha) = \phi_i$ if $\alpha \in I_i$ and i is even. Note that because of the alternating point quadrature rule, when i is odd, $\bar{K}_h\psi_i$ uses only those ψ_j with j even and vice versa. Thus for odd valued index i, we have

$$\psi_i + \bar{K}_h\psi_i = f^o(\alpha_i) + \int K^o(\alpha_i,\alpha')f^e(\alpha')d\alpha' \ ,$$

and for even valued index i,

$$\psi_i + \bar{K}_h\psi_i = f^e(\alpha_i) + \int K^e(\alpha_i,\alpha')f^o(\alpha')d\alpha' \ .$$

Let us consider first the case $\alpha \in I_i$ with i odd. We have

$$\int K^o(\alpha_i,\alpha')f^e(\alpha')d\alpha' = \sum_{(j-i)\text{ odd}} \int_{\alpha'\in I_j} 2ARe\left\{\frac{1}{2\pi i}\left[\frac{z_\alpha(\alpha_i)}{z(\alpha_i)-z(\alpha_j)}\right]\right\} f^e(\alpha')d\alpha',$$

and

$$Re\left\{\frac{2A}{2\pi i}\int \frac{z_\alpha(\alpha)f^e(\alpha')}{z(\alpha)-z(\alpha')}d\alpha'\right\} = \sum_{(j-i)\text{ odd}} \int_{\alpha'\in I_j} 2ARe\left\{\frac{1}{2\pi i}\left[\frac{z_\alpha(\alpha)}{z(\alpha)-z(\alpha')}\right]\right\} f^e(\alpha')d\alpha' \ .$$

Thus for $\alpha \in I_i$ with i odd, we may write

$$\begin{aligned}\int K^o(\alpha_i,\alpha')f^e(\alpha')d\alpha' &= Re\left\{\frac{2A}{2\pi i}\int \frac{z_\alpha(\alpha)f^e(\alpha')}{z(\alpha)-z(\alpha')}d\alpha'\right\} \\ &+ \sum_{(j-i)\text{ odd}} \int_{\alpha'\in I_j} 2ARe\left\{\frac{1}{2\pi i}\left[\frac{z_\alpha(\alpha_i)}{z(\alpha_i)-z(\alpha_j)} - \frac{z_\alpha(\alpha)}{z(\alpha)-z(\alpha')}\right]\right\} f^e(\alpha')d\alpha' \ .\end{aligned}$$

Let

$$Q(\alpha,\alpha') = Re\left\{\frac{2A}{2\pi i}\cdot\frac{z_\alpha(\alpha)}{z(\alpha)-z(\alpha')}\right\} = Re\left\{\frac{A}{\pi i(\alpha-\alpha')} + G(\alpha,\alpha')\right\} = Re\{G(\alpha,\alpha')\} \ ,$$

where $G(\alpha,\alpha')$ is smooth in both variables. Therefore $Q(\alpha,\alpha')$ is smooth. Thus

$$\begin{aligned}Q(\alpha_i,\alpha_j) - Q(\alpha,\alpha') &= Q_\alpha(\alpha_i+\eta_i,\alpha_j)(\alpha_i-\alpha) + Q_{\alpha'}(\alpha_i+\eta_i,\alpha_j+\xi_j)(\alpha_j-\alpha') \\ &= hF(\alpha_i,\alpha_j,\alpha,\alpha') \ ,\end{aligned}$$

for some bounded function F, and as a result

$$\int K^o(\alpha_i,\alpha')f^e(\alpha')d\alpha' = Re\left\{\frac{2A}{2\pi i}\int \frac{z_\alpha(\alpha)f^e(\alpha')}{z(\alpha)-z(\alpha')}d\alpha'\right\} + h\sum_{(j-i)\text{ odd}} \tilde{F}(\alpha_i,\alpha_j,\alpha)f^e(\alpha_j)h$$

for some bounded function $\tilde{F}$. Hence, for $\alpha \in I_i$ with i odd, the equation

$$\psi_i + \bar{K}_h\psi_i = \phi_i \tag{3.226}$$

is equivalent to

$$f^o + Kf^e + hL_ef^e = \phi^o \ ,$$

where L_e is a bounded linear operator generated from $\tilde{F}$. Similarly, we can show that for $\alpha \in I_i$ with i even, equation (3.226) is equivalent to

$$f^e + Kf^o + hL_of^o = \phi^e \ ,$$

where L_o is a bounded linear operator. Now we adding the equations for f^e and f^o we obtain, $f^e + f^o$ and $f^e - f^o$ as follows

$$(f^e + f^o) + K(f^e + f^o) = \phi^o + \phi^e - hL_o f^o - hL_e f^e \ .$$

Since $I + K$ has a bounded inverse [8], it follows that

$$\|f^e + f^o\|_{L^2} \leq C(\|\phi^o + \phi^e\|_{L^2} + h\|\psi\|_{l^2} \ ,$$

which implies that

$$\|\psi\|_{l^2} \leq \tilde{C}\|\phi\|_{l^2}$$

where $\tilde{C}$ is a constant independent of h. This shows $I + \bar{K}_h$ is invertible since $\phi = 0$ implies $\psi = 0$. The above estimate shows that the operator is bounded. Furthermore we note that

$$\frac{z_\alpha(\alpha_i)}{z(\alpha_i) - z(\alpha_j)} - \frac{z_\alpha(\alpha_i)}{z_h^p(\alpha_i) - z_h^p(\alpha_j)} = h^{m+3} O((\alpha_i - aj)^{-2}) = hL$$

where L is a bounded operator. Hence, for small h, $I + K_h$ is invertible with a bounded inverse independent of h. ∎

Proof of lemma 3.8.

First note Parseval's relation

$$(u \ , \ v)_h \equiv \sum_{j=-N/2+1}^{N/2} u_j v_j h = 2\pi \sum_{k=-N/2+1}^{N/2} \hat{u}_k \hat{v}_k^* \ .$$

Let us now show part (i) of this lemma. We have that

$$|(f\Lambda_h(I - P_M)\phi \ , \ (\Lambda_h - g)P_M\psi)_h| \leq |(\Lambda_h(I - P_M)\phi \ , \ f\Lambda_h P_M\psi)_h| + |(\Lambda_h(I - P_M)\phi \ , \ fgP_M\psi)_h| = L_1 + L_2 \ . \tag{3.227}$$

Now,

$$\begin{aligned} \frac{1}{2\pi} L_1 &= | \sum_{\substack{k \in I \\ |k| < M}} \rho(kh) \, |k| \, \hat{\phi}_k (f\widehat{\Lambda_h P_M \psi})_k^* \ | \\ &\leq \sum_{\substack{k \in I \\ |k| < M}} \rho(kh) \, |k| \ |\hat{\phi}_k| \sum_{\substack{l \in I \\ (k-l) \in I}} |\hat{f}_l| \, \rho((k-l)h) \, |k-l| \ |\hat{\psi}_{k-l}| \end{aligned}$$

$$
\begin{aligned}
&+ \sum_{\substack{k\in I\\ |k|<M}} \rho(kh)\,|k|\;|\hat{\phi}_k| \sum_{\substack{l\in I\\ (k-l+N)\in I}} |\hat{f}_l|\,\rho((k-l+N)h)\,|k-l+N|\;|\hat{\psi}_{k-l+N}| \\
&+ \sum_{\substack{k\in I\\ |k|<M}} \rho(kh)\,|k|\;|\hat{\phi}_k| \sum_{\substack{l\in I\\ (k-l-N)\in I}} |\hat{f}_l|\,\rho((k-l-N)h)\,|k-l-N|\;|\hat{\psi}_{k-l-N}| \\
&= L_{11} + L_{12} + L_{13}\ .
\end{aligned}
$$

For L_{11} we have,

$$
\begin{aligned}
L_{11} &\leq M \sum_{\substack{k\in I\\ |k|<M}} |\hat{\phi}_k| \sum_{\substack{l\in I\\ (k-l)\in I}} |\hat{f}_l|\,(M+|l|\,)\,|\hat{\psi}_{k-l}| \\
&\leq M \sum_{l\in I} |\hat{f}_l|\,(M+|l|\,) \sum_{k\in I} |\hat{\phi}_k|\;|\hat{\psi}_{k-l}| \;\leq C\|\phi\|_{l^2}\|\psi\|_{l^2}\ .
\end{aligned}
$$

To estimate the aliasing term L_{12}, we first note that since $|k| < M$ and $l \in I$

$$
k - l + N > -M - l + N \geq 0\ .
$$

Furthermore since $k - l + N \in I$ we have that

$$
0 \leq k - l + N \leq N/2\ , \tag{3.228}
$$

and multiplying by two (3.228) we obtain

$$
2k + N \leq 2l \quad \text{or} \quad k + k + N \leq l + l\ .
$$

Hence

$$
0 \leq k - l + N \leq l - k\ ,
$$

and thus

$$
|k - l + N| \;\leq\; |l - k| \;\leq\; |l| + M\ .
$$

Therefore

$$
\begin{aligned}
L_{12} &\leq M \sum_{\substack{k\in I\\ |k|<M}} |\hat{\phi}_k| \sum_{\substack{l\in I\\ (k-l+N)\in I}} |\hat{f}_l|\,(M+|l|\,)\,|\hat{\psi}_{k-l+N}| \\
&\leq M \sum_{l\in I} |\hat{f}_l|\,(M+|l|\,) \sum_{l\in I} |\hat{\phi}_k|\;|\hat{\psi}_{k-l+N}| \;\leq C\|\phi\|_{l^2}\|\psi\|_{l^2}\ .
\end{aligned}
$$

Similarly for the other aliasing term L_{13} we have that

$$
-N/2 + 1 \leq k - l - N \leq 0\ ,
$$

which implies that

$$\frac{N}{2} - k \leq -l - 2 \ ,$$

and again multiplying by 2 this inequality we obtain

$$|k - l - N| \ = N - k + l \leq \ |l| \ + M + 4$$

and thus the estimate for L_{12} holds also for L_{13}. Therefore

$$L_1 \leq C\|\phi\|_{l^2}\|\psi\|_{l^2} \ .$$

Finally for L_2, we have

$$\begin{aligned} L_2 &= |(\Lambda_h(I - P_M)\phi \ , \ fgP_M\psi)_h| \\ &\leq 2\pi M \sum_{|k|<M} |\hat{\phi}_k| \ |(\tilde{f}\widehat{PM\psi})_k| \leq C\|\phi\|_{l^2}\|\psi\|_{l^2} \ . \end{aligned}$$

which completes the proof for (i). Clearly, parts $(ii\text{-}iv)$ can be shown analogously. ∎

Proof of lemma 3.9.

Part (i) : We have that

$$\begin{aligned} |(\Lambda_h\psi \ , \ f\phi)_h| &= |((\Lambda_h + I)\psi \ , \ f\phi)_h - (\psi \ , \ f\phi)_h| \\ &\leq |((\Lambda_h + I)\psi \ , \ f\phi)_h| + C\|\phi\|_{l^2}\|\psi\|_{l^2} \ , \end{aligned}$$

and

$$\begin{aligned} \frac{1}{2\pi}\,|((\Lambda_h + I)\psi \ , \ f\phi)_h| &= \left|\sum_{k\in I}(\rho(kh)\,|k| \ + 1)\hat{\psi}_k(\hat{f\phi})^*_k\right| \\ &\leq \sum_{k\in I}(\rho(kh)\,|k| \ + 1)\,|\hat{\psi}_k| \sum_{\substack{l\in I \\ (k-l)\in I}} |\hat{f}_l| \ |\hat{\phi}_{k-l}| \\ &+ \sum_{k\in I}(\rho(kh)\,|k| \ + 1)\,|\hat{\psi}_k| \sum_{\substack{l\in I \\ (k-l+N)\in I}} |\hat{f}_l| \ |\hat{\phi}_{k-l+N}| \\ &+ \sum_{k\in I}(\rho(kh)\,|k| \ + 1)\,|\hat{\psi}_k| \sum_{\substack{l\in I \\ (k-l-N)\in I}} |\hat{f}_l| \ |\hat{\phi}_{k-l-N}| \\ &= R_1 + R_2 + R_3 \ . \end{aligned}$$

Now

$$\begin{aligned} R_1 &\equiv \sum_{k\in I}(\rho(kh)\,|k|\,+1)\,|\hat{\psi}_k| \sum_{\substack{l\in I\\(k-l)\in I}} |\hat{f}_l|\;|\hat{\phi}_{k-l}| \\ &= \sum_{k\in I}\sum_{\substack{l\in I\\(k-l)\in I}} |\hat{f}_l|\,(\rho(kh)\,|k|\,+1)^{1/2}\,|\hat{\psi}_k|\,(\rho((k-l)h)\,|k-l|\,+1)^{1/2}\,|\hat{\phi}_{k-l}|\,Q_{kl}\ , \end{aligned}$$

where

$$\begin{aligned} Q_{kl}^2 &\equiv \frac{\rho(kh)\,|k|\,+1}{\rho((k-l)h)\,|k-l|\,+1} = \frac{[\rho((k-l)h)+\rho'(\bar{\xi})lh]\,|k|\,+1}{\rho((k-l)h)\,|k-l|\,+1} \\ &= \frac{\rho_{kl}\,|k|\,+1}{\rho_{kl}\,|k-l|\,+1} + \frac{\rho'(\bar{\xi})\,|k|\,lh+1}{\rho_{kl}\,|k-l|\,+1}\ , \end{aligned}$$

and we have set $\rho_{kl}\equiv\rho((k-l)h)$. We observe now that

$$\frac{\rho_{kl}\,|k|\,+1}{\rho_{kl}\,|k-l|\,+1} = \begin{cases} 2\,|l|\,+1 & \text{if } |k|\le 2l \\ \frac{\rho_{kl}\,|k|+1}{\frac{1}{2}\rho_{kl}\,|k|+1} & \text{if } |k|>2l\ . \end{cases}$$

Therefore

$$Q_{kl}^2 \le C(1+\,|l|\,) \quad \text{for all } \ k\in I\ ,$$

and as a result we have for R_1,

$$\begin{aligned} R_1 &\le C\sum_{l\in I}(1+\,|l|\,)^{1/2}\,|\hat{f}_l| \\ &\quad \sum_{k\in I}(\rho(kh)\,|k|\,+1)^{1/2}\,|\hat{\psi}_k|\,(\rho((k-l)h)\,|k-l|\,+1)^{1/2}\,|\hat{\phi}_{k-l}| \\ &\le (C\sum_{l\in I}(1+\,|l|\,)^{1/2}\,|\hat{f}_l|\,)\|\phi\|_{H_h^{1/2}}\|\psi\|_{H_h^{1/2}} \le C\|\phi\|_{H_h^{1/2}}\|\psi\|_{H_h^{1/2}}\ , \end{aligned}$$

because $f\in C^2$.

We proceed now with the aliasing terms. For R_2 we first note that since k and $k-l+N\in I$ it follows that, for $|k|>2l$

$$k-l+N \ge N-(l+\,|k|\,) > N-\frac{3}{2}\,|k|\,> 2\,|k|\,-\frac{3}{2}\,|k|\,=\frac{1}{2}\,|k|\ , \tag{3.229}$$

that is

$$|k-l+N|\,\ge\frac{1}{2}\,|k| \quad \text{for } |k|>2l\ . \tag{3.230}$$

Consequently

$$\frac{\rho_{kl}\,|k|\,+1}{\rho_{kl}\,|k-l+N|\,+1} \leq \begin{cases} 2\,|l|\,+1 & \text{if } |k| \leq 2l \\ \\ \frac{\rho_{kl}\,|k|+1}{\frac{1}{2}\rho_{kl}\,|k|+1} & \text{if } |k| > 2l\ . \end{cases}$$

Therefore the same type of estimate for R_1 can be applied to R_2. A similar argument can be used for the other aliasing term R_3. Thus, we conclude that

$$|((\Lambda_h + I)\phi\ ,\ f\psi)_h| \leq C\|\phi\|_{H_h^{1/2}}\|\psi\|_{H_h^{1/2}}$$

which proves part (i). Part (ii) follow exactly the same argument as before.

For part (iii) we have that

$$\left|(\Lambda_h\psi\ ,\ fS_hG_h^p\phi)_h\right| \leq \left|((\Lambda_h + I)\psi\ ,\ fS_hG_h^p\phi)_h\right| + C\|\phi\|_{l^2}\|\psi\|_{l^2}\ ,$$

and using Parseval's relation we obtain for the first term,

$$A \equiv \left|((\Lambda_h + I)\psi\ ,\ fS_hG_h^p\phi)_h\right| = 2\pi|\sum_{k\in I}(\rho(kh)\,|k|\,+1)\hat{\psi}_k \sum_{\substack{k_1+k_2=k \bmod N \\ k_1,k_2\in I}} \hat{f}^*_{k_1} ik_2 (\widehat{G_h^p\phi})^*{}_{k_2}|\ ,$$

but

$$(\widehat{G_h^p\phi})_{k_2} = \sum_{\substack{l_1+l_2=k_2 \bmod N \\ l_1,l_2\in I}} (\rho(l_2h) - \rho(k_2h))\hat{g}_{l_1}\hat{\phi}_{l_2} = h\sum_{\substack{l_1+l_2=k_2 \bmod N \\ l_1,l_2\in I}} \rho'(\bar{\xi})l_1\hat{g}_{l_1}\hat{\phi}_{l_2}\ ,$$

because

$$\rho(l_2h) - \rho(k_2h) = \rho((k_2 - l_1 \pm N)h) - \rho(k_2h) = \rho((k_2 - l_1)h) - \rho(k_2h) = \rho'(\bar{\xi})l_1h\ .$$

Thus

$$A \leq C\sum_{k\in I}(\rho(kh)\,|k|\,+1)\,|\hat{\psi}_k| \sum_{\substack{k_1+k_2=k \bmod N \\ k_1,k_2\in I}} |\hat{f}_{l_1}| \sum_{\substack{l_1+l_2=k_2 \bmod N \\ l_1,l_2\in I}} |l_1|\ |\hat{g}_{l_1}|\ |\hat{\phi}_{l_2}|\ .$$

Let us consider now the case $k_1 + k_2 = k$. Then we have the following terms

$$\begin{aligned} B_1 \ &\equiv\ \sum_{k\in I}(\rho(kh)\,|k|\,+1)\,|\hat{\psi}_k| \sum_{\substack{l\in I \\ k-l\in I}} |\hat{f}_{l_1}| \sum_{\substack{m\in I \\ k-l-m\in I}} |m|\ |\hat{g}_m|\ |\hat{\phi}_{k-l-m}| \\ &+\ \sum_{k\in I}(\rho(kh)\,|k|\,+1)\,|\hat{\psi}_k| \sum_{\substack{l\in I \\ k-l\in I}} |\hat{f}_{l_1}| \sum_{\substack{m\in I \\ k-l-m\pm N\in I}} |m|\ |\hat{g}_m|\ |\hat{\phi}_{k-l-m\pm N}| \\ &=\ B_{11} + B_{12}\ . \end{aligned}$$

Just as we did in part (i) we write B_{11} as follows,

$$\begin{aligned} B_{11} &= \sum_{k\in I}(\rho(kh)\,|k|\,+1)^{1/2}\,|\hat{\psi}_k| \sum_{\substack{l\in I\\ k-l\in I}} |\hat{f}_{l_1}| \\ &\quad\cdot \sum_{\substack{m\in I\\ k-l-m\in I}} |m|\;|\hat{g}_m|\,(\rho((k-l-m)h)\,|k-l-m|\,+1)^{1/2}\,|\hat{\phi}_{k-l-m}|\,Q\;, \end{aligned}$$

where

$$Q^2 \equiv \frac{\rho(kh)\,|k|\,+1}{\rho((k-l-m)h)\,|k-l-m|\,+1} = \frac{\rho(kh)\,|k|\,+1}{\rho((k-\tilde{l})h)\,|k-\tilde{l}|\,+1}\;,$$

and we have set $\tilde{l} \equiv l+m$. Clearly we can use the same argument as in part (i) to conclude that

$$Q^2 \le C(1+\,|\tilde{l}|\,) \le C(1+\,|l|\,+\,|m|\,)\;.$$

Hence

$$\begin{aligned} B_{11} &\le C\sum_{k\in I}\sum_{m\in I}(1+\,|l|\,^{1/2}+\,|m|\,^{1/2})\,|m|\;|\hat{f}_l|\;|\hat{g}_m| \\ &\quad\cdot\sum_{k\in I}(\rho(kh)\,|k|\,+1)^{1/2}\,|\hat{\psi}_k|\,(\rho((k-l-m)h)\,|k-l-m|\,+1)^{1/2}\,|\hat{\phi}_{k-l-m}|\;. \end{aligned}$$

Thus, using Schwarz inequality and the smoothness of f and g, we obtain

$$B_{11} \le C\|\phi\|_{H_h^{1/2}}\|\psi\|_{H_h^{1/2}}\;.$$

On the other hand,

$$\begin{aligned} B_{12} &= \sum_{k\in I}(\rho(kh)\,|k|\,+1)^{1/2}\,|\hat{\psi}_k| \sum_{l\in I} |\hat{f}_l| \\ &\quad\cdot \sum_{\substack{m\in I\\ k-l-m\pm N\in I}} |m|\;|\hat{g}_m|\,(\rho((k-l-m\pm N)h)\,|k-l-m\pm N|\,+1)^{1/2}\,|\hat{\phi}_{k-l-m\pm N}|\,Q_\pm\;, \end{aligned}$$

where

$$Q_\pm^2 \equiv \frac{\rho(kh)\,|k|\,+1}{\rho((k-l-m)h)\,|k-l-m\pm N|\,+1}\;.$$

Let us consider the case Q_+. The other case, Q_-, can be handled similarly. We have,

$$Q_+^2 \equiv \frac{\rho(kh)\,|k|\,+1}{\rho((k-\tilde{l})h)\,|k-\tilde{l}+N|\,+1}\;, \quad \text{with } \tilde{l} = l+m\;.$$

Exactly by the same argument as in (3.229), with $\tilde{l}$ instead of l, it follows that

$$Q_+^2 \le C(1+\,|\tilde{l}|\,) \le C(1+\,|l|\,+\,|m|\,)\;,$$

and therefore, the estimate for B_{11} applies also for B_{12}. Thus,

$$B_{12} \leq C\|\phi\|_{H_h^{1/2}}\|\psi\|_{H_h^{1/2}} \tag{3.231}$$

Now consider the case $k_1+k_2 = k+N$ (the other case $k_1+k_2 = k-N$, can be treated analogously). Its contribution is a term of the following form,

$$\begin{aligned} B_2 \;\equiv\; & \sum_{k\in I}(\rho(kh)\,|k|\,+1)\,|\hat{\psi}_k| \sum_{l\in I}|\hat{f}_{l_1}| \sum_{\substack{m\in I \\ k-l-m+N\in I}} |m|\;|\hat{g}_m|\;|\hat{\phi}_{k-l-m+N}| \\ + \;& \sum_{k\in I}(\rho(kh)\,|k|\,+1)\,|\hat{\psi}_k| \sum_{l\in I}|\hat{f}_{l_1}| \sum_{\substack{m\in I \\ k-l-m+2N\in I}} |m|\;|\hat{g}_m|\;|\hat{\phi}_{k-l-m+2N}| \;, \end{aligned}$$

Which has the same structure as B_{12}, and consequently similar arguments show that (3.231) also holds for B_2. Thus in all cases we have

$$\left|\left(\Lambda_h\psi\;,\; fS_hG_h^p\phi\right)_h\right| \leq C\|\phi\|_{H_h^{1/2}}\|\psi\|_{H_h^{1/2}}\;.$$

Clearly, similar arguments can be used to show part (iv) of this lemma. ∎

4. Water Waves with Surface Tension

An extreme case of interfacial flow occurs when the density of one of the fluids is negligible compared with the density of the other. This is the case for waves on water or a single fluid falling on vacuum. Wave breaking is one of the most complex examples of this kind of flows; the mechanisms that cause the wave profile to break, are not well understood yet. Without surface tension, numerical simulations show [11, 41] that the interface profile remains smooth even until the tip of the wave reaches the lower part of the free surface. Thus, it is natural to ask how surface tension affects the nonlinear behavior of the interface, once the wave starts to overturn. Although we could use our method for two density fluid interfaces, setting the Atwood number to one, to simulate water waves motion with surface tension, it turns out that a more specialized formulation performs better numerically. We devote this chapter to present this formulation, give a numerical method, and establish its convergence for sufficiently smooth solutions. We also present a method to compute water waves with bottom topography at the end of the chapter.

4.1. A Tangent Angle-Arclength Stretching Formulation for Water Waves on a Fluid of Infinite Depth

We consider one layer of incompressible, irrotational and inviscid fluid of infinite depth in two dimensions. The position of the fluid interface, at any instant, is given by the complex variable $z(\alpha, t) = x(\alpha, t) + iy(\alpha, t)$, with α a Lagrangian parameter. In the interior of the fluid, we can write a complex potential $\Phi = \phi + i\psi$, where ϕ is the real velocity potential and ψ a stream function, in the double layer representation

$$\Phi(\xi, t) = \frac{1}{2\pi i} \int \frac{\mu(\alpha', t)}{\xi - z(\alpha', t)} z_{\alpha'} d\alpha' \quad ,$$

where μ is the dipole strength. Using the Plemelj formula [44], we may evaluate ϕ on the interface to obtain

$$\phi(\alpha,t) = \frac{1}{2}\mu(\alpha,t) + Re\left\{\frac{1}{2\pi i}\int \frac{\mu(\alpha',t)}{z(\alpha,t)-z(\alpha',t)} z_{\alpha'} d\alpha'\right\} .$$

To simplify the notation we drop the time variable from now on, but keep in mind that all the variables are time-dependent. Differentiating this expression with respect to α and integrating by parts we get,

$$\phi_\alpha(\alpha) = \frac{1}{2}\gamma(\alpha) + Re\left\{\frac{z_\alpha(\alpha)}{2\pi i}\int \frac{\gamma(\alpha')}{z(\alpha)-z(\alpha')} d\alpha'\right\} , \tag{4.1}$$

where $\gamma = \mu_\alpha$ is the (unnormalized) vortex sheet strength. On the other hand, we can obtain the complex velocity $W = U - iV$ differentiating Φ with respect to z. Thus,

$$W(\xi) = \frac{d\Phi}{dz} = \frac{1}{2\pi i}\int \frac{\gamma(\alpha')}{\xi - z(\alpha')} d\alpha' ,$$

and using again the Plemelj formula, we obtain the limiting velocity on the interface,

$$W(\alpha) = \frac{\gamma(\alpha)}{2z_\alpha(\alpha)} + \frac{1}{2\pi i}\int \frac{\gamma(\alpha')}{z(\alpha)-z(\alpha')} d\alpha' .$$

Now, Bernoulli's equation evaluated on the curve, in Eulerian variables reads

$$\left.\frac{\partial\phi}{\partial t}\right|_z + \frac{1}{2}|W|^2 = -gy + \tau\kappa .$$

We define the velocity $\tilde{W}$ of the Lagrangian particles on the interface as

$$\tilde{W} = W + \frac{z_\alpha}{|z_\alpha|}U^A .$$

With this velocity, we still satisfy the kinematics and have freedom to select U^A to gain some control over the positioning of the Lagrangian particles. Thus

$$\frac{\partial z}{\partial t}(\alpha,t) = \tilde{W}^*(\alpha,t) . \tag{4.2}$$

Bernoulli's equation can be evaluated in this Lagrangian frame, by noting that

$$\left.\frac{\partial\phi}{\partial t}\right|_\alpha = \left.\frac{\partial\phi}{\partial t}\right|_z + Re\{W^*\tilde{W}\} = \left.\frac{\partial\phi}{\partial t}\right|_z + |W|^2 + U^A U^T ,$$

where $U^T = |z_\alpha|^{-1} Re\{z_\alpha W\}$. Hence, we obtain

$$\left.\frac{\partial\phi}{\partial t}\right|_\alpha = \frac{1}{2}|W|^2 + U^A U^T - gy + \tau\kappa . \tag{4.3}$$

Equations (4.1), (4.2) and (4.3) determine the time evolution of the interface, and in terms of the tangent angle θ and the arclength stretching σ introduced in Section 2.1, the equations of motion become

$$\sigma_t = -R(\alpha) < \theta_\alpha U^N > \tag{4.4}$$

$$\theta_t = \frac{1}{\sigma}[U^N_\alpha + \theta_\alpha (U^T + U^A)] \tag{4.5}$$

$$\phi_t = \frac{\tau}{\sigma}\theta_\alpha + \frac{1}{2}|W|^2 + U^A U^T - gIm\{z\} \tag{4.6}$$

$$\phi_\alpha = \frac{1}{2}\gamma + \int_{-\pi}^{\pi} Re\left\{\frac{\sigma(\alpha)e^{i\theta(\alpha)}}{4\pi i}\cot\frac{1}{2}(z(\alpha)-z(\alpha'))\right\}\gamma(\alpha')d\alpha' \tag{4.7}$$

$$z = \alpha + \int_0^\alpha (\sigma e^{i\theta} - < \sigma e^{i\theta} >)d\alpha' \tag{4.8}$$

$$W = \frac{\gamma}{2\sigma}e^{-i\theta} + \frac{1}{4\pi i}\int_{-\pi}^{\pi}\gamma(\alpha')\cot\frac{1}{2}(z(\alpha)-z(\alpha'))d\alpha' \tag{4.9}$$

$$U^T = Re\{e^{i\theta}W\} \quad ; \quad U^N = -Im\{e^{i\theta}W\} \tag{4.10}$$

$$U^A = -U^T + \int_0^\alpha (\theta_\alpha U^N - R < \theta_\alpha U^N >)d\alpha' \ . \tag{4.11}$$

Note that the integral equation (4.7) has to be solved for γ at each time in order to update the velocity.

The terms that cause the high order stiffness may be extracted out as before, but now we use the integral equation to write γ in terms of ϕ. The evolution equations for θ and ϕ may be written as

$$\theta_t = \frac{1}{\sigma}\left(\frac{1}{\sigma}\mathcal{H}[\phi_\alpha]\right)_\alpha + P \tag{4.12}$$

$$\phi_t = \frac{\tau}{\sigma}\theta_\alpha + Q \ , \tag{4.13}$$

where P is defined as the right hand side of (4.5) minus the high mode leading term and Q is the right hand side of (4.6) without the surface tension term. As we discussed in Chapter 2, the high order stiffness can be removed by an implicit time-discretization of the leading order terms.

4.2. A Convergent Numerical Method for Water Waves with Surface Tension

We present now, a scheme based on the formulation (4.4-4.11) for water waves and a spectral discretization obtained with the pseudo-spectral operators S_h, D_h and Int_h, the

alternate point trapezoidal rule to approximate the velocity integral, and the de-aliasing filtering, which we indicate with the super index p. We refer to Section 3.1 for the definition of these approximations and for notation.

Our numerical method for water waves of infinite depth takes the following form

$$\frac{d\sigma_i}{dt} = -R(\alpha_i) < S_h \theta U^N >_h \tag{4.14}$$

$$\frac{d\theta_i}{dt} = \frac{1}{\sigma_i}[S_h U_i^N + D_h \theta_i (U_i^T + U_i^A)] \tag{4.15}$$

$$\frac{d\phi_i}{dt} = \tau(\frac{1}{\sigma_i} D_h \theta_i)^p + \frac{1}{2}|W_i|^2 + U_i^A U_i^T - gIm\{z_i\} \tag{4.16}$$

$$\sigma_i(\frac{1}{\sigma_i} S_h \phi_i)^p = \frac{1}{2}\gamma_i + Re\{\frac{\sigma_i e^{i\theta_i^p}}{4\pi i} \sum_{\substack{j=-N/2+1 \\ (j-i)\text{odd}}}^{N/2} \gamma_j \cot\frac{1}{2}(z_i^p - z_j^p) 2h\} \tag{4.17}$$

$$z_i = \alpha_i + Int_h(\sigma e^{i\theta} - < \sigma e^{i\theta} >_h)_i \tag{4.18}$$

$$W_i = \frac{\gamma_i}{2\sigma_i} e^{-i\theta_i^p} + \frac{1}{4\pi i} \sum_{\substack{j=-N/2+1 \\ (j-i)\text{odd}}}^{N/2} \gamma_j \cot\frac{1}{2}(z_i^p - z_j^p) 2h \tag{4.19}$$

$$U_i^T = Re\{e^{i\theta_i^p} W_i\} \quad ; \quad U_i^N = -Im\{e^{i\theta_i^p} W_i\} \tag{4.20}$$

$$U_i^A = -U_i^T + Int_h(D_h \theta U^N - R < D_h \theta U^N >_h)_i \ . \tag{4.21}$$

Note that we are not filtering γ when computing the velocity W. Through the discrete form of the integral equation (4.17), we will show that γ has already the desired filtering. Just as in the two fluid interface we needed to approximate γ by $\sigma\tilde{\gamma}^p$, now we require a special discretization of ϕ_α, the left hand side of (4.17), to maintain balance among leading order terms when σ is α-dependent, that is, $R \not\equiv 1$. We also filter the surface tension term in (4.16).

In the same spirit as in the scheme for two fluid interfaces, we can prove the convergence of this method for water waves, provided the exact solution is sufficiently smooth. More precisely, we have the following result.

THEOREM 4.1. *Assume that for $0 \le t \le T$ there exist a regular solution of the water wave equations (4.4-4.11) with $\sigma(\cdot,t)$, $\theta(\cdot,t)$ and $\phi(\cdot,t)$ belonging to $C^{m+3}[-\pi,\pi]$ for $m > 4$ and that $|z(\alpha,t) - z(\beta,t)| \ge C|\alpha - \beta|$ holds for some $C > 0$. If σ_h, θ_h and ϕ_h denote*

the numerical solution of (4.14 -4.21), then for $h \le h_0(T)$, we have

$$\begin{aligned} \|\sigma_h(t) - \sigma(\cdot,t)\|_{l^2} &\le C(T)h^m \\ \|\theta_h(t) - \theta(\cdot,t)\|_{H_h^{1/2}} &\le C(T)h^m \\ \|\phi_h(t) - \phi(\cdot,t)\|_{H_h^1} &\le C(T)h^m \end{aligned}$$

where

$$\|u\|_{H_h^1} \equiv \|u\|_{l^2} + \|D_h u\|_{l^2}\,.$$

4.3. Sketch of Proof

Consistency of the scheme (4.14-4.21) follows from (3.18-3.22) and the spectral accuracy to approximate the principal value integral (3.32).

In order to obtain evolution equations for the errors $\dot\sigma$, $\dot\theta$ and $\dot\phi$, we need to estimate $\dot W$. Proceeding as in Section 3.3.1, we find

LEMMA 4.1. *For $t \le T^*$ we have*

$$\begin{aligned} \dot W_i &= \frac{1}{2z_\alpha(\alpha_i)}(I - iH_h)(\dot\gamma_i - i\gamma(\alpha_i)\dot\theta_i^p) + E(\dot\theta_i) + f(\alpha_i)H_h G_h^p \dot\theta_i \\ &+ A_{-2}(\dot\sigma_i, \dot\theta_i, \dot\gamma_i) + O(h^{m+2}) \end{aligned} \tag{4.22}$$

where

$$T^* = \{t | t \le T, \quad \|\dot\sigma\|_{l^2},\ \|\dot\theta\|_{l^2},\ \|\dot\gamma\|_{l^2} \le h^{7/2}\}\,. \tag{4.23}$$

Now from (4.17) we get,

$$\begin{aligned} \sigma(\alpha_i)\left(\frac{1}{\sigma(\alpha_i)} S_h \dot\phi_i\right)^p &= (\frac{1}{2} + K_h)\dot\gamma_i - Re\{\frac{\gamma(\alpha_i)}{2z_\alpha(\alpha_i)} H_h (z_\alpha \dot\theta_i)^p\} \\ &- Im\{W_0 z_\alpha\}\dot\theta_i^p + A_{-2}(\dot\sigma_i, \dot\theta_i) + O(h^{m+2}) \end{aligned} \tag{4.24}$$

where

$$W_0(\alpha_i) = \frac{1}{2\pi i}\int \frac{\gamma(\alpha')}{z(\alpha_i) - z(\alpha')} d\alpha'\,, \tag{4.25}$$

and K_h is the operator defined by

$$K_h\dot\gamma_i \equiv Re\{\frac{\sigma(\alpha_i)e^{i\theta^p(\alpha_i)}}{2\pi i} \sum_{(j-i)\ \text{odd}} \frac{\dot\gamma_j}{z^p(\alpha_i) - z^p(\alpha_j)} 2h\}\,. \tag{4.26}$$

We can rewrite (4.24) as

$$
\begin{aligned}
(\frac{1}{2}I + K_h)\dot{\gamma}_i &= \sigma(\alpha_i)\dot{\psi}_i^p + Re\{\frac{\gamma(\alpha_i)}{2z_\alpha(\alpha_i)}H_h(z_\alpha\dot{\theta}_i)^p\} \\
&- \sigma(\alpha_i)U^N(\alpha_i)\dot{\theta}_i^p + A_{-2}(\dot{\sigma}_i,\dot{\theta}_i) + O(h^{m+2}) \equiv \dot{Q}_i\,,
\end{aligned} \tag{4.27}
$$

where we have defined $\dot{\psi} \equiv S_h\dot{\phi}_i/\sigma(\alpha_i)$. Hence, if $(\frac{1}{2}I + K_h)$ has a bounded inverse, we can bound $\dot{\gamma}$ in terms of $\dot{\psi}$, $\dot{\sigma}$, and $\dot{\theta}$. With little modification, we can adapt the proof of Lemma (3.7) to show the following result.

LEMMA 4.2. *Assume $z(\cdot;t) \in C^3$, $z_\alpha \neq 0$, then there exit constants $h_0 > 0$ and $C > 0$ such that for all h with $0 < h \leq h_0$ we have*

$$
\|(\frac{1}{2}I + K_h)^{-1}\|_{l^2} \leq C\,. \tag{4.28}
$$

We now show that $K_h\dot{\gamma}_i$ is a lower order term. We have,

$$
K_h\dot{\gamma}_i = K_h(\frac{1}{2}I + K_h)^{-1}\dot{Q}_i = (\frac{1}{2}I + K_h)^{-1}K_h\dot{Q}_i\,,
$$

but

$$
K_h\dot{Q}_i = Re\{\frac{1}{2\pi i}\sum_{(j-i)\text{ odd}}\frac{\dot{Q}_j}{\alpha_i - \alpha_j}2h\} + \sum_{(j-i)\text{ odd}} g(\alpha_i, aj)\dot{Q}_j 2h = \sum_{(j-i)\text{ odd}} g(\alpha_i, aj)\dot{Q}_j 2h\,,
$$

for some smooth function g. Thus K_h is an operator of the type (3.79), that is $K_h = R_h$, thus

$$
\begin{aligned}
K_h\dot{Q}_i &= R_h\dot{Q}_i = R_h(\dot{\psi}_i^p) + R_h(\dot{\theta}_i^p) + R_h[(H_h(z_\alpha\dot{\theta}_i))^p] \\
&+ A_{-2}(\dot{\sigma}_i,\dot{\theta}_i) + O(h^{m+2}) = A_{-2}(\dot{\sigma}_i,\dot{\theta}_i,\dot{\psi}_i) + O(h^{m+2})
\end{aligned}
$$

Therefore, we have

$$
\begin{aligned}
\dot{\gamma}_i &= 2\sigma(\alpha_i)[\dot{\psi}_i^p - U^N(\alpha_i)\dot{\theta}_i^p] + \gamma(\alpha_i)H_h\dot{\theta}_i^p + f(\alpha_i)H_hG_h^p\dot{\theta}_i \\
&+ A_{-2}(\dot{\sigma}_i,\dot{\theta}_i,\dot{\psi}_i) + O(h^{m+2})\,,
\end{aligned}
$$

and substituting this expression into (4.22) we obtain

$$
\begin{aligned}
\dot{W}_i &= \frac{1}{z_\alpha(\alpha_i)}(I - iH_h)[\sigma(\alpha_i)\dot{\psi}_i^p - \sigma(\alpha_i)U^N(\alpha_i)\dot{\theta}_i^p + \frac{\gamma(\alpha_i)}{2}H_h\dot{\theta}_i^p - i\frac{\gamma(\alpha_i)}{2}\dot{\theta}_i^p] \\
&+ E(\dot{\theta}_i) + f(\alpha_i)H_hG_h^p\dot{\theta}_i + A_{-2}(\dot{\sigma}_i,\dot{\theta}_i,\dot{\psi}_i) + O(h^{m+2})
\end{aligned}
$$

Now use $(I - iH_h)H_h = (I - iH_h)i$, we get

$$\begin{aligned}\dot{W}_i &= \frac{\sigma(\alpha_i)}{z_\alpha(\alpha_i)}(I - iH_h)[\dot{\psi}_i^p - U^N(\alpha_i)\dot{\theta}_i^p] + E(\dot{\theta}_i) + f(\alpha_i)H_h G_h^p \dot{\theta}_i \\ &+ A_{-2}(\dot{\sigma}_i, \dot{\theta}_i, \dot{\psi}_i) + O(h^{m+2})\end{aligned}$$

It is natural to define a new variable,

$$\dot{\eta}_i \equiv \dot{\psi}_i - U^N(\alpha_i)\dot{\theta}_i = \frac{1}{\sigma(\alpha_i)} S_h \dot{\phi}_i - U^N(\alpha_i)\dot{\theta}_i \,. \tag{4.29}$$

With this definition we obtain

$$\begin{aligned}\dot{W}_i &= \frac{\sigma(\alpha_i)}{z_\alpha(\alpha_i)}(I - iH_h)\dot{\eta}_i^p + E(\dot{\theta}_i) + f(\alpha_i)H_h G_h^p \dot{\theta}_i \\ &+ A_{-2}(\dot{\sigma}_i, \dot{\theta}_i, \dot{\eta}_i) + O(h^{m+2}) \,.\end{aligned} \tag{4.30}$$

We now use this expression for $\dot{W}$ to obtain estimates for $\dot{U}^T$ and $\dot{U}^N$. Repeating the procedure in Chapter 3 we have

$$\begin{aligned}\dot{U}_i^T &= \dot{\eta}_i^p + U^N(\alpha_i)\dot{\theta}_i^p + E(\dot{\theta}_i) + f(\alpha_i)H_h G_h^p \dot{\theta}_i \\ &+ A_{-2}(\dot{\sigma}_i, \dot{\theta}_i, \dot{\eta}_i) + O(h^{m+2})\end{aligned} \tag{4.31}$$

$$\begin{aligned}\dot{U}_i^N &= H_h \dot{\eta}_i^p - U^T(\alpha_i)\dot{\theta}_i^p + E(\dot{\theta}_i) + f(\alpha_i)H_h G_h^p \dot{\theta}_i \\ &+ A_{-2}(\dot{\sigma}_i, \dot{\theta}_i, \dot{\eta}_i) + O(h^{m+2}) \,,\end{aligned} \tag{4.32}$$

and for the variation of the added tangential velocity U^A we obtain

$$\dot{U}_i^A = -\dot{U}_i^T + U^N(\alpha_i)\dot{\theta}_i^p + A_{-1}(\dot{\sigma}_i, \dot{\theta}_i, \dot{\eta}_i) \,. \tag{4.33}$$

We can find an evolution equation for $\dot{\theta}$ just as we did in Section (3.3.2) but now using the estimates (4.31-4.33). Skipping the algebra, we obtain

$$\begin{aligned}\frac{d\dot{\theta}_i}{dt} &= \frac{1}{\sigma(\alpha_i)}\Lambda_h \dot{\eta}_i + \frac{U^A(\alpha_i)}{\sigma(\alpha_i)} D_h \dot{\theta}_i + f(\alpha_i)\dot{\theta}_i^p + S_h E(\dot{\theta}_i) \\ &+ S_h f H_h G_h^p \dot{\theta}_i + A_{-1}(\dot{\sigma}_i, \dot{\theta}_i, \dot{\eta}_i) + O(h^{m+1}) \,.\end{aligned} \tag{4.34}$$

We need to get an evolution equation for $\dot{\eta}$; first we we obtain an equation for $\dot{\phi}$. Using consistency and estimating the nonlinear terms we have

$$\begin{aligned}\frac{d\dot{\phi}_i}{dt} &= \tau(\frac{1}{\sigma(\alpha_i)} D_h \dot{\theta}_i)^p + Re\{W(\alpha_i)^* \dot{W}_i\} + U^T(\alpha_i)\dot{U}_i^A + U^A(\alpha_i)\dot{U}_i^T + gIm\{\dot{z}_i\} \\ &+ A_{-1}(\dot{\sigma}_i, \dot{\theta}_i, \dot{\eta}_i) + O(h^{m+1}) \\ &= \tau(\frac{1}{\sigma(\alpha_i)} D_h \dot{\theta}_i)^p + U^N(\alpha_i)H_h \dot{\eta}_i + U^A(\alpha_i)[\dot{\eta}_i + U^N(\alpha_i)\dot{\theta}_i^p] + gIm\{\dot{z}_i\} \\ &+ A_{-1}(\dot{\sigma}_i, \dot{\theta}_i, \dot{\eta}_i) + O(h^{m+1}) \,.\end{aligned}$$

Furthermore we note that

$$\frac{d\dot{\eta}_i}{dt} = \frac{1}{\sigma(\alpha_i)}\frac{d}{dt}S_h\dot{\phi}_i - U^N(\alpha_i)\frac{d\dot{\theta}_i}{dt} + A_0(\dot{\theta}_i, \dot{\eta}_i)\,,$$

We substitute (4.34) and applying the operator S_h to (4.35); there are some cancellations and we obtain

$$\frac{d\dot{\eta}_i}{dt} = \frac{\tau}{\sigma}D_h(\frac{1}{\sigma}D_h\dot{\theta}_i) + \frac{U^A}{\sigma}D_h\dot{\eta}_i + A_0(\dot{\sigma}_i, \dot{\theta}_i, \dot{\eta}_i) + O(h^m)\,.$$

On the other hand, the evolution equation for $\dot{\sigma}$ contains only lower order terms, just as in the case for two-dentity fluid interface. Therefore, the system of evolution equations for the error is

$$\frac{d\dot{\sigma}_i}{dt} = A_{-2}(\dot{\sigma}_i, \dot{\theta}_i, \dot{\eta}_i) + O(h^{m+2}) \tag{4.35}$$

$$\frac{d\dot{\theta}_i}{dt} = \frac{1}{\sigma(\alpha_i)}\Lambda_h\dot{\eta}_i + \frac{U^A(\alpha_i)}{\sigma(\alpha_i)}D_h\dot{\theta}_i + \Theta(\dot{\theta}_i) + A_{-1}(\dot{\sigma}_i, \dot{\theta}_i, \dot{\eta}_i) + O(h^{m+1}) \tag{4.36}$$

$$\frac{d\dot{\eta}_i}{dt} = \frac{\tau}{\sigma(\alpha_i)}D_h\left(\frac{1}{\sigma(\alpha_i)}D_h\dot{\theta}_i\right) + \frac{U^A(\alpha_i)}{\sigma(\alpha_i)}D_h\dot{\eta}_i + A_0(\dot{\sigma}_i, \dot{\theta}_i, \dot{\eta}_i) + O(h^m)\,, \tag{4.37}$$

where the $\Theta(\dot{\theta})$ is of the form

$$\Theta(\dot{\theta}_i) = f(\alpha_i)\dot{\theta}_i^p + S_hE(\dot{\theta}_i) + S_hf(\alpha_i)H_hG_h^p\dot{\theta}_i\,. \tag{4.38}$$

To perform energy estimates on this system, we take the discrete inner product of equation (4.36) and $\Lambda_h\dot{\theta}$, and of equation (4.37) with $\frac{\sigma}{\tau}\dot{\eta}$. When we add these two equations, the leading order terms cancel each other, more precisely

$$\left(\Lambda_h\dot{\theta}\ ,\ \frac{1}{\sigma}\Lambda_h\dot{\eta}\right)_h + \left(\dot{\eta}\ ,\ D_h(\frac{1}{\sigma}D_h\dot{\theta})\right)_h = \left(A_0(\dot{\theta})\ ,\ \dot{\eta}\right)_h\ ,$$

because

$$\begin{aligned}\left(\Lambda_h\dot{\theta}\ ,\ \frac{1}{\sigma}\Lambda_h\dot{\eta}\right)_h &= -\left(D_h\dot{\eta}\ ,\ H_h(\frac{1}{\sigma}\Lambda_h\dot{\theta})\right)_h \\ &= -\left(D_h\dot{\eta}\ ,\ \frac{1}{\sigma}H_h^2D_h\dot{\theta}\right)_h + \left(A_{-1}(\dot{\theta})\ ,\ D_h\dot{\eta}\right)_h \\ &= \left(D_h\dot{\eta}\ ,\ \frac{1}{\sigma}D_h\dot{\theta}\right)_h + \left(A_0(\dot{\theta})\ ,\ \dot{\eta}\right)_h\ .\end{aligned}$$

The rest of the terms can be estimated as in the two-density case, except that now we do not need to separate the modes.

4.4. Water Waves with Bottom Topography

With a few modification we can include bottom topography in our model to study water waves. In addition to the boundary conditions on the free surface, we now require that the normal velocity at the bottom, which we assume stationary, be equal to zero because the fluid cannot penetrate a solid boundary, this translates into a Neumann boundary condition for the potential.

A dipole-layer potential has jump discontinuities, but its normal derivative varies continuously as the surface is approached along the normal direction. On the other hand, the potential due to a layer of sources varies continuously as the interface is penetrated, but the normal derivative has a jump discontinuity. Thus it is natural to impose a distribution of sources on the solid boundary to satisfy the Neumann boundary condition.

We describe the interface position with the complex variable $z_F(\alpha)$ and the solid bottom with $z_B(\alpha)$, where α is a Lagrangian parameter. Assuming both boundaries are 2π periodic in the horizontal direction, we may write the complex potential as

$$\begin{aligned} \Phi(\xi) &= \frac{1}{4\pi i}\int_{-\pi}^{\pi} \mu_F(\alpha') z_{F\alpha}(\alpha') \cot\frac{1}{2}[\xi - z_F(\alpha')] d\alpha' \\ &+ \frac{1}{2\pi}\int_{-\pi}^{\pi} \eta(\alpha') \log[\sin\frac{1}{2}[\xi - z_B(\alpha')]] d\alpha' , \end{aligned} \tag{4.39}$$

where $\mu_F(\alpha)$ is the dipole strength associated with the free surface and $\eta/|z_B|$ is the source strength on the solid boundary. Defining $\eta = \mu_{B\alpha}$ and integrating by parts, we obtain

$$\begin{aligned} \Phi(\xi) &= \frac{1}{4\pi i}\int_{-\pi}^{\pi} \mu_F(\alpha') z_{F\alpha}(\alpha') \cot\frac{1}{2}[\xi - z_F(\alpha')] d\alpha' \\ &+ \frac{1}{4\pi}\int_{-\pi}^{\pi} \mu_B(\alpha') z_{B\alpha}(\alpha') \cot\frac{1}{2}[\xi - z_B(\alpha')]] d\alpha' . \end{aligned} \tag{4.40}$$

Evaluating the real velocity potential $\phi = Re\{\Phi\}$ on the free surface, differentiating with respect to α and integrating by parts, we find

$$\begin{aligned} \phi_\alpha(\alpha) &= \frac{\gamma(\alpha)}{2} + Re\{\frac{z_{F\alpha}(\alpha)}{4\pi i}\int_{-\pi}^{\pi} \gamma(\alpha') \cot\frac{1}{2}[z_F(\alpha) - z_F(\alpha')] d\alpha'\} \\ &+ Re\{\frac{z_{F\alpha}(\alpha)}{4\pi}\int_{-\pi}^{\pi} \eta(\alpha') \cot\frac{1}{2}[z_F(\alpha) - z_B(\alpha')] d\alpha'\} . \end{aligned} \tag{4.41}$$

where $\gamma = \mu_{F\alpha}$ is again, the vortex sheet strength.

We obtain the complex velocity $W = U - iV$ at an interior point ξ taking the derivative of Φ we respect to ξ, that is

$$
\begin{aligned}
(4.42) \qquad W(\xi) &= \frac{d\Phi}{d\xi} = \frac{1}{4\pi i}\int_{-\pi}^{\pi}\gamma(\alpha')\cot\frac{1}{2}[\xi - z_F(\alpha')]d\alpha' \\
&+ \frac{1}{4\pi}\int_{-\pi}^{\pi}\eta(\alpha')\cot\frac{1}{2}[\xi - z_B(\alpha')]d\alpha' .
\end{aligned}
$$

We impose now the condition that the normal velocity vanishes at the solid bottom, that is, $Im\{z_{B\alpha}W^*|_{bottom}\} = 0$ and this condition implies

$$
\begin{aligned}
(4.43) \qquad \eta(\alpha) &= 2Im\{\frac{z_{B\alpha}(\alpha)}{4\pi i}\int_{-\pi}^{\pi}\gamma(\alpha')\cot\frac{1}{2}[z_B(\alpha) - z_F(\alpha')]d\alpha'\} \\
&+ 2Im\{\frac{z_{B\alpha}(\alpha)}{4\pi}\int_{-\pi}^{\pi}\eta(\alpha')\cot\frac{1}{2}[z_B(\alpha) - z_B(\alpha')]d\alpha'\} .
\end{aligned}
$$

This expression together with (4.41) gives us a coupled system of Fredholm integral equations of second type. As noted in [BMO] these equations retain the property of having a globally convergent Neumann series.

In the especial case of a flat horizontal bottom, that is, $z_B = \alpha + ib$ with b a constant, equation (4.43) simplifies to

$$
(4.44) \qquad \eta(\alpha) = 2Im\{\frac{1}{4\pi i}\int_{-\pi}^{\pi}\gamma(\alpha')\cot\frac{1}{2}[z_B(\alpha) - z_F(\alpha')]d\alpha'\} ,
$$

and the system becomes a single integral equation for γ.

We find the evolution equations for the interface, proceeding as in the infinite depth case discussed at the beginning of this chapter. First we evaluate the complex velocity on the free surface. We obtain

$$
\begin{aligned}
(4.45) \qquad W(\alpha) &= \frac{\gamma(\alpha)}{2z_{F\alpha}(\alpha)} + \frac{1}{4\pi i}\int_{-\pi}^{\pi}\gamma(\alpha')\cot\frac{1}{2}[z_F(\alpha) - z_F(\alpha')]d\alpha' \\
&+ \frac{1}{4\pi}\int_{-\pi}^{\pi}\eta(\alpha')\cot\frac{1}{2}[z_F(\alpha) - z_B(\alpha')]d\alpha' ,
\end{aligned}
$$

and we allow the Lagrangian particles on the free interface to move according to

$$
(4.46) \qquad \frac{\partial z^*}{\partial t}(\alpha, t) = W + \frac{z_{F\alpha}}{|z_{F\alpha}|}U^A.
$$

Finally, the evolution equation for ϕ comes from Bernoulli's law evaluated on the free surface, in Lagrangian variables, that is, equation (4.3).

We present now a discretization for the whole system of equations determining the motion of the free interface with surface tension and influenced by bottom topography. We reformulate again the problem using the variables σ and γ and follow our stable, and convergent method, for the case of infinite depth. The scheme may be written as

$$\frac{d\sigma_i}{dt} = -R(\alpha_i) < S_h \theta U^N >_h \tag{4.47}$$

$$\frac{d\theta_i}{dt} = \frac{1}{\sigma_i}[S_h U_i^N + D_h \theta_i (U_i^T + U_i^A)] \tag{4.48}$$

$$\frac{d\phi_i}{dt} = \tau(\frac{1}{\sigma_i} D_h \theta_i)^p + \frac{1}{2}\left|W_i\right|^2 + U_i^A U_i^T - gIm\{z_i\} \tag{4.49}$$

$$\begin{aligned} \sigma_i(\frac{1}{\sigma_i} S_h \phi_i)^p &= \frac{1}{2}\gamma_i + Re\{\frac{\sigma_i e^{i\theta_i^p}}{4\pi i} \sum_{\substack{j=-N/2+1 \\ (j-i)\text{odd}}}^{N/2} \gamma_j \cot\frac{1}{2}(z_{Fi}^p - z_{Fj}^p)2h\} \\ &+ Re\{\frac{\sigma_i e^{i\theta_i^p}}{4\pi} \sum_{j=-N/2+1}^{N/2} \eta_j \cot\frac{1}{2}(z_{Fi}^p - z_{Bj})h\} \end{aligned} \tag{4.50}$$

$$\begin{aligned} \eta_i &= 2Im\{\frac{D_h z_{Bi}}{4\pi i} \sum_{j=-N/2+1}^{N/2} \gamma_j \cot\frac{1}{2}(z_{Bi} - z_{Fj}^p)h\} \\ &+ 2Im\{\frac{D_h z_{Bi}}{4\pi} \sum_{\substack{j=-N/2+1 \\ (j-i)\text{odd}}}^{N/2} \eta_j \cot\frac{1}{2}(z_{Bi} - z_{Bj})2h\} \end{aligned} \tag{4.51}$$

$$z_{Fi} = \alpha_i + Int_h(\sigma e^{i\theta} - < \sigma e^{i\theta} >_h)_i + z_{F0} \tag{4.52}$$

$$\begin{aligned} W_i &= \frac{\gamma_i}{2\sigma_i} e^{-i\theta_i^p} + \frac{1}{4\pi i} \sum_{\substack{j=-N/2+1 \\ (j-i)\text{odd}}}^{N/2} \gamma_j \cot\frac{1}{2}(z_{Fi}^p - z_{Fj}^p)2h \\ &+ \frac{1}{4\pi} \sum_{j=-N/2+1}^{N/2} \eta_j \cot\frac{1}{2}(z_{Fi}^p - z_{Bj})h \end{aligned} \tag{4.53}$$

$$U_i^T = Re\{e^{i\theta_i^p} W_i\} \quad ; \quad U_i^N = -Im\{e^{i\theta_i^p} W_i\} \tag{4.54}$$

$$U_i^A = -U_i^T + Int_h(D_h \theta U^N - R < D_h \theta U^N >_h)_i \tag{4.55}$$

We may evolve the translation constant z_{F0} in time by solving explicitly the ODE

$$\frac{dz_{F0}^*}{dt} = W_0 + e^{-i\theta_0^p} U_0^A \,. \tag{4.56}$$

Note that it is not necessary to filter z_B, because it is assumed smooth and does not change in time. It is clear that the convergence analysis for the case of infinite depth applies,

with minor modifications, to bottom topography. Also, the same high-mode leading order terms decomposition (4.12-4.13) can be used for an semi-implicit time-discretization to remove the stiffness.

5. Numerical Examples

5.1. Time Discretization

We implement our numerical methods for two fluid interfaces and water waves, with a fourth order accurate implicit-explicit scheme studied by Ascher, Ruuth, and Wetton [4]. The scheme is suitable for time dependent PDEs whose spatial derivatives have been discretized by central finite differences or by some spectral method, giving rise to a large system of ODEs of the form

$$\frac{du}{dt} = f(u) + \nu g(u) \ , \tag{5.1}$$

where g is a linear operator containing derivatives of high order, f is a collection of nonlinear terms which we prefer not to integrate implicitly, and ν is a positive parameter. Typically f contains only first order derivatives, thus the main stiffness is introduced by the linear operator g. The implicit-explicit time integration scheme is given by

$$\begin{aligned} \frac{1}{\Delta t}\left(\frac{25}{12}u^{n+1} - 4u^n + 3u^{n-1} - \frac{4}{3}u^{n-2} + \frac{1}{4}u^{n-3}\right) = \\ 4f(u^n) - 6f(u^{n-1}) + 4f(u^{n-2}) - f(u^{n-3}) + \nu g(u^{n+1}) \ . \end{aligned} \tag{5.2}$$

This discretization seems to have good stability properties. For example, if $f(u) = au_x$ and $g(u) = u_{xx}$, that is, the Convection-Diffusion Equation, and a spectral discretization in space is used, then the von Neumann analysis shows that the scheme is stable for $\Delta t \leq 0.52h/a$. Larger time steps are permitted as ν increases [4].

We discuss now the application of the implicit-explicit scheme (5.2) to our method for two fluid interfaces. The time integration for the water waves method presented in Chapter 4, follows the same philosophy.

The evolution equation for σ does not contribute to the high order stiffness. Therefore, an explicit method can be used to update σ in time. In our implementation, we employ

the following fourth order Adams-Bashforth scheme,

$$\sigma_i^{n+1} = \sigma_i^n + \frac{\Delta t}{24}(55F_i^n - 59F_i^{n-1} + 37F_i^{n-2} - 9F_i^{n-3}) \ , \tag{5.3}$$

where F_i^n is the right hand side of (3.8) computed at time $n\Delta t$.

To remove the stiffness, we rewrite the spectral discretization in space of the evolution equations for θ and γ, extracting the high mode leading order terms (2.34-2.35). The resulting system of ODEs can be written as

$$\frac{d\theta_i}{dt} = \frac{1}{2\sigma_i} D_h \left(\frac{1}{\sigma_i} H_h \gamma_i \right) + P_i \ , \tag{5.4}$$

$$\frac{d\gamma_i}{dt} = S D_h \left(\frac{1}{\sigma_i} D_h \theta_i \right) + Q_i \ , \tag{5.5}$$

where P_i is the right hand side of (3.9) minus the first term in the right hand side of (5.4) and Q_i is the right hand side of (3.10) without the surface tension term. Applying now the implicit-explicit scheme to (5.4-5.5), we obtain the following system of equations

$$\theta_i^{n+1} - \frac{\Delta t}{2}\frac{12}{25}\frac{1}{\sigma_i^{n+1}} D_h \left(\frac{1}{\sigma_i^{n+1}} H_h \gamma_i^{n+1} \right) = A_i \ , \tag{5.6}$$

$$\gamma_i^{n+1} - S\Delta t \frac{12}{25} D_h \left(\frac{1}{\sigma_i^{n+1}} D_h \theta_i^{n+1} \right) = B_i \ , \tag{5.7}$$

where A_i and B_i depend only on the previous time steps and are given by

$$\begin{aligned} A_i = {} & \frac{12}{25}(4\theta_i^n - 3\theta_i^{n-1} + \frac{4}{3}\theta_i^{n-2} - \frac{1}{4}\theta_i^{n-3}) \ + \\ & \frac{12}{25}\Delta t(4P_i^n - 6P_i^{n-1} + 4P_i^{n-2} - P_i^{n-3}) \end{aligned} \tag{5.8}$$

$$\begin{aligned} B_i = {} & \frac{12}{25}(4\gamma_i^n - 3\gamma_i^{n-1} + \frac{4}{3}\gamma_i^{n-2} - \frac{1}{4}\gamma_i^{n-3}) \ + \\ & \frac{12}{25}\Delta t(4Q_i^n - 6Q_i^{n-1} + 4Q_i^{n-2} - Q_i^{n-3}) \ . \end{aligned} \tag{5.9}$$

In the Equal Arclength Frame, that is, $R \equiv 1$, the system (5.6-5.7) becomes diagonal in Fourier space, because σ is everywhere equal to its average, and varies only in time. Thus, if $R \equiv 1$, we have a diagonal system for the Fourier Transforms:

$$\hat{\theta}_k^{n+1} - \frac{6}{25}\frac{\Delta t |k|}{(\sigma^{n+1})^2}\hat{\gamma}_k^{n+1} = \hat{A}_k \tag{5.10}$$

$$\hat{\gamma}_k^{n+1} + \frac{12}{25}\frac{S\Delta t k^2}{\sigma^{n+1}}\hat{\theta}_k^{n+1} = \hat{B}_k \ , \tag{5.11}$$

which is now trivial to solve.

However, if we select $R \not\equiv 1$, then σ varies in space and the Lagrangian markers are not uniformly separated in arclength on the interface. Thus, some iterative procedure has to be applied to solve for θ^{n+1} and γ^{n+1}. In [33], HLS recast the equations in a form suitable for a Preconditioned Conjugate Gradient method (PCG) [60]. First, γ^{n+1} from (5.7) is substituted into (5.6) and the resulting equation is multiplied by σ^{n+1}.

$$\sigma_i^{n+1}\theta_i^{n+1} - \frac{S}{2}(\frac{12}{25}\Delta t)^2 D_h \left(\frac{1}{\sigma_i^{n+1}} \Lambda_h [\frac{1}{\sigma_i^{n+1}} D_h \theta_i^{n+1}] \right) = N_i \ , \tag{5.12}$$

where N_i depends only on the previous time steps and $\Lambda_h = H_h D_h$. Note that the left hand side of (5.12) defines a symmetric positive definite operator. This property allows us to use a PCG to solve for θ^{n+1}. The preconditioner proposed by HLS is the constant coefficient operator given by,

$$M(\theta_i^{n+1}) = \sigma_{max}^{n+1}\theta_i^{n+1} - \frac{S}{2(\sigma_{min}^{n+1})^2}(\frac{12}{25}\Delta t)^2 D_h \Lambda_h D_h \theta_i^{n+1} \ , \tag{5.13}$$

where $\sigma_{min} = \min_i \sigma_i$ and $\sigma_{max} = \max_i \sigma_i$. Note that M can be inverted in $N \log N$ operations. We accelerate the convergence of the PCG with a forth order extrapolated initial guess for θ^{n+1}, obtained from previous time steps. Typically, it takes only a few iterations (about 12) for the PCG to converge with a error of 10^{-10}. The error we consider is the maximum change of successive iterates. Finally, the vortex sheet strength γ^{n+1} is obtained by substituting θ^{n+1} back into (5.7).

Of course, to take advantage of the adaptive refinement, we need to know in advance the location of possible singular points about which we wish to cluster particles to improve resolution. This information can be obtained from an equal arclength computation. This adaptive refinement technique has been used successfully in the high accuracy vortex sheet computations of HLS [33].

5.2. Some Details about the Implementation

We believe it is important to provide as many details as possible about the implementation of the numerical methods. This is the purpose of this section.

5.2.1. Equal Arclength Initialization

Suppose that initially the interface is parametrized by $\alpha_i = ih$, with $h = 2\pi/N$ and $i = 0(1)N$. We need to find a mapping $\beta_i = \beta(\alpha_i)$, such that $\sigma(\beta_i) =< \sigma >$. This can be

accomplished with a procedure presented in [9, 15]. The idea is to use Newton's method to solve the following nonlinear equation for β_i,

$$\int_0^{\beta_i} \sigma(\alpha')d\alpha' = \frac{ih}{2\pi}\int_0^{2\pi} \sigma(\alpha')d\alpha' = ih < \sigma > \quad . \tag{5.14}$$

The mean $< \sigma >$ is computed as before, using trapezoidal rule. The rest of the terms needed in Newton's method are obtained by a combination of pseudo-spectral integration and Fourier interpolation.

Once computed β_i, we must rescale the unnormalized vortex sheet strength γ. If $\gamma(\alpha, 0)$ is given, then the initial data for the equal arclength frame is $\gamma(\beta_i, 0) \cdot S_h\beta_i$, where S_h is the pseudo-spectral derivative operator defined in (3.3).

5.2.2. Solving the Integral Equation

The evolution equation (3.10) for γ, is a discrete version of a Fredholm integral equation of the second kind. Unless the Atwood number A is zero, as it is the case for a vortex sheet or Boussinesq flow, we must solve for $d\gamma_i/dt$. The solution is found efficiently using fixed point iteration accelerated with a fourth order extrapolated initial guess [8]. For most of the time, $d\gamma_i/dt$ can be computed to a tolerance of 10^{-10} with just 2 or 3 iterations. We then set to zero all the modes of $d\gamma_i/dt$ below 1.5×10^{-10} to prevent them from polluting the rest of the numerics. The same procedure is used to solve for γ_i in the method for water waves. However, if bottom topography is considered, we require to solve a couple system of integral equations for γ_i and the source strength η_i. Again, fixed point iteration works efficiently, though the convergence is slower than for the case of infinite depth. For a smooth fixed bottom, η_i need not be filtered.

5.2.3. Constructing R for the Nonuniform Mesh

If we desire to improve the resolution of our computation for a short interval of time, by clustering grid points around the positions where the interface is most singular, then R has to be determined accordingly. For example, if we wish to refine near α_1 and α_2, then R should be small close to these two points. The following construction of R was proposed and used by HLS [33]. The idea is to look for a parametrization β, such that

$$\sigma(\beta, t) = s_\beta(\beta, t) = R(\beta) < \sigma > , \quad \text{with} \quad < R >= 1 , \tag{5.15}$$

where s is the arclength and the brackets denote average over one period. If α is the equal arclength parametrization, then by chain rule $R(\beta) = d\alpha/d\beta$, that is, the mapping relating the two parametrizations is given by

$$\alpha(\beta) = \int_0^\beta R(\beta')d\beta' \ . \tag{5.16}$$

Note that since R is chosen positive, the mapping is strictly monotone and thus, the inverse always exists. In general, we do not know the values $\beta_1 = \beta(\alpha_1)$ and $\beta_2 = \beta(\alpha_2)$. However, if we select R to be the step function given by

$$R(\beta) = \begin{cases} R_{min} & \text{for } \beta \in [\beta_1 - \delta, \beta_1 + \delta] \cup [\beta_2 - \delta, \beta_2 + \delta] \\ \\ R_{max} & \text{otherwise} \ , \end{cases} \tag{5.17}$$

we can obtain all the information we need. First, given R_{min} and δ, the constant R_{max} is uniquely determined by imposing the condition that R should have mean one. We get

$$R_{max} = \frac{1 - 4\delta R_{min}}{1 - 4\delta} \ . \tag{5.18}$$

Now, using (5.16) we find that

$$\beta_1 = \delta + \frac{\alpha_1 - \delta R_{min}}{R_{max}} \tag{5.19}$$

$$\beta_2 = 3\delta + \frac{\alpha_2 - 3\delta R_{min}}{R_{max}} \ . \tag{5.20}$$

However, we need R to be sufficiently smooth. This can be accomplished by mollifying the step function (5.17) with a heat kernel, that is, we solve the Heat Equation for a small time interval with (5.17) as initial data. This diffusion does not change the position of the local extrema. Thus, the formulae (5.19-5.20) are still valid after this smoothing process. For example, if $\delta = 0.05$, $R_{min} = 0.06$ after a diffusion time of 0.0005 , the minimum value of R is about 0.1 near β_1 and β_2. This construction gives approximately 10 more points around the singular region. Once R is constructed , the grid mapping $\alpha_i = \alpha(\beta_i)$ with $\beta_i = ih$ can be found. Using spectral interpolation the initial data is recomputed at the new parametrization $\{\alpha_i\}_{i=1}N$. Again, the unnormalized vortex sheet strength has to be rescaled.

5.2.4. Fourier Filtering

In all our computations, Fourier filtering is applied only at the places specified by our methods. Following HLS [34], we first clean the spectrum of the variable to be filtered, by setting to zero all the modes below a tolerance ϵ of the order of round-off level. We use $\epsilon = 10^{-12}$. This is Krasny filtering [37]. As remarked in [34], Krasny filtering is only a precautionary measure to keep the spectrum clean and is not necessary for numerical stability, provided of course, that surface tension is not zero or that the problem is stably stratified. As defined in Chapter 3 ,our Fourier filtering is obtained multiplying the Fourier transform by a cutoff function ρ, that is

$$(\widehat{f^p})_k = \rho(kh)\hat{f}_k \ . \tag{5.21}$$

For our computations, ρ is constructed from the following function

$$P(\xi) = 35\xi^4 - 84\xi^5 + 70\xi^6 - 20\xi^7 \ . \tag{5.22}$$

We set

$$\rho(x) = \begin{cases} 1 & \text{for } x \in [0, \lambda\pi] \\ \\ P\left(\frac{\pi - x}{\pi - \lambda\pi}\right) & \text{for } x \in [\lambda\pi, \pi] \ , \end{cases} \tag{5.23}$$

where $0 < \lambda < 1$. Typically, we take λ equal to $1/2$ or $3/4$. Note also that ρ given by (5.23), satisfies all the properties demanded for the cutoff function. In particular, $\rho \in C^3$ and vanishes, along with its first, second, and third derivatives, at $x = \lambda\pi$ and $x = \pi$.

In the case of nonuniform mesh, that is, $R \not\equiv 1$, we need to filter the PCG-computed θ^{n+1} to eliminate the modes below the iteration tolerance level. However, this filtering produces a jump in the spectrum at the highest mode k_c above the tolerance. If the solution is over-resolved, then the Fourier smoothing (5.21-5.23) modifies little or not at all the spectrum. To produce a smooth transition near the mode k_c, we adapt our filtering to work on the interval $[0, k_c h]$ rather than in $[0, \pi]$.

5.3. Numerical Experiments

We present in this section some numerical simulations of two fluid interfaces and water waves with surface tension, using the schemes studied in this thesis, and with the time

discretization described at the beginning of this chapter. Most of our computations are for 1-periodic interfaces. The simulations in $[0,1]$ are achieved by a simple scaling of the 2π-periodic case. All our calculations were performed with double precision on a Sparc10 workstation.

A useful check for the accuracy of the numerics is the monitoring of the energy. For a two fluid interface, the total perturbation energy given by

$$\begin{aligned} E_T &= S\Big(\int_0^1 \sigma(\alpha')d\alpha' - 1\Big) + \frac{1}{2}\int_0^1 \gamma(\alpha)\psi(\alpha)d\alpha \\ &+ A\left[\int_0^1 \psi(\alpha)\phi_\alpha(\alpha)d\alpha + g\int_0^1 y^2(\alpha)x_\alpha(\alpha)g\alpha\right] , \end{aligned} \tag{5.24}$$

where ϕ and ψ are the velocity potential and stream function respectively, that is,

$$\phi(\alpha) + i\psi(\alpha) = \frac{1}{2\pi i}\int_0^1 \gamma(\alpha')\log[\sin\pi(z(\alpha) - z(\alpha')]d\alpha' , \tag{5.25}$$

is conserved in time. E_T can be computed with spectral accuracy [6]. In our computations, we monitor the number of digits in the fractional change of energy, that is,

$$\text{Number of Digits} = -\log_{10}\frac{|E_T(t) - E_T(t_0)|}{|E_T(t_0)|} ,$$

where $E_T(t)$ is the total energy at time t.

5.3.1. An Interfacial Standing Wave

Our first example is nearly an air-water situation. We take the Atwood number $A = 0.9$, the surface tension coefficient $S = 0.01$, the gravity constant $g = 1$ and the following initial position and vortex sheet strength for the interface.

$$\begin{aligned} x(\alpha,0) &= \alpha + 0.01\sin(2\pi\alpha) , \\ y(\alpha,0) &= -0.01\sin(2\pi\alpha) , \\ \gamma(\alpha,0) &= 0.01\sin(2\pi\alpha) . \end{aligned}$$

This corresponds to a small perturbation about the equilibrium state. The interface behaves like a standing wave, completing one full oscillation at about $t = 2.4$. The position of the interface, as it evolves in time, is plotted in Figure 5.1. In this computation, $N = 128$ and $\Delta t = 0.0025$. Figure 5.2(a) shows the spectrum of y versus the wavenumber k, plotted

at $t = 0, 1.2, 2.4, \ldots, 12$. The wave performs about 5 complete oscillations by the time $t = 12$, that is, after 4800 time steps. The spectra clearly shows that the numerical solution is stable and smooth. It appears that there exist a smooth solution for all times. In Figure 5.2(b), we plot the l^2 norm of the difference in the position variable y between the numerical solutions obtained with $N = 128$ and $N = 256$. Here $\Delta t = 0.0025$. For this simple case in which the amplitude of the wave is small and the interface profile remains smooth, few points are needed to obtain high resolution. Figure 5.3 shows the number of digits in the fractional change of energy against time, for $N = 128$ and $\Delta t = 0.0025$.

5.3.2. Raleigh-Taylor Instability

One of the classical examples of hydrodynamic instability occurs when a layer of heavy fluid sits on top of a lighter fluid, or equivalently when the interface is accelerated toward the heavy fluid. This is called Raleigh-Taylor Instability [24].

Raleigh-Taylor Instability plays an important role in many natural and industrial phenomena. Examples can be found in confinement fusion [54], laser-driven burnthrough experiments [22], mixing of fluids [40] and the formation of bubbles from a vapor film beneath a liquid.

We can simulate pure Rayleigh-Taylor instability by considering negative values of the product of the Atwood number and the gravity acceleration, that is, $Ag < 0$, and taking the following initial data

$$\begin{aligned} z(\alpha, 0) &= \alpha + i\epsilon \cos(2\pi\alpha) \ , \\ \gamma(\alpha, 0) &= 0 \ . \end{aligned}$$

For all our computations we use $\epsilon = 0.1$. Following Tryggvason [62], we fix $Ag = -1$, while considering different Atwood numbers and surface tension coefficients. Figure 5.4 shows the time evolution of an interface with $A = -0.1$ ($g = 10$) and $S = 0.005$. For this calculation we use $N = 1024$ and $\Delta t = 2.5 \times 10^{-4}$. Near $t = 0.8$, the interface becomes vertical in two symmetric positions about $x = 0.5$. Before $t = 0.9$ two small fingers appear and the interface begins to roll up. The fingers in the lighter fluid are thicker than those in the heavy fluid. Capillary waves are produced near $t = 1.2$ and move outwards from the centers of roll-up. Figure 5.5(a) shows the number of digits in the fractional change

of energy for $N = 1024$ and $N = 2048$ plotted against time. There is a sudden loss of accuracy between $t = 0.8$ and $t = 0.9$ close to the time when the fingers appear. From this time on, and up to $t = 1.4$, the accuracy stays at about 4.66 digits for $N = 1024$ and about 7.2 digits for $N = 2048$. Convergence under refinement is illustrated in Figure 5.5(b) where the l^2-norm of difference in the y coordinate between both resolutions $N = 1024$ and $N = 2048$ is plotted against time. Before $t = 0.8$, both computations agree within almost 12 digits of accuracy. The spectra of y and γ plotted in Figure 5.6(a)-(b), show clearly the transition that occurs between $t = 0.8$ and $t = 0.9$ when the sudden loss of accuracy is observed. After $t = 0.9$, the spectrum saturates and the Fourier components begin to decrease.

The computations can proceed further with still good accuracy for $N = 2048$. Figure 5.7 shows a sequence of the interface position in time from $t = 1.5$ to $t = 1.75$. Note that the tips of the fingers broaden as they continue to roll, and that the interface bends towards the tip of the fingers. At $t = 1.75$, the minimum separation between the tip of the fingers and the opposite side of the interface is about 0.016. This minimum distance continues to approach zero. By $t = 1.785$ (Figure 5.8), the separation is approximately 5×10^{-4} and the computations have to be stopped soon after this time.

This process of bubble formation through self-intersection of a fluid interface has been observed by HLS [33] for a vortex sheet. Based on their numerical results and a local model, HLS have suggested that the interface minimum separation decreases proportional to $(t_c - t)^{2/3}$, reaching zero at finite $t = t_c$. In Figure 5.9, we compare the computed minimum separations d_i, represented as circles in the plot, and a fitted curve of the form $d(t) = C(t_c - t)^{2/3}$ as a solid line. There is good agreement between the values d_i and $d(t_i)$ up to $t = 1.76$. Beyond this time, we see a deviation of the computed values d_i from the fitted curve. However, the accuracy is not high enough to resolve a separation of order $0(10^{-3})$ or smaller (Figure 5.10) and thus, more resolution is needed near the pinch-off time to give a more conclusive answer about the rate at which the minimum interface separation goes to zero. High accuracy can be achieved through the adaptive refinement technique that we described in the beginning of this chapter. The results will be reported elsewhere [18].

Roll-up has been also observed in other numerical simulations of Rayleigh-Taylor insta-

bility such as the early marker-in-cell computations of Daly [21], the vortex-in-cell method of Tryggvason [62] and the projection method for variable density of Bell and Marcus [16]. However, unlike these methods, the only regularization we use here is surface tension. Thus, the structure of the roll up and the formation of trapped bubbles through self-intersection of the interface are genuinely due to surface tension.

In our next example, we take the Atwood number $A = -0.5$, that is, the density of the fluid above the interface is three times the density of the fluid below. To keep $Ag = -1$, we use $g = 2$. Figure 5.11 shows the interface position at time $t = 1.0$ for two different surface tension coefficients: $S = 0.005$ and $S = 0.01$. In the upper plot, where $S = 0.005$, we already see the appearance of two thin fingers with a sharper tip than those observed in our previous example with $A = -0.1$. If the surface tension is doubled (lower plot), no fingers appear up to $t = 1.0$. Away from the location of the fingers, the interface in both cases behaves similarly. A detailed numerical study of the surface tension effects for different Atwood numbers will be presented elsewhere [18].

5.3.3. Drop Formation in a Single Fluid

A drop falling from a faucet is a common example in which there is a change of topology in the interface and physical quantities become discontinuous.

Pullin [51] has provided indications that surface tension may cause drop formation in a falling fluid. However, his computations could not go very far due to instability.

We can simulate the process of drop formation in a falling fluid with our method for water waves by reversing the sign of the gravity acceleration. In the numerical example we present next, $g = -10$ and the surface tension coefficient is $\tau = 0.25$. Recall that $S = 2\tau/(\rho_1 + \rho_2)$. We use the same initial data as in our Rayleigh-Taylor examples, but with a change of sign in the y coordinate.

A sequence of the interface position for different times is presented in Figures 5.12-5.13. As the fluid falls, the interface stretches forming a pendant drop. By the time $t = 1.3$ (Figure 5.13) the fluid has a long neck whose minimum thickness decreases in time. At time $t = 1.5$, the interface length is more than 10 times its initial length and the minimum thickness of the fluid neck, just above the drop is about 0.02. The interface is about to pinch off.

Figure 5.14 shows an apparent linear decrease of the neck thickness, and thus, possibly a different rate than that in the Rayleigh-Taylor roll-up. Of course, we still do not know the behavior of the thickness closer to the pinch-off.

The accuracy in the energy is plotted in Figure 5.15, from $t = 1.4$ to $t = 1.5$. The calculation was performed with $N = 2048$ and $\Delta t = 1.25 \times 10^{-4}$. Before $t = 1.4$ the interface is well resolved even with $N = 1024$ and the accuracy in the energy is about 9 digits. Close to $t = 1.46$ the accuracy decreases as the thickness of the fluid neck approaches zero and the interface continues to stretch, leaving fewer Lagrangian grid points near the regions of high curvature. We find that an adaptive refinement through the selection of a fixed parametrization function R constructed as in Section 5.2.3, does not work efficiently in this case because the position of the points about which we need to refine changes too fast, and soon the advantage of the parametrization determined by R is lost. However, this difficulty may be overcome by allowing the parametrization function R to change in time according to the position of the points with largest curvature. We will implement this idea in the future.

The experiments of Shi *et al.* [57] show that the fluid forms a thin long neck before breaking up. The neck decreases in width just above the drop to form a secondary neck. At a later time this secondary neck suffers instability and forms a third neck. It has been suggested by Shi *et al.* that the repeated formation of necks can proceed ad infinitum whenever a small but finite amount of noise is present in the experiment. Shi *et al.* argue that it is the noise what leads to this complex structure of singularity formation. Our simulations do not show this complex behavior. However, our computations give evidence that surface tension effects alone can lead to drop formation and that a topological singularity occurs in finite time. In future work [18], we will introduce small fluctuations in the thickness of the neck to simulate experimental noise.

5.3.4. Breaking Waves

Another challenging test for our methods is the simulation of breaking waves. Without surface tension, recent boundary integral methods have been able to compute close to the time when the tip of the wave reaches the lower part of the free surface [11, 41]. Moreover, the computations in [11] also show that the interface profile remains smooth though the

magnitude of the curvature is very large at the wave tip.

Next we present a calculation of a breaking wave over a flat horizontal bottom, including surface tension effects. The computations are performed with our scheme (4.47-4.55) and the following initial data

$$\begin{aligned} z_F(\alpha,0) &= \alpha + 0.5i\cos(\alpha) \quad ; \quad z_B(\alpha) = \alpha - i \\ \gamma(\alpha,0) &= 0.5\tanh(1)\cos(\alpha)\ , \end{aligned}$$

where, z_F is the complex position of the free interface and z_B gives the location of the fixed flat bottom. Note that in this case, the source strength η is determined from γ. Here we take $\tau = 0.001$ and $g = 1$.

In Figure 5.16 we show the interface profile plotted at three different times. The computations were performed with $N = 512$ and $\Delta t = 5 \times 10^{-4}$. By the time $t = 2.3$ the wave is already overturning. Although the interface profile appears to be fairly smooth at $t = 2.3$, the curvature has a sharp spike just below the wave crest. Figure 5.17 shows that the curvature is still smooth at $t = 2.1$ but subsequently loses regularity at one point. We performed the same computation but without surface tension and found that the curvature remains smooth at $t = 2.3$, but it is larger in the wave tip than that in the case with $\tau = 0.001$. Figure 5.18(a) shows the curvature at $t = 2.3$ for the computation without surface tension. In Figure 5.18(b) we plot the curvature also at $t = 2.3$ but with $\tau = 0.001$ for two computations: one with $N = 512$ and the other with $N = 1024$. Both agree with plotting resolution.

In Figure 5.19 we plot the number of digits in the fractional change of energy, that is $-\log_{10}|(E_T(t) - E_T(0))/E_T(0)|$, where $E_T(t)$ is the total energy at time t . Here, $N = 512$ and $\Delta t = 5 \times 10^{-4}$. There are about 11 digits of accuracy up to $t = 2.3$. The spectrum of the vortex sheet strength γ is presented in Figure 5.20 where no signs of numerical instability are observed.

We continue our computations beyond $t = 2.3$ using $N = 1024$. Figure 5.21 shows the interface profile at $t = 2.5$ and $t = 2.6$. By these times, the effect of the curvature spike can be seen in the interface profile. The number of digits in the fractional change of energy is presented in Figure 5.23. About $t = 2.56$ the accuracy in the energy drops to less than 4 digits by $t = 2.6$.

The curvature at time $t = 2.5$ is presented in Figure 5.22 . Oscillations can be observed on one side of the spike which suggets a possible onset of capillary waves. However, we need more resolution to go beyond $t = 2.6$ and for water waves with bottom topography (a flat bottom in this case) this turns out to be very expensive computationally. Instead we perform a calculation of a breaking wave on water of infinite depth. The breaker can be generated by introducing a shear velocity through the initial vortex sheet strengh. The initial data is

$$\begin{aligned} z(\alpha, 0) &= \alpha + 0.1i\cos(2\pi\alpha) \\ \gamma(\alpha, 0) &= -1 + 0.1\sin(2\pi\alpha) \ . \end{aligned}$$

We use $\tau = 0.005$, $g = 10$, $N = 1024$ and $\Delta t = 2.5 \times 10^{-4}$. Figure 5.24 shows the interface position at $t = 0.2$, $t = 0.3$, and $t = 0.35$. By $t = 0.3$ (middle plot) the interface has developed a strong vortical region, or roller [42]. At $t = 0.35$ (lower plot) the interfaces begins to overturn. Figure 5.25(a) shows the interface position at $t = 0.4$ where a capillary wave can be seen at the forward edge of the roller. Figure 5.25(b) gives a close-up of this region. The curvature at time $t = 0.4$ is plotted in Figure 5.25(c) where clear oscillations are observed on one side of a very sharp spike, consistent with those seen in the breaker over a flat bottom. The formation of the roller and the appearance of capillary waves at the forward edge of the roller seems to be a generic phenomenon due to surface tension. This has been observed experimentally [25]. It has also been argued by Longuet-Higgins [42] that the roller is generated by the (parasitic) capillary waves. We intend to investigate this phenomenon further in the future.

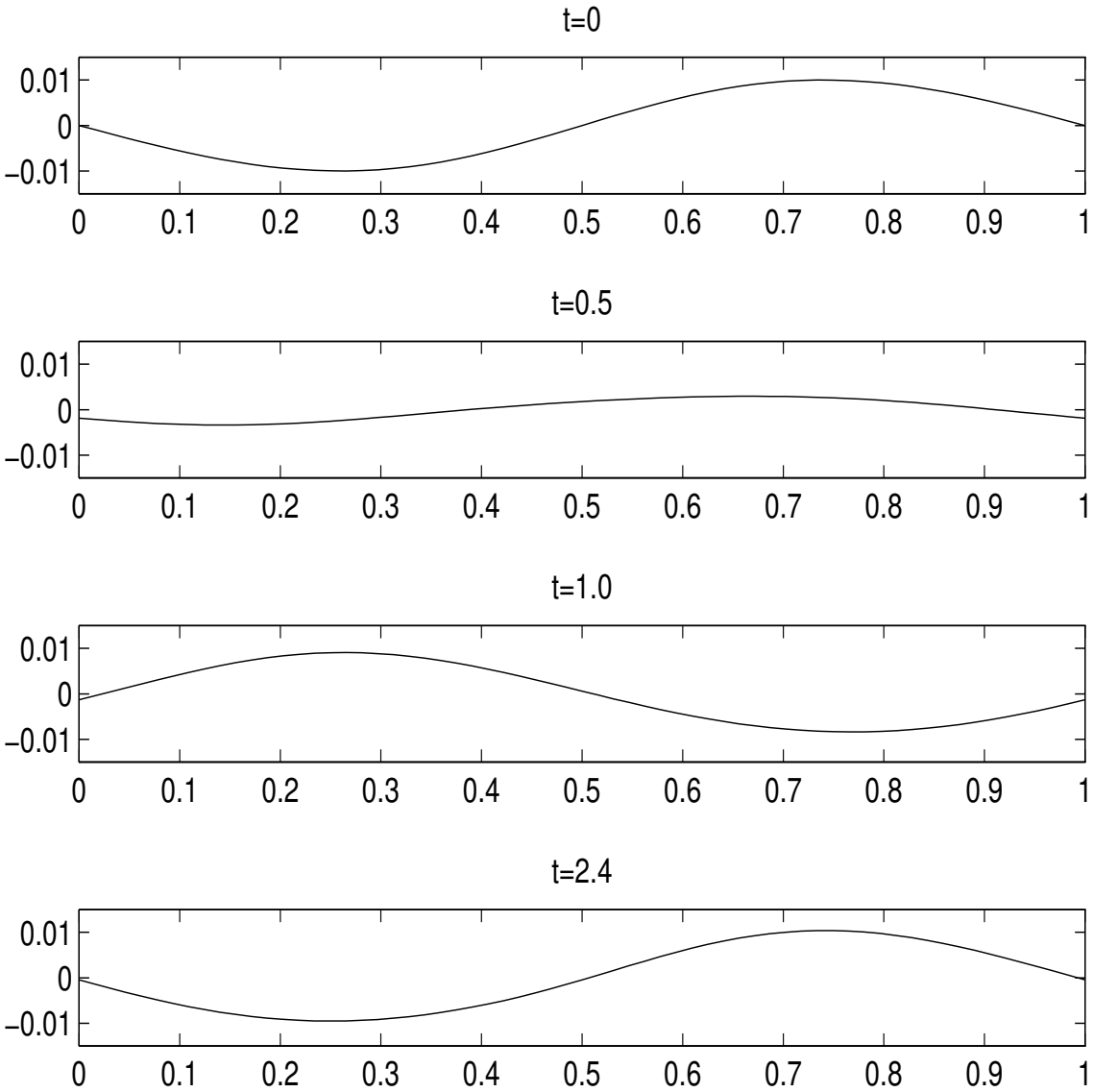

Figure 5.1: A standing wave for time $t = 0, 0.5, 1.0, 2.4$. $A = 0.9$, $S = 0.01$ and $g = 1$. $N = 128$ and $\Delta t = 0.0025$.

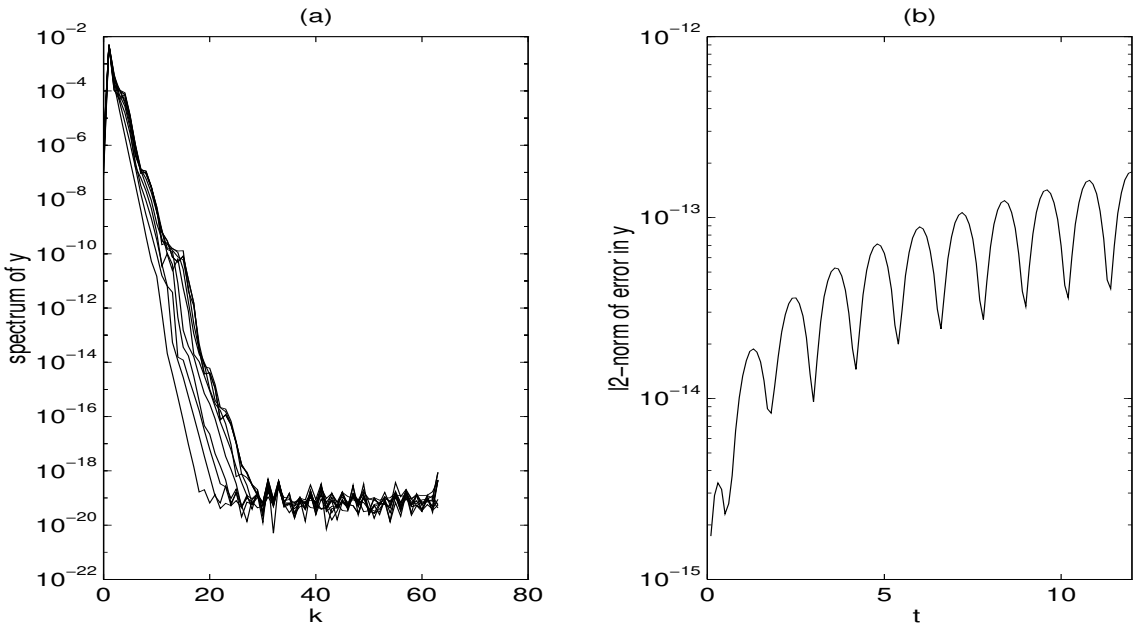

Figure 5.2: Standing Wave: (a) Spectrum of y at $t = 1.2, 2.4, \ldots, 12$. (b) l^2-norm of the difference in y between the numerical solutions for $N = 128$ and $N = 256$ with $\Delta t = 0.0025$.

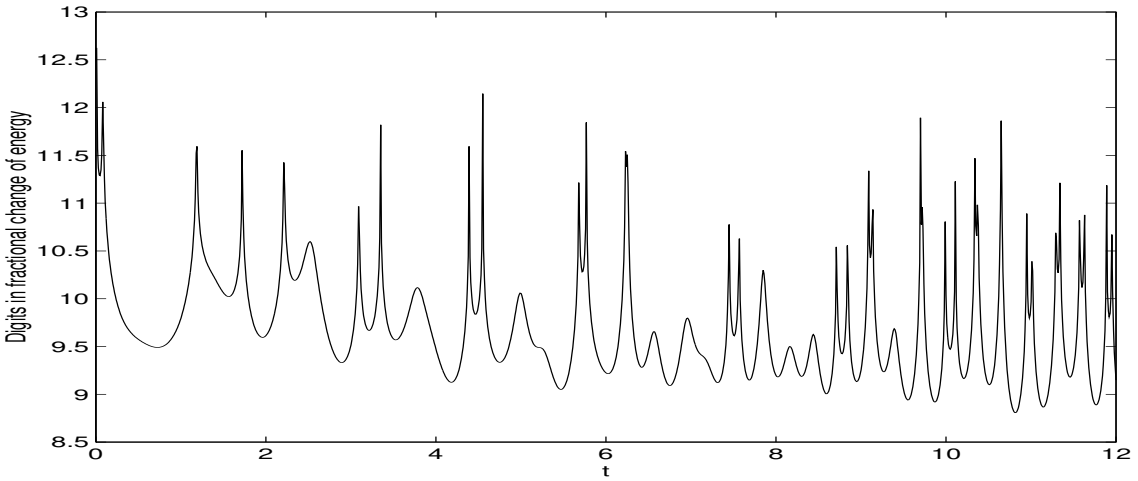

Figure 5.3: Standing Wave: Numbers of digits in the fractional change of the total energy versus time.

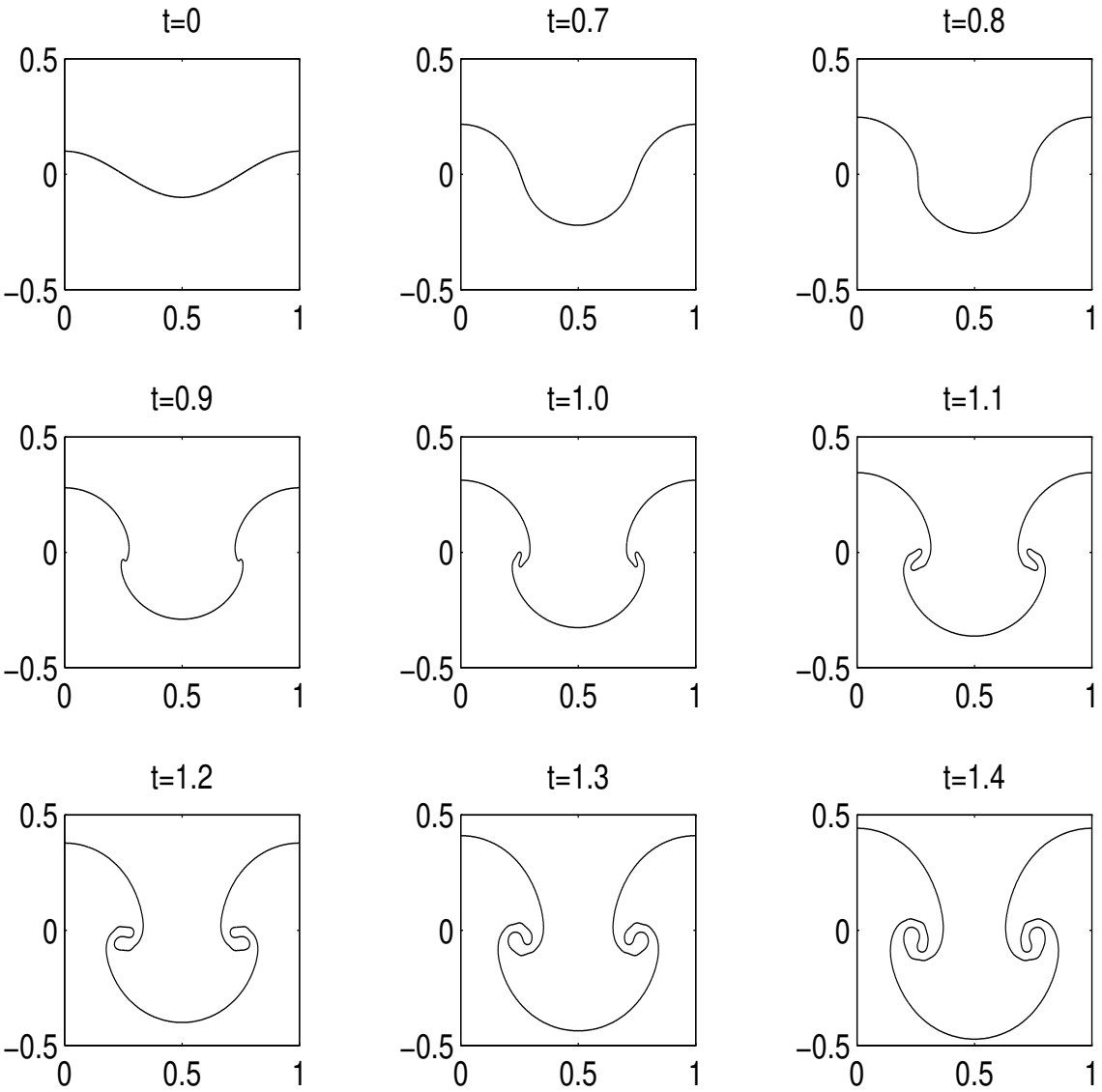

Figure 5.4: Rayleigh-Taylor Instability: Time evolution of the interface with $A = -0.1$ and $S = 0.005$. Computations performed with $N = 1024$ and $\Delta t = 2.5 \times 10^{-4}$.

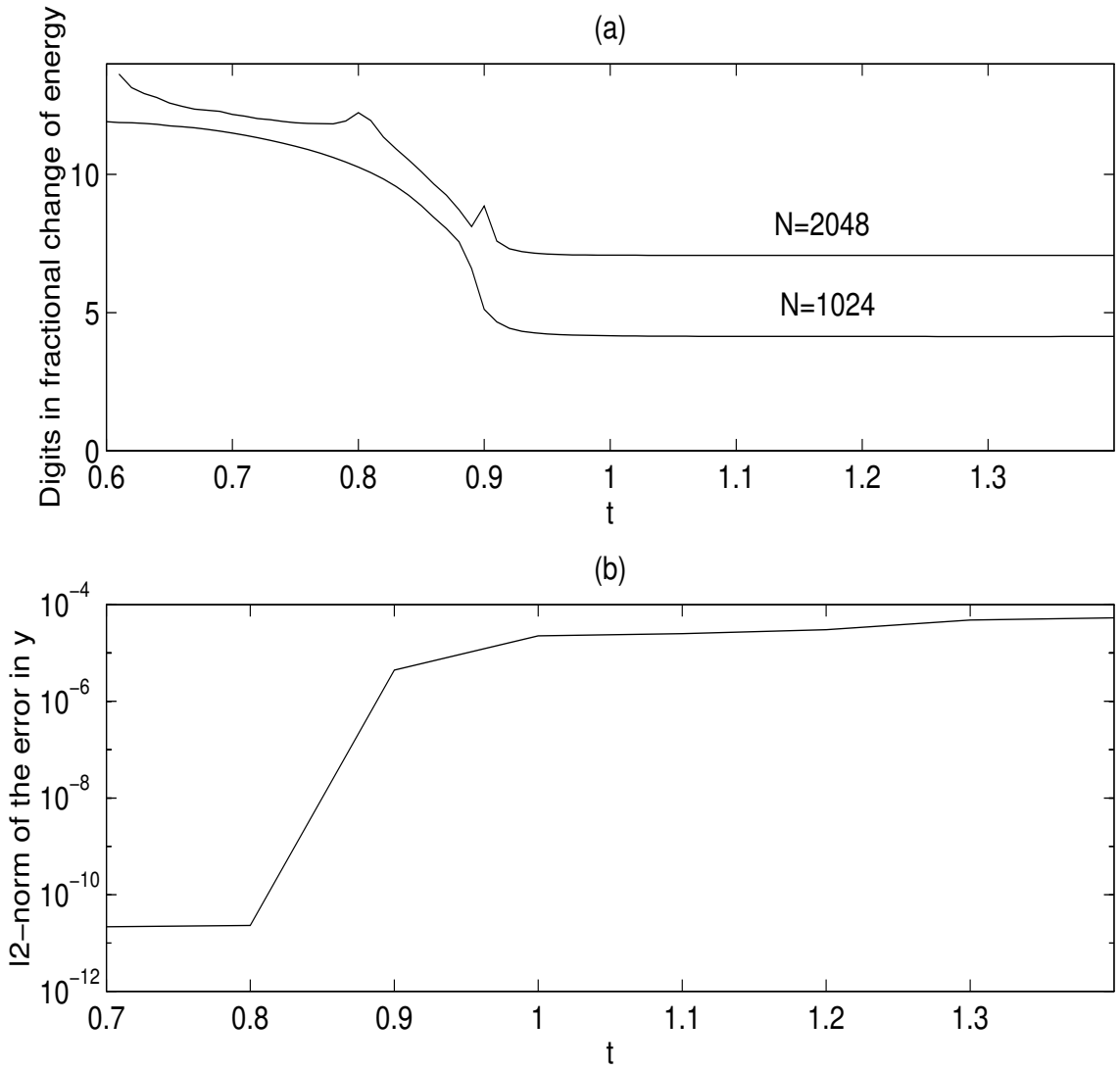

Figure 5.5: Rayleigh-Taylor Instability: $A = -0.1$ and $S = 0.005$. (a) Number of accurate digits in energy for $N = 1024$ and $\Delta t = 2.5^{-4}$, and $N = 2048$ and $\Delta t = 1.25^{-4}$. (b) l^2-norm of the difference in y between the computations obtained with $N = 1024$ and $N = 2048$.

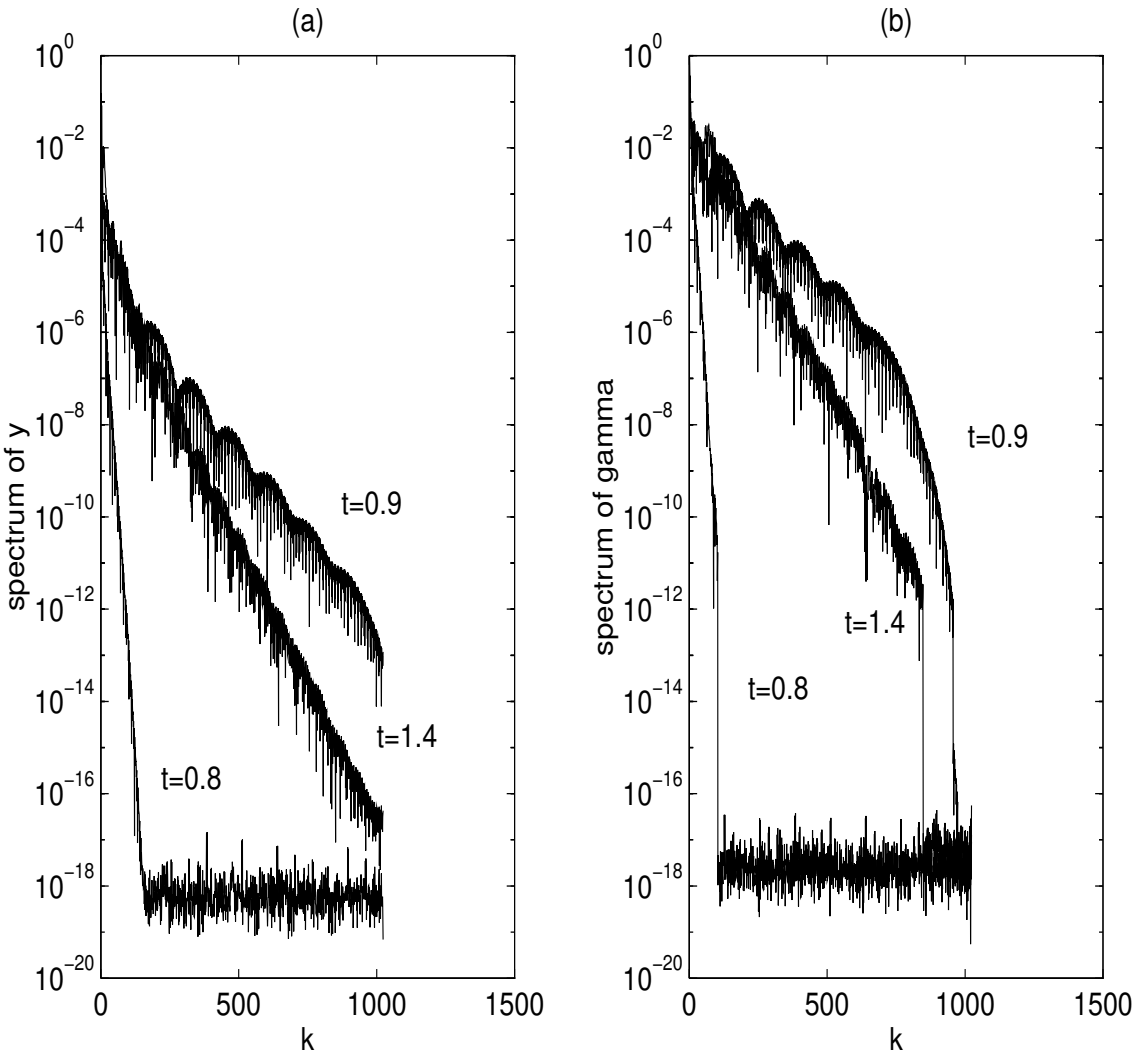

Figure 5.6: Rayleigh-Taylor Instability: $A = -0.1$ and $S = 0.005$. (a) Spectrum of y at $t = 0.8, 0.9$ and 1.4. (b) Spectrum of γ at $t = 0.8, 0.9$ and 1.4.

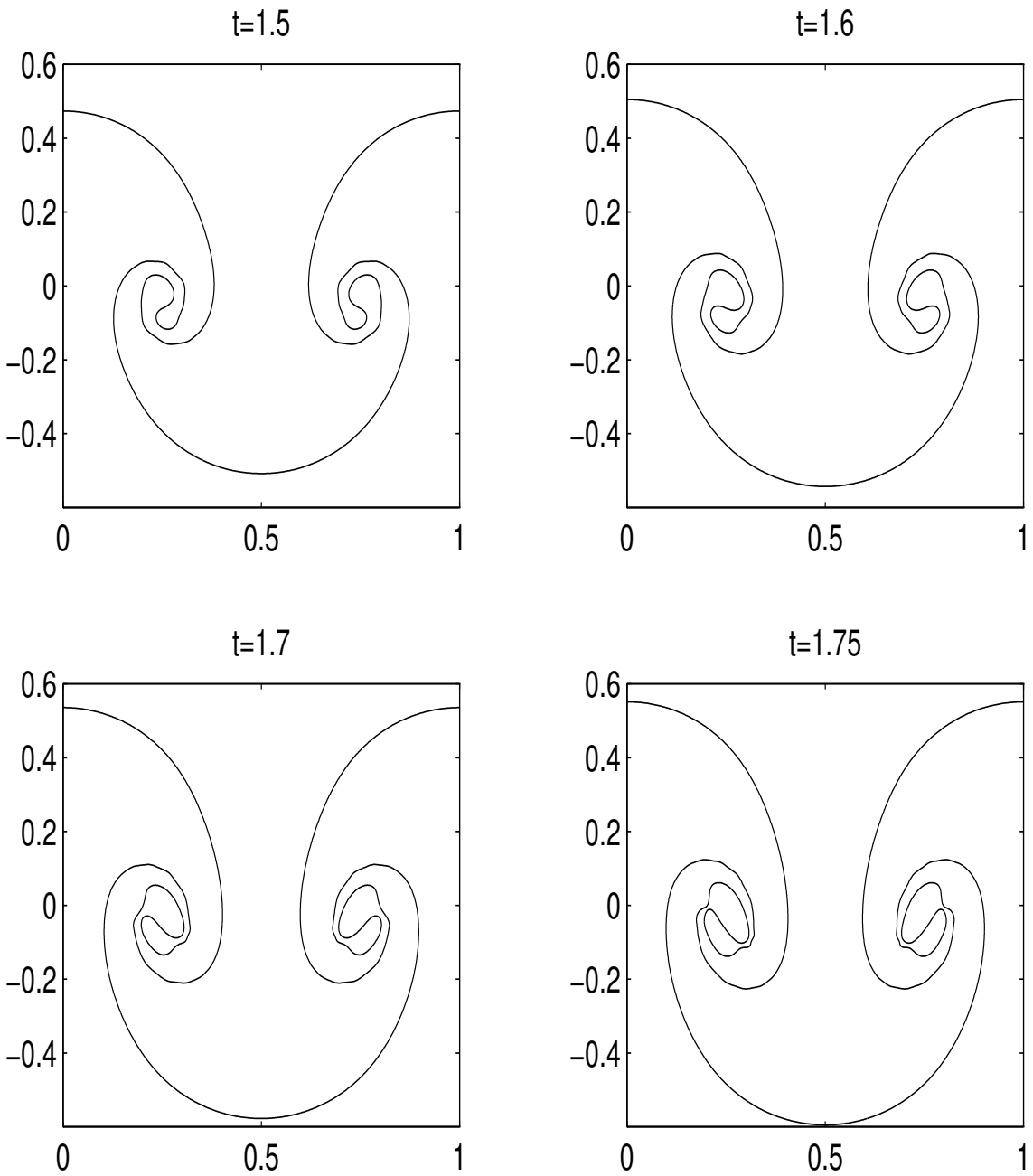

Figure 5.7: Rayleigh-Taylor Instability: $A = -0.1$ and $S = 0.005$. Sequence of interface positions. $N = 2048$ and $\Delta t = 1.25 \times 10^{-4}$.

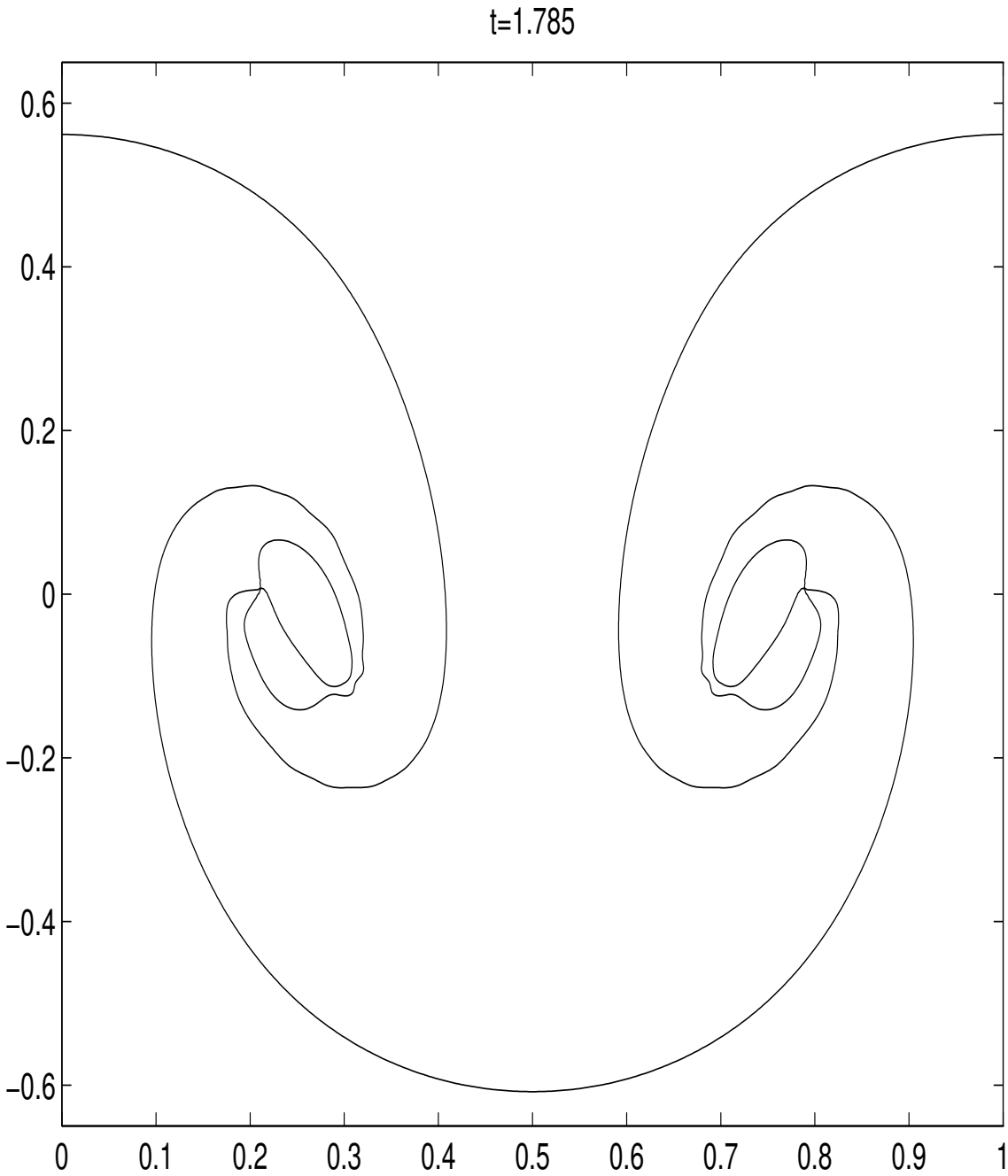

Figure 5.8: Rayleigh-Taylor Instability: $A = -0.1$ and $S = 0.005$. Interface position at $t = 1.785$

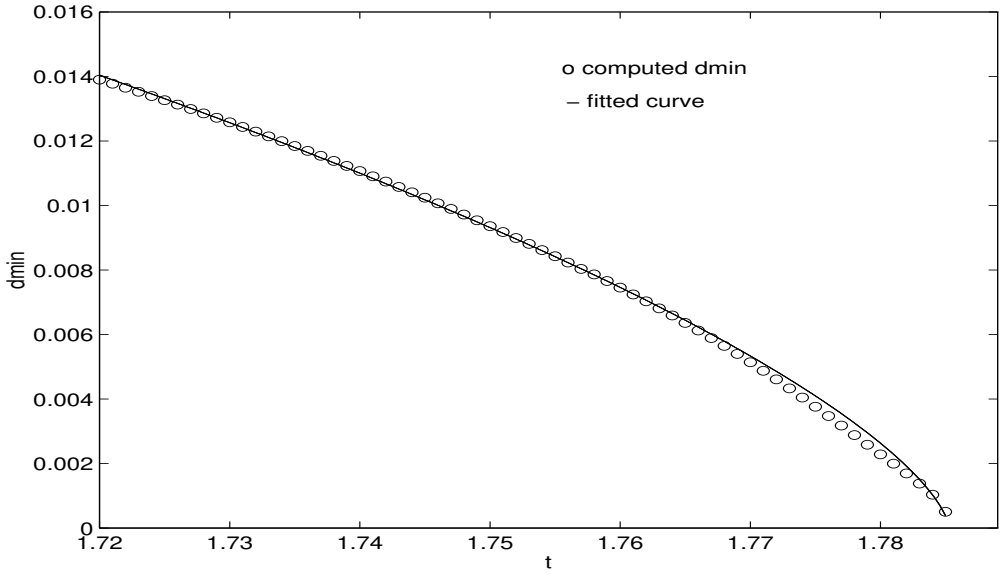

Figure 5.9: Rayleigh-Taylor Instability: $A = -0.1$ and $S = 0.005$. Minimum separation against time. The circles are the minimum distance between the tip of the fingers and the opposite side of the interface computed with $N = 2048$ and $\Delta t = 1.25 \times 10^{-4}$. The solid line is a fitted curve of the form $d(t) = C(t_c - t)^{2/3}$.

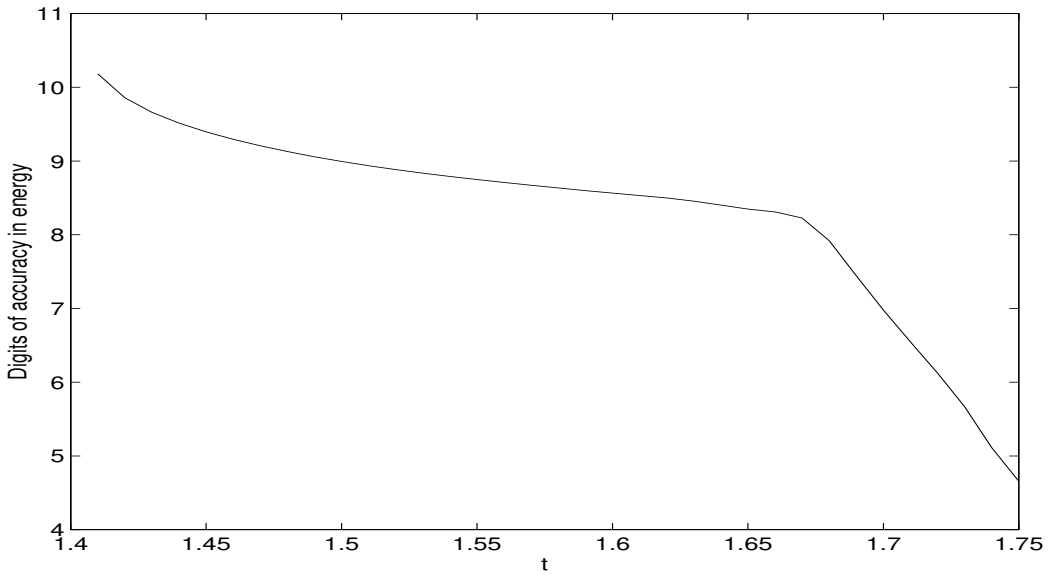

Figure 5.10: Rayleigh-Taylor Instability: $A = -0.1$ and $S = 0.005$. Number of accurate digits in the fractional change of energy against time.

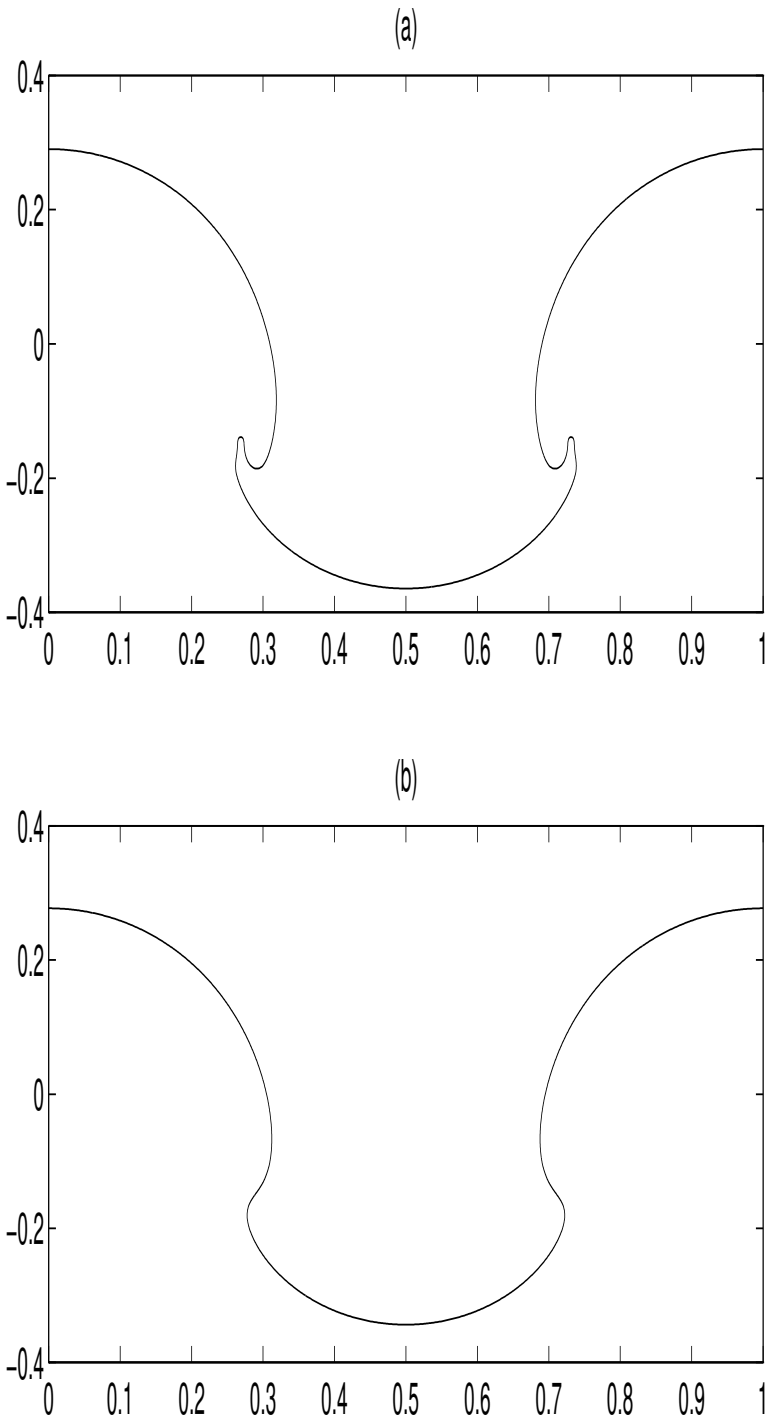

Figure 5.11: Rayleigh-Taylor Instability: $A = -0.5$. Interface position at $t = 1.0$. Computations performed with $N = 1024$ and $\Delta t = 2.5 \times 10^{-4}$. (a) $S = 0.005$. (b) $S = 0.01$

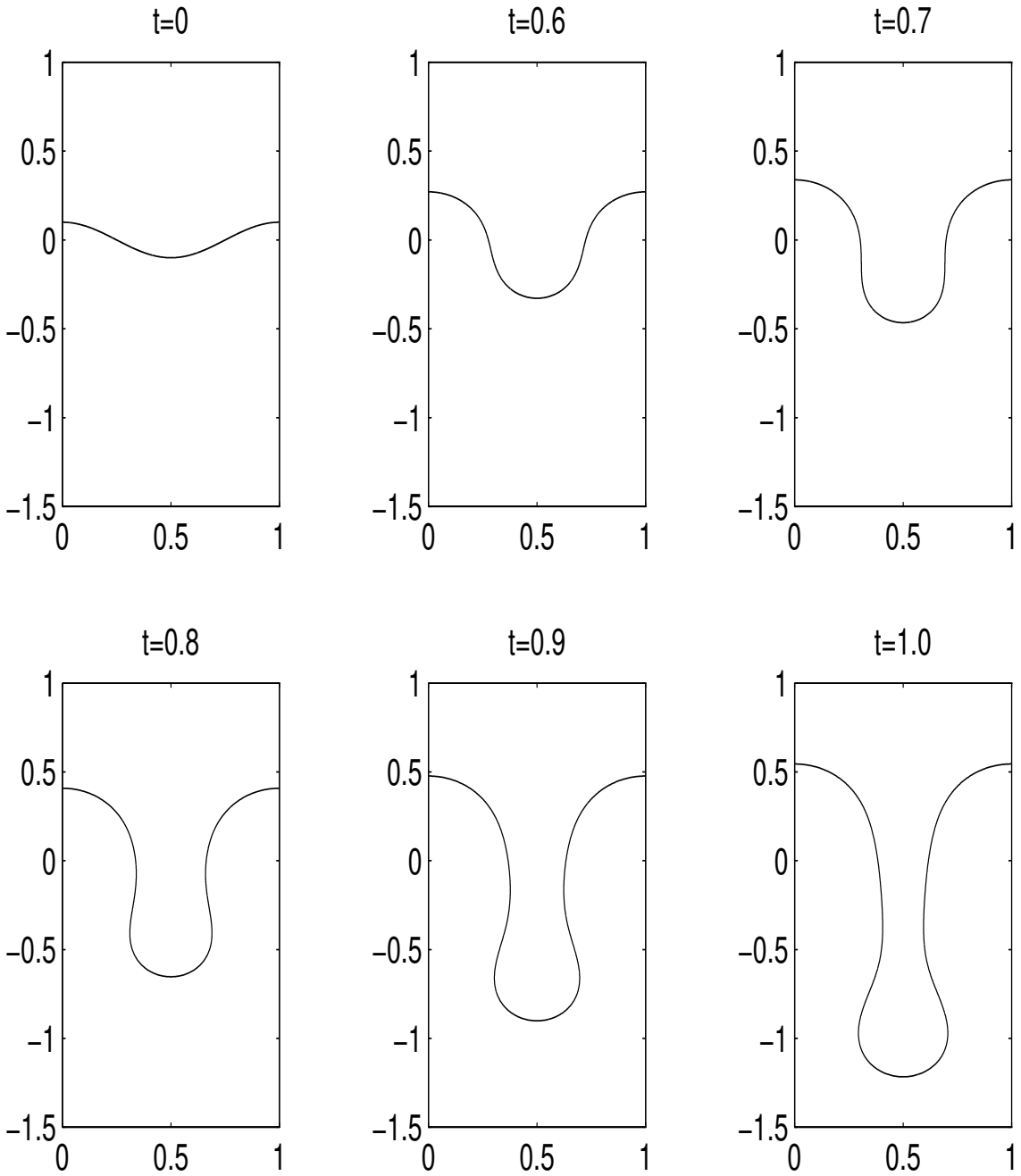

Figure 5.12: Falling of a Single Fluid. Sequence of interface positions at different times t. $\tau = 0.25$, $g = -10$, $N = 1024$ and $\Delta t = 2.5 \times 10^{-4}$.

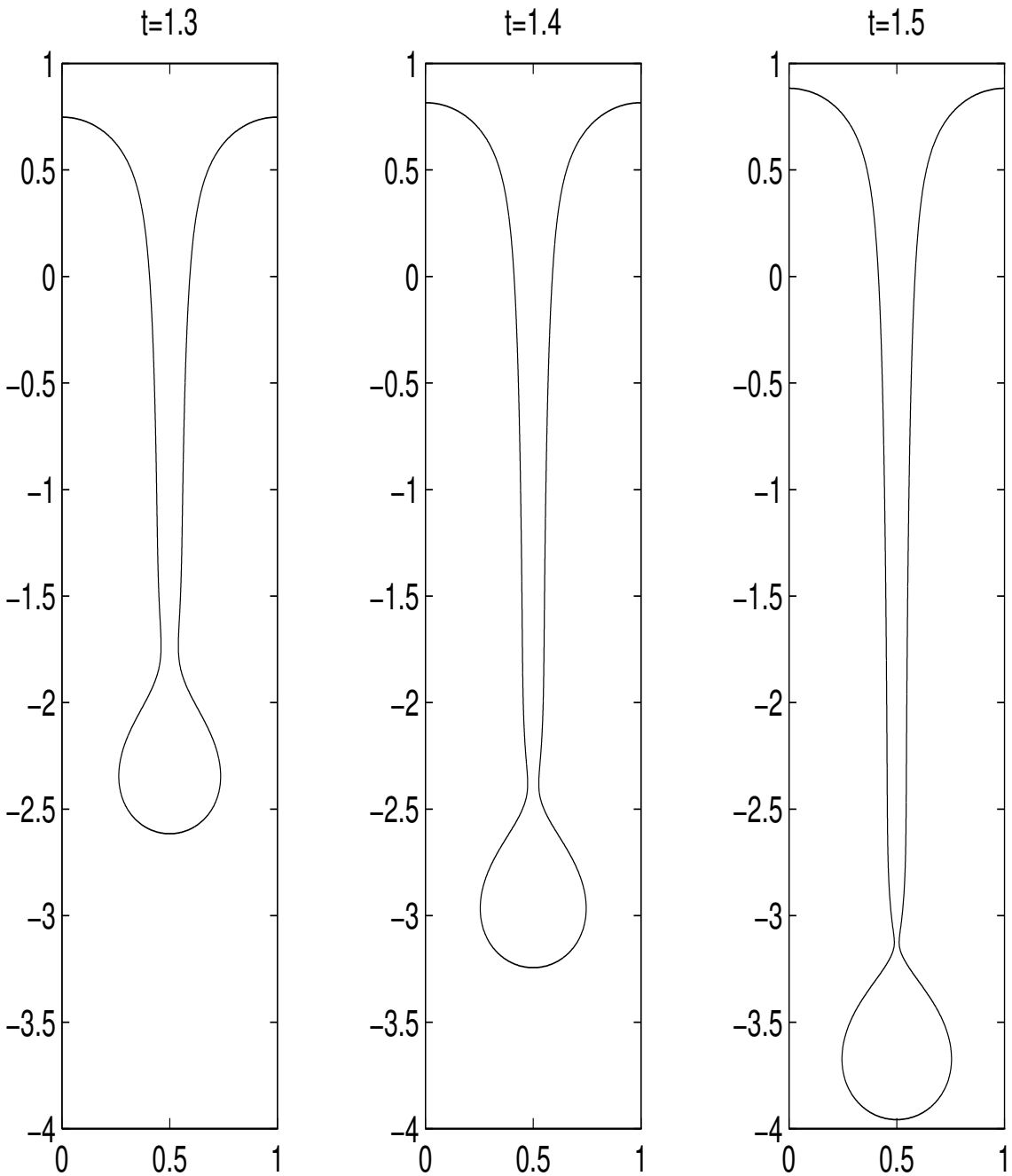

Figure 5.13: Falling of a Single Fluid: Sequence of interface positions at times $t = 1.3$, $t = 1.4$, and $t = 1.5$. $g = -10$, $\tau = 0.25$, $N = 2048$ and $\Delta t = 1.25 \times 10^{-4}$.

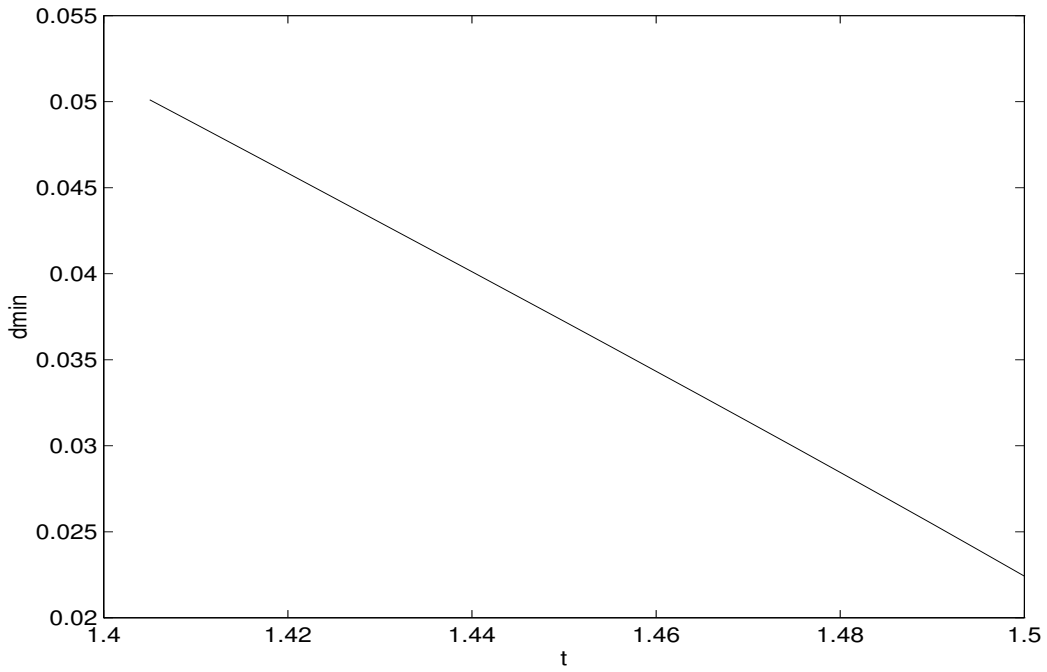

Figure 5.14: Falling of a Single Fluid: Minimum thickness in the neck of the fluid. $N = 2048$ and $\Delta t = 1.25 \times 10^{-4}$.

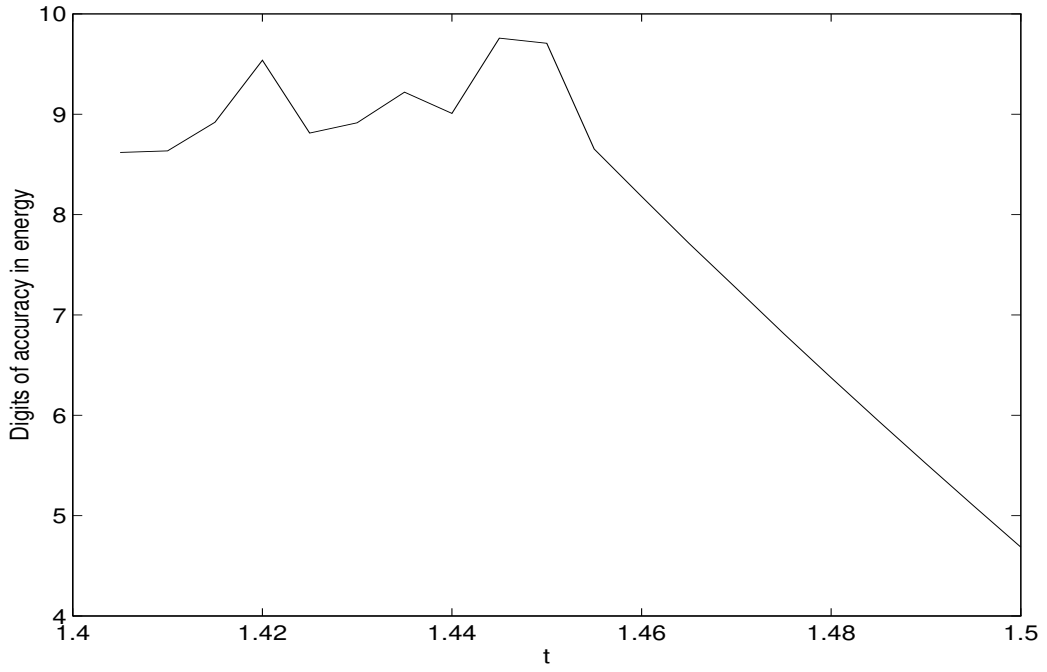

Figure 5.15: Falling of a Single Fluid: Number of accurate digits in the fractional change of energy against time. $N = 2048$ and $\Delta t = 1.25 \times 10^{-4}$.

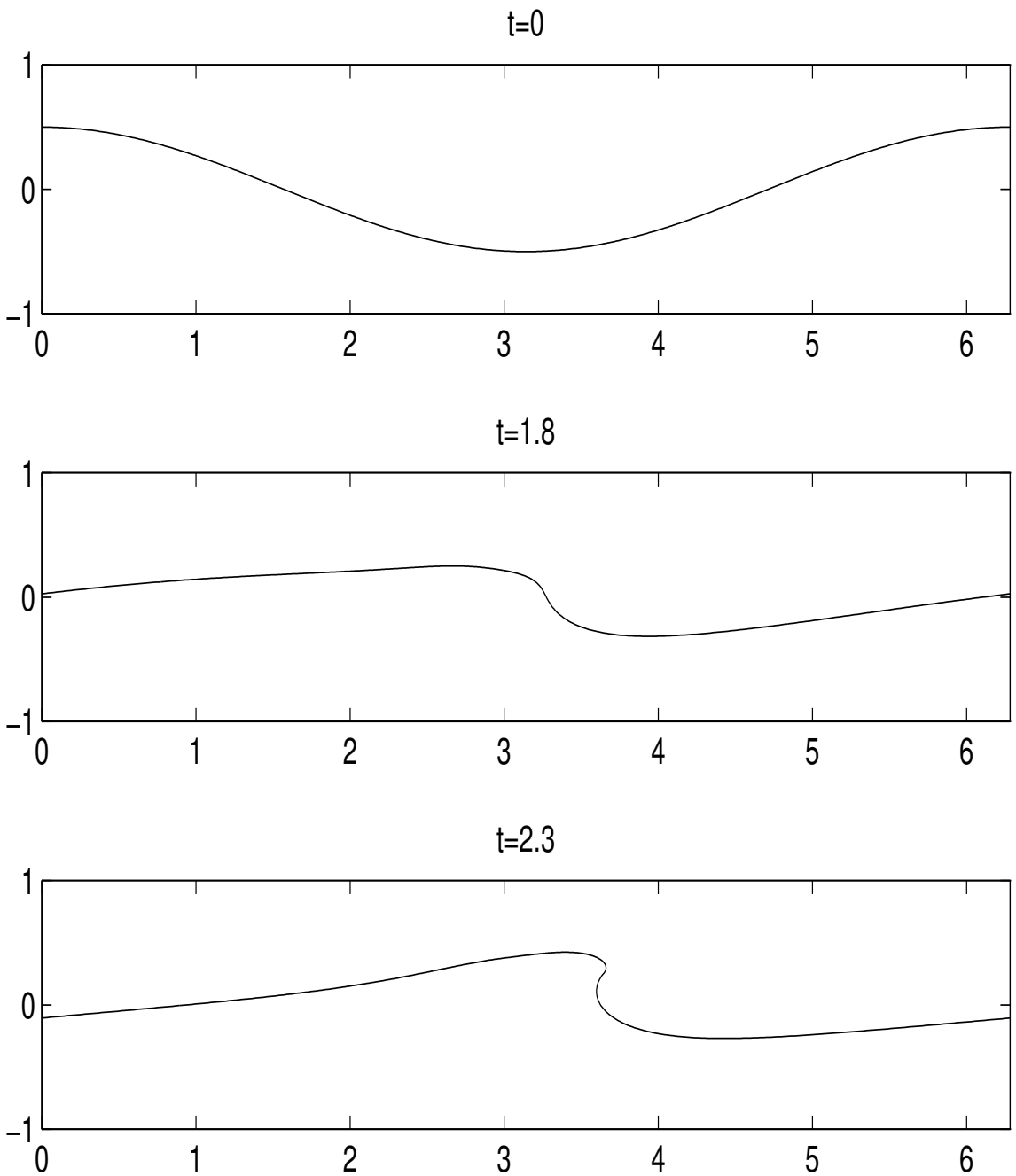

Figure 5.16: Breaking Wave: $\tau = 0.001$ Interface positions at times $t = 0$, $t = 1.8$, and $t = 2.3$. $N = 512$ and $\Delta t = 5 \times 10^{-4}$.

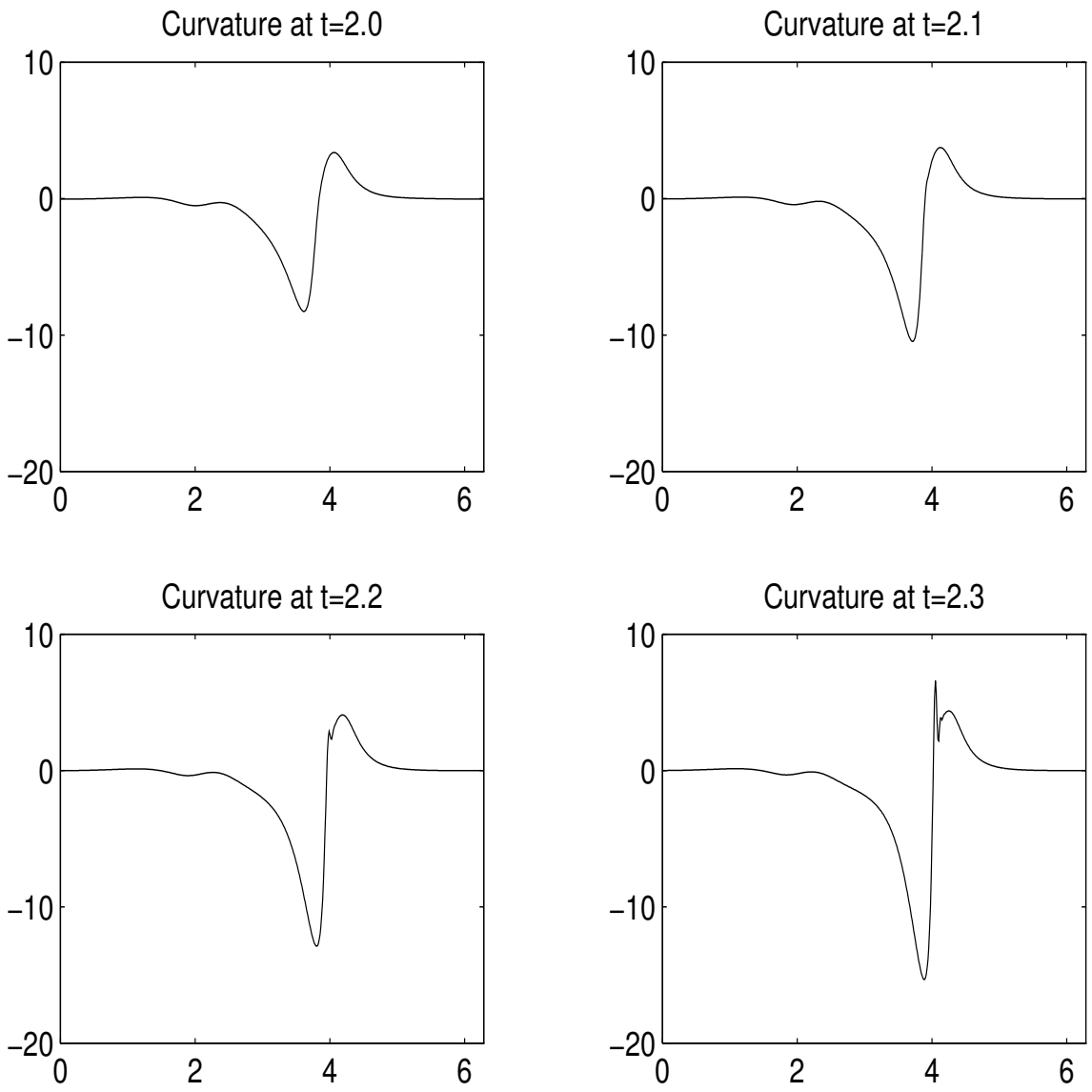

Figure 5.17: Breaking Wave: $\tau = 0.001$ Plots of the curvature. $t = 2.0, 2.1, 2.2, 2.3$. $N = 512$ and $\Delta t = 5 \times 10^{-4}$.

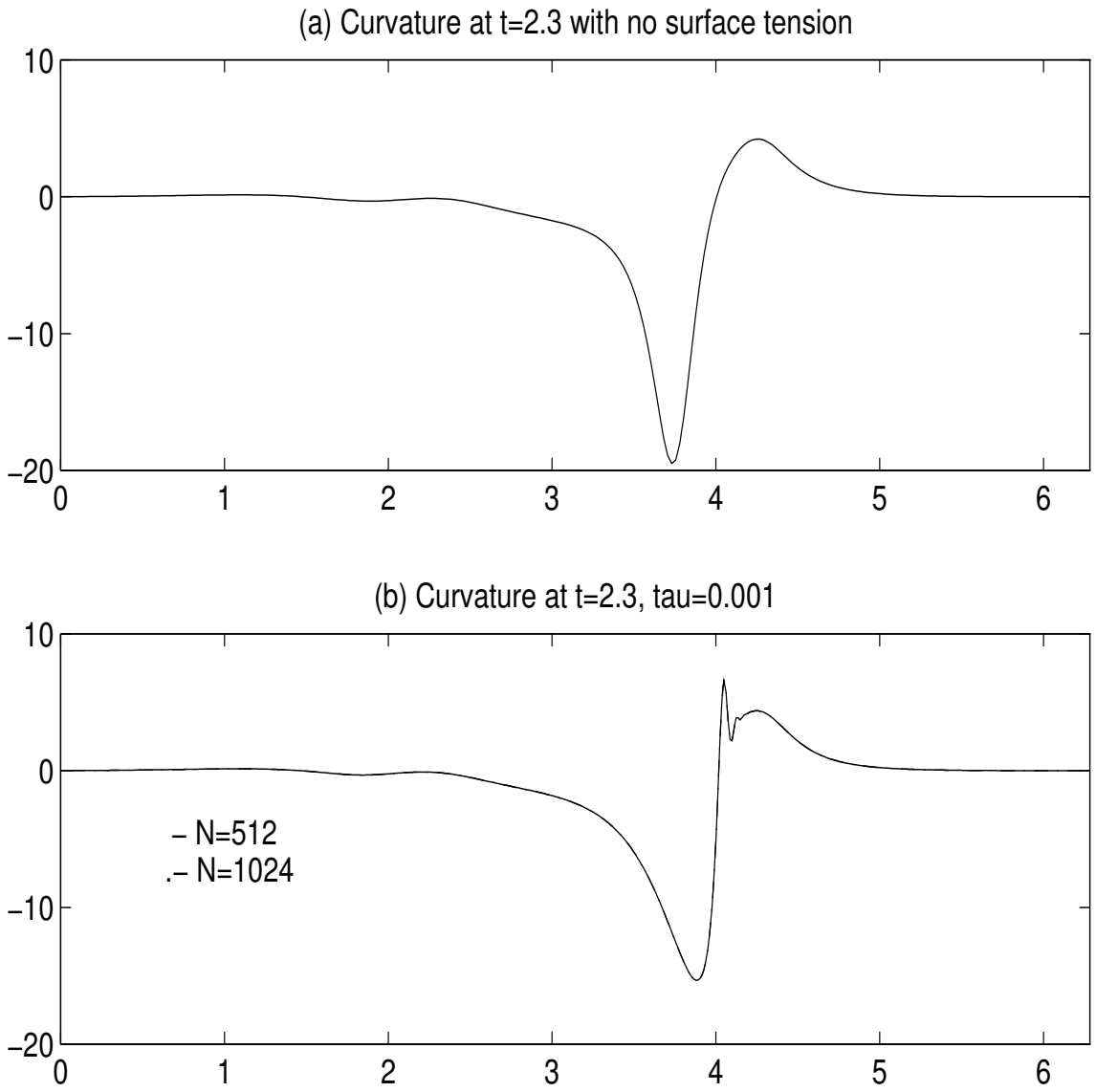

Figure 5.18: Breaking Wave: Plots of the curvature at time t=2.3 for (a) $\tau = 0$ and (b) $\tau = 0.001$ for both $N = 512$ and $N = 1024$.

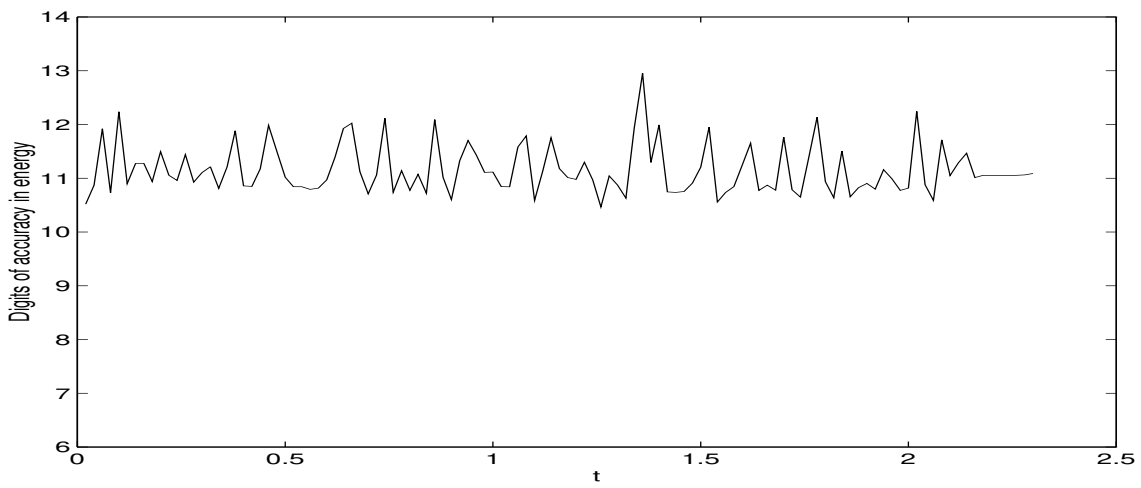

Figure 5.19: Breaking Wave: $\tau = 0.001$: Number of accurate digits in the fractional change of energy against time. $N = 512$ and $\Delta t = 5 \times 10^{-4}$.

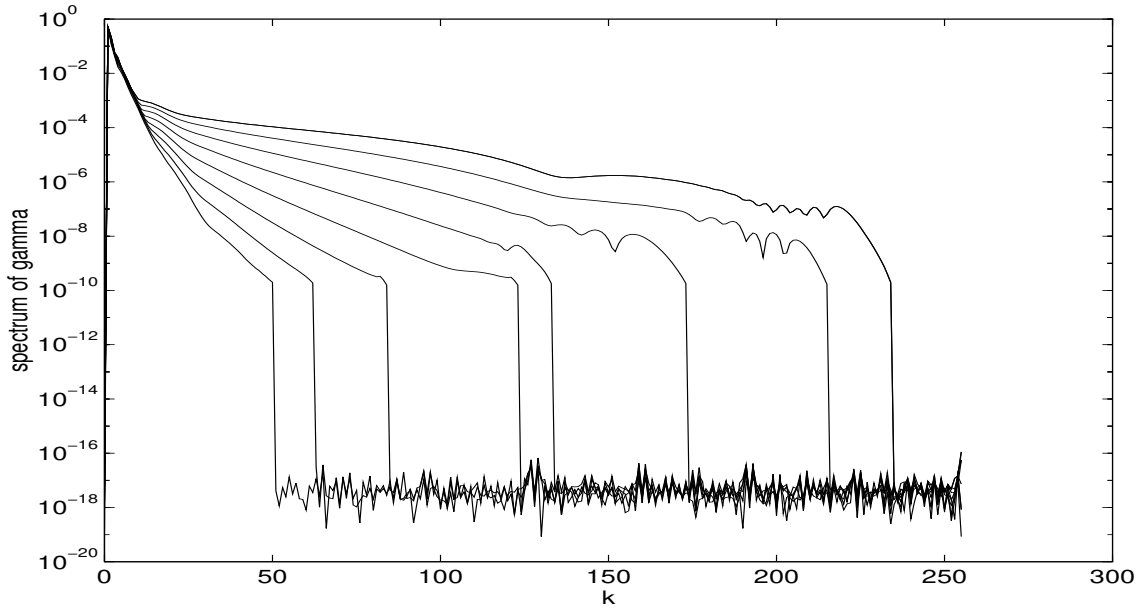

Figure 5.20: Breaking Wave: $\tau = 0.001$: Spectrum of γ at $t = 1.6, 1.7, \cdots, 2.3$.

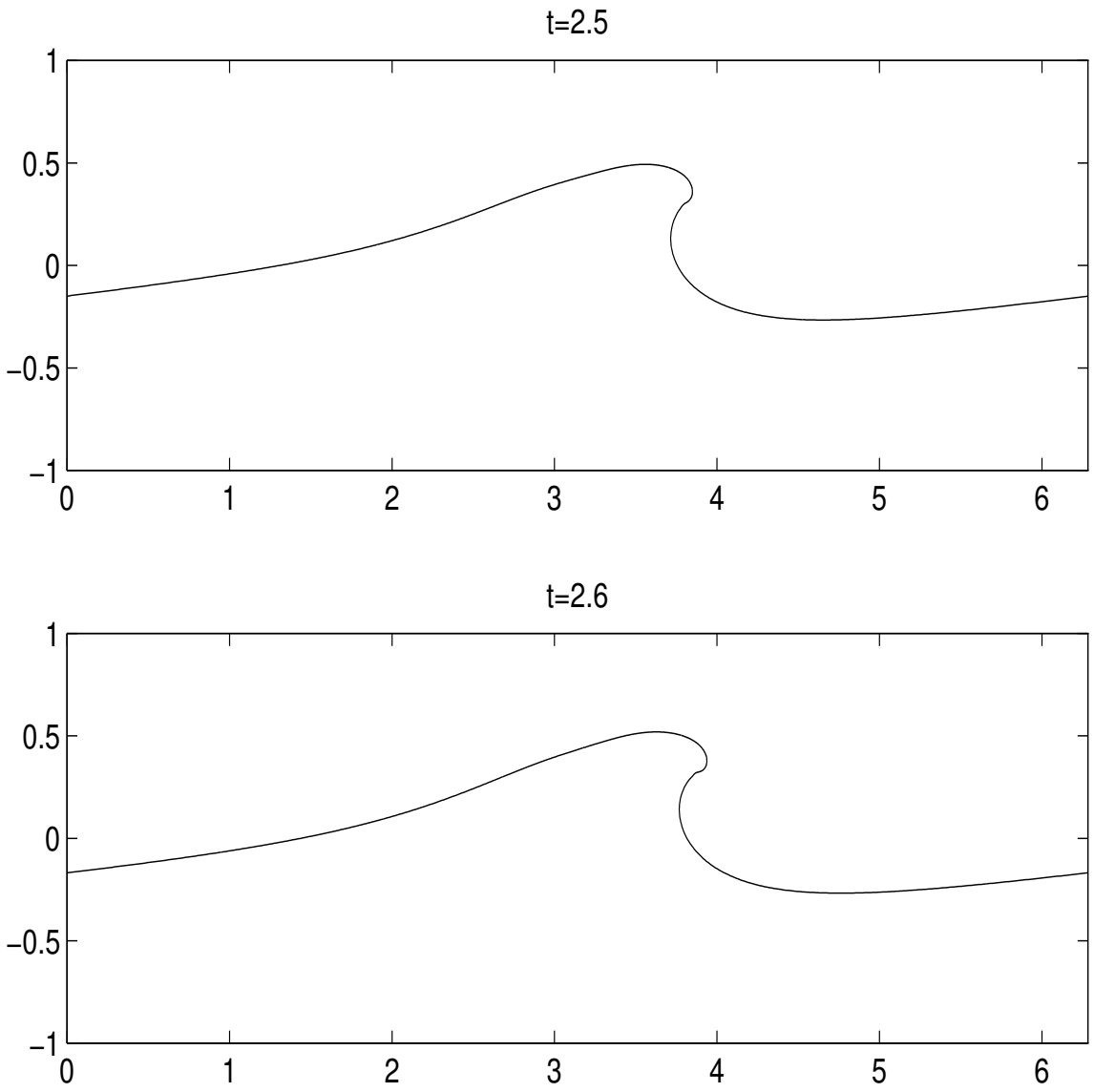

Figure 5.21: Breaking Wave: $\tau = 0.001$: Interface profile at $t = 2.5$ and $t = 2.6$. $N = 1024$ and $\Delta t = 2.5 \times 10^{-4}$.

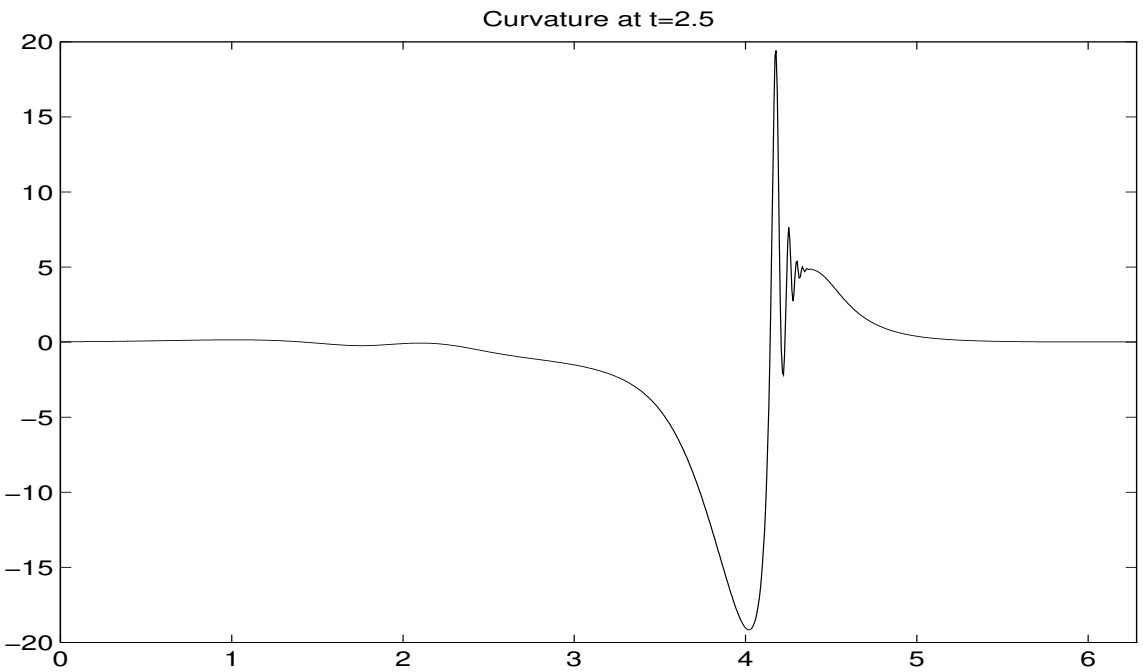

Figure 5.22: Breaking Wave: $\tau = 0.001$: Plot of the curvature at $t = 2.5$.

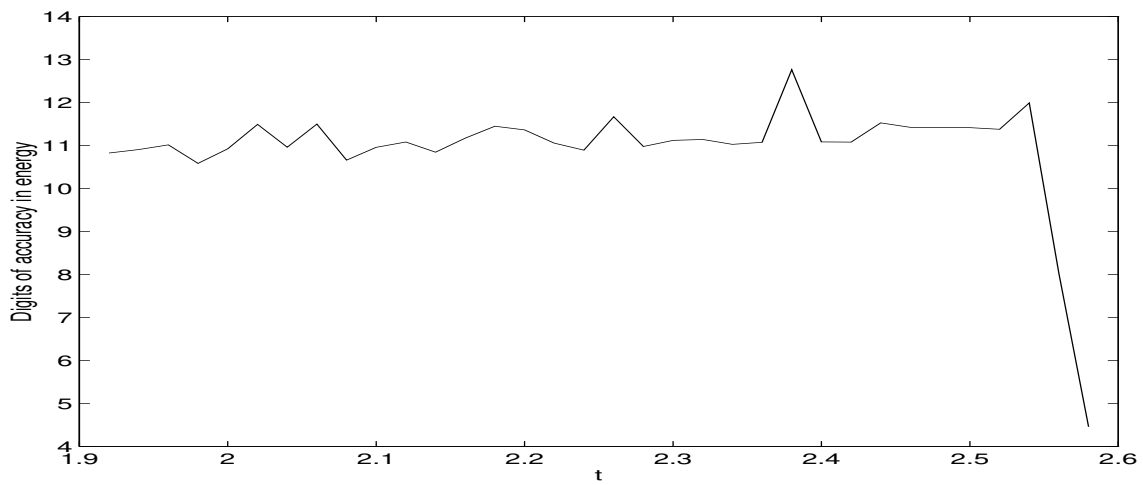

Figure 5.23: Breaking Wave: $\tau = 0.001$: Number of accurate digits in the fractional change of energy against time. $N = 1024$ and $\Delta t = 2.5 \times 10^{-4}$.

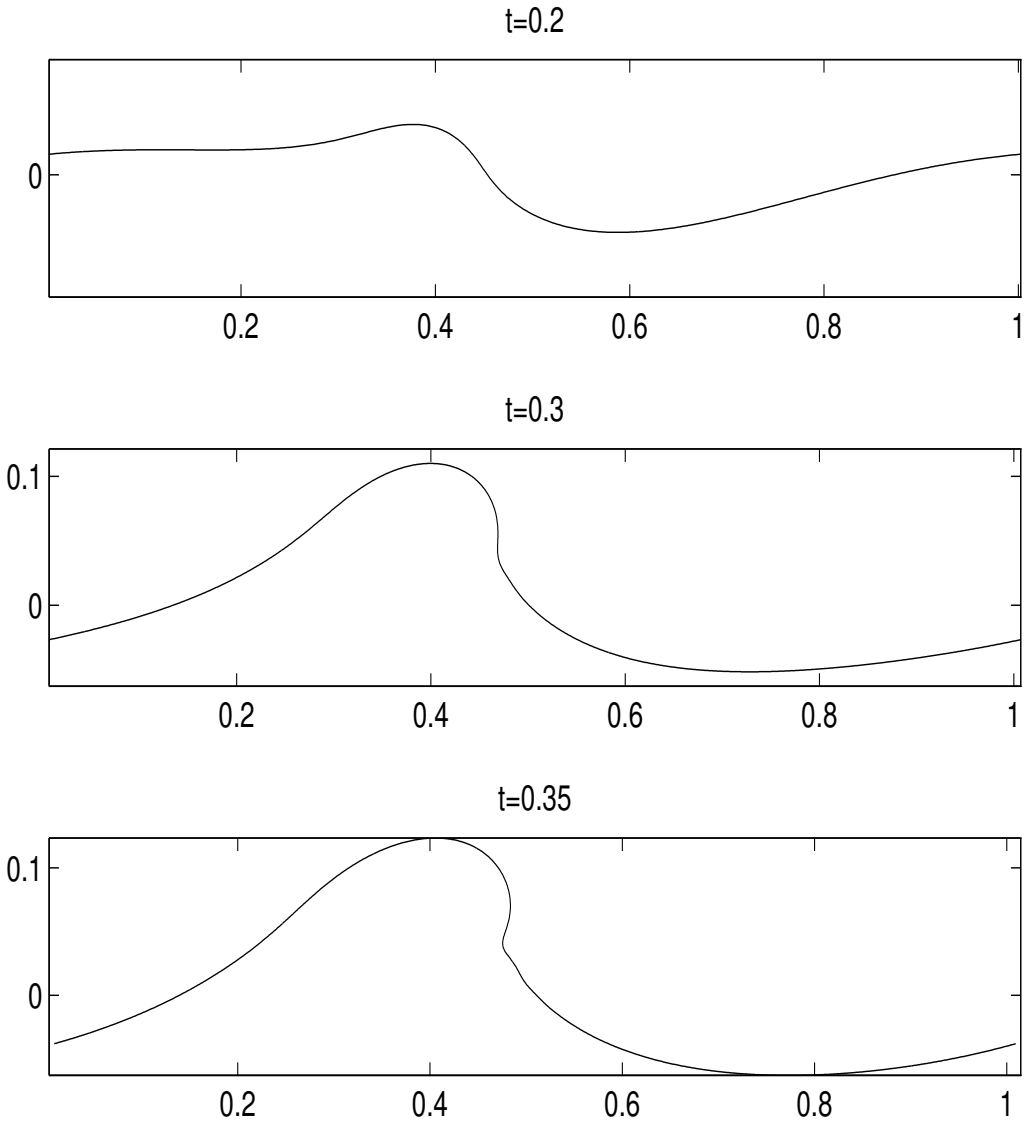

Figure 5.24: Breaking Wave: $\tau = 0.005$, $g = 10$: Interface position at (a) $t = 0.2$. (b)$t = 0.3$. (c) $t = 0.35$. $N = 1024$ and $\Delta t = 2.5 \times 10^{-4}$.

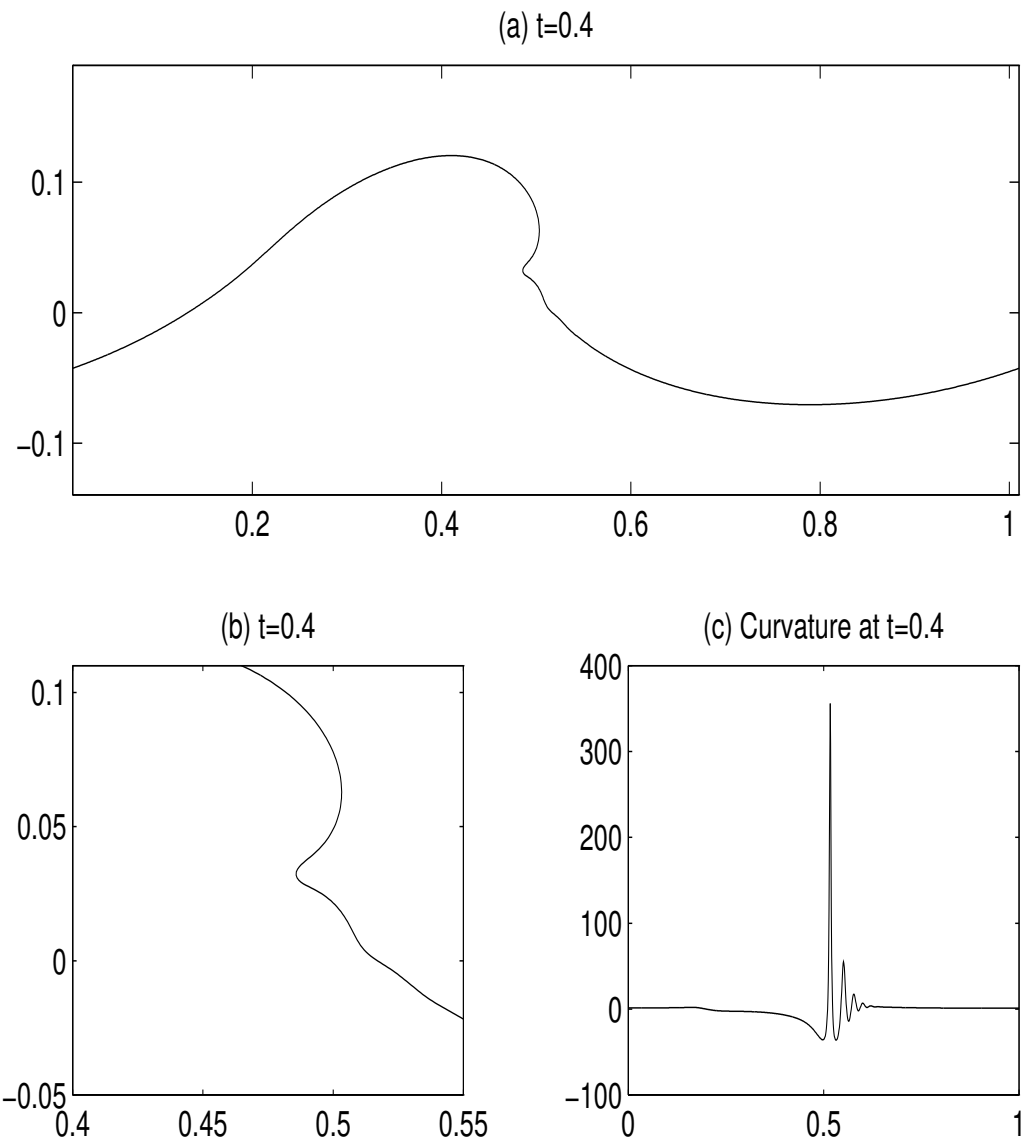

Figure 5.25: Breaking Wave: $\tau = 0.005$, $g = 10$: (a)Interface profile at $t = 0.4$. (b)Close-up of the high curvature region at $t = 0.4$. (c)Plot of the curvature at $t = 0.4$. $N = 1024$ and $\Delta t = 2.5 \times 10^{-4}$.

Bibliography

[1] J. Adler and L. Sowerby. Shalow three-dimensional flows with variable surface tension. *J. Fluid Mech.*, 42:549–559, 1970.

[2] C. Anderson. A vortex method for flows with slight density variations. *J. Comp. Phys.*, 61:417–444, 1985.

[3] L. K. Antanovskii. Influence of surfactants on a creeping free-boundary flow induced by two counter-rotating horizontal thin cylinders. *Eur. J. Mech., B/Fluids*, 13(1):73–92, 1994.

[4] U. M. Ascher, S. J. Ruuth, and B. Wetton. Implicit-explicit methods for time-dependent pde's. To appear in *SIAM J. Numer. Anal.*, 1995.

[5] G. Baker. Generalized vortex methods for free-surface flows. In R. Meyer, editor, *Waves on Fluid Interfaces*, pages 53–81. Univ. Wisc. Press, 1983.

[6] G. Baker and A. Nachbin. Stable methods for vortex sheet motion in presence of surface tension. Submitted to *J. Comp. Phys.*

[7] G. R. Baker, D. I. Meiron, and S. A. Orszag. Vortex simulations of the Rayleigh-Taylor instability. *Phys. Fluids*, 23:1485–1490, 1980.

[8] G. R. Baker, D. I. Meiron, and S. A. Orszag. Generalized vortex methods for free-surface flow problems. *J. Fluid Mech.*, 123:477–501, 1982.

[9] G. R. Baker and M. J. Shelley. On the connection between thin vortex layers and vortex sheets. *J. Fluid Mech.*, 215:161–194, 1990.

[10] G. K. Batchelor. *An introduction to fluid dynamics.* Cambridge University Press, Cambridge, 1967.

[11] J. T. Beale, T. Y. Hou, and J. S. Lowengrub. Convergence of a boundary integral method for water waves. To appear in *SIAM J. Num. Anal.*

[12] J. T. Beale, T. Y. Hou, and J. S. Lowengrub. The stability of two-fluid flows with surface tension, part 1: Growth rates for the linear motion far from equilibrium; part 2: Convergence of suitably modified vortex methods. In preparation.

[13] J. T. Beale, T. Y. Hou, and J. S. Lowengrub. Growth rates for the linear motion of fluid interfaces away from equilibrium. *Comm. Pure Appl. Math.*, 46:1269–1301, 1993.

[14] J. T. Beale, T. Y. Hou, and J. S. Lowengrub. On the well-posedness of two fluid interfacial flows with surface tension. In R. C. Caflisch and G. C. Papanicolaou, editors, *Singularities in Fluids, Plasmas and Optics*, London, 1993. Kluwer Academic.

[15] J. T. Beale, T. Y. Hou, J. S. Lowengrub, and M. J. Shelley. Spatial and temporal stability issues for interfacial flows with surface tension. *Mathl. Comput. Modelling*, 20(10/11):1–27, 1994.

[16] J. B. Bell and D. L. Marcus. A second-order projection method for variable-density flows. *J. Comp. Phys.*, 101:334–348, 1992.

[17] J. U. Brackbill, D. B. Kothe, and C. Zemach. A continuum method for modeling surface tension. *J. Comp. Phys.*, 100:335–354, 1992.

[18] H. D. Ceniceros and T. Y. Hou. Numerical studies of surface tension effects in interfacial flows. In preparation.

[19] A. J. Chorin and P. S. Bernard. Discretization of a vortex sheet, with an example of roll-up. *J. Comp. Phys.*, 13:423, 1973.

[20] W. S. Dai and M. J. Shelley. A numerical study of the effect of surface tension and noise on an expanding Hele-Shaw bubble. *Phys. Fluids A*, 5(9):2131–2146, 1993.

[21] B. J. Daly. Numerical study of the effect of surface tension on interface instability. *Phys. Fluids*, 12(7):1340–1354, July 1969.

[22] J. Delettrez, D. K. Dradley, and C. P. Verdon. The role of the Rayleigh-Taylor instability in laser-driven burnthrough experiments. *Phys. Plasma*, 1(7):2342–2349, 1994.

[23] J. W. Dold. An efficient surface-integral algorithm applied to unsteady gravity waves. *J. Comp. Phys.*, 103:90–115, 1992.

[24] P. G. Drazin and W. H. Reid. *Hydrodynamic stability.* Cambridge monographs on mechanics and applied mathematics. Cambridge University Press, New York, 1981.

[25] N. Ebuchi, H. Kawamure, and Y. Toba. Fine structure of laboratory wind-waves surfaces studied using an optical method. *Boundary Layer Met.*, 39:133–151, 1987.

[26] J. S. Ely and G. R. Baker. High-precision calculations of vortex sheet motion. *J. Comp. Phys.*, 111:275–281, 1993.

[27] R. Goldstein and D. M. Petrich. The Korteweg-de Vries heirarchy as dynamics of closed curves in the plane. *Phys. Rev. Let.*, 67:3203–3206, 1991.

[28] J. Goodman, T. Hou, and E. Tadmor. On the stability of the unsmoothed Fourier method for hyperbolic equations. *Numer. Math.*, 67:93–129, 1994.

[29] D. Gottlieb and S. A. Orszag. *Numerical Analysis of Spectral Methods: Theory and Applications*, volume 26 of *CBMS-NSF Regional Conference Series in Applied Mathematics.* SIAM, Philadelphia, 1977.

[30] H. P. Greenspan. On the deformation of a viscous droplet caused by variable surface tension. *Stud. Appl. Math.*, 57:45–58, 1977.

[31] G. Hammerlin and K. H. Hoffmann. *Numerical Mathematics.* Springer-Verlag, New York, 1991. Translation of: Numerische Mathematik.

[32] T. Y. Hou, J. S. Lowengrub, and R. Krasny. Convergence of a point vortex method for vortex sheets. *SIAM J. Numer. Anal.*, 28:308–320, 1991.

[33] T. Y. Hou, J. S. Lowengrub, and M. J. Shelley. The roll-up and self-intersection of vortex sheets under surface tension. Preprint. Courant Institute.

[34] T. Y. Hou, J. S. Lowengrub, and M. J. Shelley. Removing the stiffness from interfacial flows with surface tension. *J. Comp. Phys.*, 114:312–338, 1994.

[35] R. M. Kerr. Simulation of Rayleigh-Taylor flows using vortex blobs. *J. Comp. Phys.*, 76:48–84, 1988.

[36] R. Krasny. Desingularization of periodic vortex sheet roll-up. *J. Comp. Phys.*, 65:292–313, 1986.

[37] R. Krasny. A study of singularity formation in a vortex sheet by the point vortex approximation. *J. Comp. Phys.*, 167:65–93, 1986.

[38] L. D. Landau and E. M. Lifshitz. *Fluid Mechanics*. Pergamon Press, London, 1959. Translated from the Russian.

[39] J. S. Langer. Instabilities and pattern formation in crystal growth. *Rev. Modern Phys.*, 52:1–28, 1980.

[40] P. F. Linden, J. M. Redondo, and D. L. Youngs. Molecular mixing in Rayleigh-Taylor instability. *J. Fluid Mech.*, 265:97–124, 1994.

[41] P. L.-F. Liu, H.-W. Hsu, and M. H. Lean. Applications of boundary integral equation methods for two-dimensional non-linear water wave problems. *International Journal For Numerical Methods in Fluids*, 15:1119–1141, 1992.

[42] M. S. Longuet-Higgins. Capillary rollers and bores. *J. Fluid Mech.*, 240:569–679, 1992.

[43] M. S. Longuet-Higgins and E. D. Cokelet. The deformation of steep surface waves on water I. a numerical method of computation. *Proc. R. Soc. Lond. A.*, 350:1–26, 1976.

[44] A. I. Markushevich. *Theory of Functions of a Complex Variable*. Chelsea Publishing Company, New York, second edition, 1985.

[45] D. M. Moore. On the point vortex method. *SIAM J. Sci. Stat.*, 2:65–84, 1981.

[46] A. L. New, P. McIver, and D. H. Peregrine. Computations of overturning waves. *J. Fluid Mech.*, 150:233–251, 1985.

[47] P. Pelcé. *Dynamics of Curved Fronts.* Academic Press, Inc., San Diego, 1988.

[48] D. H. Peregrine, G. Shoker, and A. Symon. The bifurcation of liquid bridges. *Journal of Fluid Mechanics*, 212:25–39, 1990.

[49] C. Pozrikidis. *Boundary Integral and Singularity Methods for Linearized Viscous Flow.* Cambridge University Press, 1992.

[50] A. Prosperetti, L. A. Crum, and H. C. Pumphrey. The underwater noise of rain. *J. Geophys. Res.*, 94:3255–3259, 1989.

[51] D. I. Pullin. Numerical studies of surface-tension effects in nonlinear Kelvin-Helmholtz and Rayleigh-Taylor instability. *J. Fluid Mech.*, 119:507–532, 1982.

[52] R. Rangel and W. Sirignano. Nonlinear growth of Kelvin-Helmholtz instability: Effect of surface tension and density ratio. *Phys. Fluids*, 31(7):1845–1855, 1988.

[53] A. J. Roberts. A stable and accurate numerical method to calculate the motion of a sharp interface between fluids. *IMA J. Appl. Math.*, 31:13–35, 1983.

[54] J. Sanz. Self-consistent analytical model of the Rayleigh-Taylor instability in inertial confinement fusion. *Physical Review Letters*, 73:2700–2703, 1994.

[55] J. Sethian and J. Strain. Crystal growth and dendritic solidification. *J. comp. Phys.*, 98:231–253, 1992.

[56] M. J. Shelley. A study of singularity formation in vortex sheet motion by a spectrally accurate vortex method. *J. Fluid Mech.*, 244:493–526, 1992.

[57] X. D. Shi, M. P. Brenner, and S. R. Nagel. A cascade of structure in a drop falling from a faucet. *Science*, 265:157–288, 1994.

[58] A. Sidi and M. Israeli. Quadrature methods for periodic singular and weakly singular Fredholm integral equations. *J. Sci. Comp.*, 3:201–231, 1988.

[59] J. Strain. A boundary integral approach to unstable solidification. *J. Comp. Phys.*, 85:342–389, 1989.

[60] J. C. Strikwerda. *Finite Difference Schemes and Partial Differential Equations.* Wadsworth & Brooks/Cole, Pacific Grove, California, 1989.

[61] E. Tadmor. Stability analysis of finite-difference, pseudospectral and Fourier-Galerkin approximations for time-dependent problems. *SIAM Review*, 29(4):525–555, December 1987.

[62] G. Tryggvason. Numerical simulations of the Rayleigh-Taylor instability. *J. Comp. Phys.*, 75:253–282, 1988.

[63] G. Tryggvason and H. Aref. Numerical experiments in Hele-Shaw flows with a sharp interface. *J. Fluid Mech.*, 136:1–30, 1983.

[64] G. B. Whitham. *Linear and Nonlinear Waves.* Pure & Applied Mathematics. A Wiley-Interscience Series of Texts, Monographs & Tracts. John Wiley & Sons, Inc., New York, 1974.